Olfactory capabilities of sharks: An anatomical and molecular comparative approach

By

Maria Pozo Montoro

Department of Biological Sciences, Macquarie University, Sydney, NSW 2109

Date of Submission: 1st February 2021

A thesis submitted as part of the requirements for the completion of the degree of Master of Research

Statement of Originality

This work has not previously been submitted for a degree or diploma in any university. To the best of my knowledge and belief, the thesis contains no material previously published or written by another person except where due reference is made in the thesis itself.

Chapters 2 and 3 are written in the form of a journal article for *PLoS ONE*. The formatting is slightly modified to meet formatting requirements in line with Macquarie University Thesis Submission Guidelines. Due to space constraints, separate abstracts for each of the chapters were not included. Moreover, the results obtained for each chapter as they relate to the ecology, phylogeny and olfactory capabilities of each species are jointly discussed in Chapter 4 to avoid repetition and comply with the length restrictions of this thesis.

All research performed on animals was approved by Macquarie University's Animal Ethics Committee, Animal Research Authority 2017/039 and Scientific NSW Department of Primary Industries and Fisheries scientific collection permit P17/0055-1.0.

I wish to acknowledge the following assistance in the research detailed in this report:

Professor Nathan Hart and Dr Laura Ryan for their assistance in conceiving and designing this project's experimental design, field and lab training, and overall guidance throughout this project.

Associate Professor Drew Allen and Dr Laura Ryan for their assistance with modelling of the data and statistical analysis

Dr Jemma Geoghegan and Dr Oliver Griffith for assistance with transcriptome assembly, characterisation and expression analyses.

Professor Nathan Hart and Dr Oliver Griffith for assistance in editing this manuscript.

The numerous volunteers for their assistance in data collection.

Blind shark image in abstract page © Sarah Han-de-Beaux (sydneydives.com)

Mako shark image in abstract page © Isaias Cruz (makopako.es)

Date: _____1st - February - 2021_____

(Signed)_____

Maria Pozo Montoro

Candidate's Statement About The Impact Of COVID-19 Changes On The Thesis.

Dear Examiner,

Many of our HDR candidates have had to make changes to their research due to the impact of COVID-19. Below you will find a statement from the candidate, approved by their Supervisory Panel, that indicates how their original research plan has been affected by COVID-19 restrictions. Relevant ongoing restrictions in place caused by COVID-19 will also be detailed by the candidate.

Candidate's Statement:

Due to COVID-19, most fishing competitions where I would have obtained the tissue from mako shark were cancelled during 2020. This affected my original plan to obtain tissue from a diverse set of specimens. Moreover, only olfactory organs from female individuals were available for the molecular characterisation of olfactory receptors. Additionally, once the data collection was completed, I had to go back to Spain to take care of an aged dependent, given the potential risk of infection of other working family members. Therefore, I completed the data analysis and writing of my thesis in Spain. Current travel restrictions mean that it is unlikely I will be able to return to Australia in 2021, but I will certainly be able to address the examiners comments from Spain.

Abstract

Sharks rely heavily on the sense of smell, and their olfactory apparatus has likely evolved to suit the differing lifestyle requirements of each species. Unfortunately, the selective pressures that shape the various physical traits of the olfactory organ of sharks, and their effect on olfactory capabilities, are poorly understood. Here, a multidisciplinary approach combining microscopic and transcriptomic techniques was used to characterise the olfactory organs of two shark species: the pelagic, shortfin mako (*Isurus oxyrinchus*) and the benthic blind shark (*Brachaelurus waddi*). The total sensory surface area of the olfactory organs—a traditional proxy of olfactory capabilities—is relatively larger in *I. oxyrinchus* due to greater coverage of sensory epithelium and more extensive secondary folding of the lamellae. However, examination of the *de novo* transcriptomes reveals a more diversified olfactory receptor repertoire in *B. waddi*. These findings suggest that sharks may rely on different olfactory strategies (i.e.: more extensive olfactory organs and/or more diversified receptor repertoires) that may be related to the characteristics of the flow within their olfactory organs, their ecology or phylogeny. Consequently, multidisciplinary studies considering the anatomical and molecular traits of the olfactory system of sharks are required to fully comprehend the olfactory capabilities of this group.

Mako shark (*Isurus oxyrinchus*)

Blind shark (*Brachaelurus waddi*)

Acknowledgements

Finalmente, nada de esto hubiera sido posible sin el apoyo incondicional de mi familia que me ha animado siempre a seguir mis propósitos a pesar de los quebraderos de cabeza que eso les supone. Especialmente agradecer a mi hermana Loreto por involucrase tantísimo en este proyecto. Así mismo, tengo que agradecerle a mi madre por ser siempre mi mayor confidente, consejera y fuente de apoyo a pesar de la distancia. Quisiera agradecer también a mis padrinos por permitir que me refugiara en su piso para poder escribir esta tesis y a mi abuela por cuidarme y soportarme los días previos a la entrega. Por último, quiero darle las gracias a mi padre, por inculcarme desde pequeña que los sueños pueden despegar con esfuerzo y superación. Gracias por aguantar.

Table of Contents

Supplementary Material Index

Chapter 1 – General Introduction

Chemoreception is considered to be the oldest and most widespread of all the senses [1,2]. Olfaction, the sense of smell, is a form of chemoreception that most vertebrates rely on to detect a range of chemicals (odorants) that inform behaviours such as foraging, predator avoidance, kin recognition and navigation [2,3]. The successful detection and discrimination of odorants is highly dependent on a variety of factors, including the chemical properties and relative concentrations of the odorants, the characteristics of the medium (air or water) in which the odorants are dispersed, the morphology and physiological responses of the olfactory organs, and the processing that occurs once the olfactory stimuli have been transduced into a neural signal [1,2,4–6]. In consequence, over evolutionary time, the olfactory organs of vertebrates have undergone numerous adaptations in their morphology [7–9], physiology [10–13], and associated behavioural responses to given odours [14,15] to maximise the amount and quality of information obtained from olfactory cues.

Sharks are a type of cartilaginous fish (Chondrichthyes) that have become an important group of predators in the aquatic environment since their appearance around 400 million years ago [16,17]. Many shark species fulfil critical roles as apex predators and help to maintain the diversity and functioning of ecosystems by controlling the population and habitat use of species from lower trophic levels [18,19]. The sense of smell of sharks is a critical element in this regulatory mechanism, as the olfactory system is usually the first sense utilized for tracking of prey given the potential of odorant stimuli to travel longer distances [20–22] and the ability of sharks to detect chemical compounds such as amino acids or amines at remarkably low concentrations [23–25]. Additionally, sharks are thought to rely heavily on olfactory cues for their survival and reproduction. For instance, the ammonium acetate emanating from rotten shark flesh has been observed to have a deterrent effect on some species, while others are able to detect chemical compounds exuded from their predators and toxic prey that potentially alert them to danger [2,16]. Similarly, behavioural observations indicate that olfaction may play an important role in the reproduction of this group [26], which may be mediated by bile salts as observed in agnathans and teleosts [27]. Furthermore, recent studies have started to provide evidence of the importance of this sensory modality for navigation [28,29], whereas the possibility of olfactory cues mediating conspecific recognition for species that show social structures remains to be examined [30,31].

The substantial morphological variability observed in the olfactory system of sharks suggests that this sensory modality has adapted to the different environmental and sensory requirements of each species

[32–37], and this is supported by behavioural studies that have revealed interspecific differences in the degree of reliance on olfaction for feeding. For example, the nurse shark (*Ginglymostoma cirratum*) and the dusky smooth-hound (*Mustelus canis*) are unable to detect and capture prey without olfactory cues, whereas the common blacktip (*Carcharhinus limbatus*) and bonnethead sharks (*Sphyrna tiburo*) can still forage providing that visual and electric cues are available [20,38]. Given the complications associated with performing behavioural experiments on species that are difficult to keep in captivity and/or study in the laboratory, morphological differences of the olfactory system have been used to infer the olfactory capabilities and degree of reliance in several shark species [32–34,36,37,39–43]. Unfortunately, the selective pressures shaping these morphological traits and how they may modify the olfactory capabilities of sharks are still poorly understood. Addressing this knowledge gap is critical not only for a better understanding of the evolutionary and behavioural ecology of this group [44], but also for providing new opportunities to reduce negative interactions between humans and sharks, including the reduction of bycatch in commercial fisheries [45], improved shark deterrent technologies [16], and mitigating the impacts of pollution [46] and climate change [47,48].

One of the main morphological traits used as a proxy of olfactory capabilities in sharks is the available surface area of their peripheral olfactory organs [32,33,37,39,40]. The olfactory organs (olfactory rosettes) comprise a series of sensory lamellae (primary folds) that vary in number, shape, and size between species [49,50]. Species with relatively larger available surface area within their olfactory organs are assumed to rely more heavily on olfaction on the basis that more olfactory receptor neurons (ORNs) and olfactory receptors will be available to sample the water passing through the olfactory organ [24,32,36,37]. Bentho-pelagic elasmobranchs (sharks and rays) tend to have larger sensory surface areas than benthic species, which has been suggested to be an adaptation to the open water environment that may be deficient in visual, mechanical or electrical sensory cues [32]. However, it is unclear how differences in the total sensory surface area of the olfactory organs relate to the diversity of odorants that can be perceived and their detection thresholds for two main reasons.

Firstly, studies characterizing the surface area of the olfactory organs of sharks rarely consider interspecific differences in the distribution of the sensory epithelium and the degree of secondary folding of the lamellae. In several studies, the surface area of the olfactory organs has been calculated by simply multiplying the number of lamellae by their surface area [24,36,39,40]. However, ORNs are not distributed uniformly across the surface of the lamellae and instead are confined to a sensory epithelium, which is distinguished by the presence of cilia from supporting cells, that covers only a proportion of the lamella in a species-specific manner [32,37]. Moreover, the surface area of the lamellae is significantly

2

increased by the presence of secondary folds that vary in complexity between species [35]. Whereas differences in each of these factors have been reported independently in different studies, it is unclear how these two factors interact with each other and with the number and size of the lamellae to determine the total sensory surface area of the olfactory organs of each species. Additionally, it is unclear how differences in the degree of secondary folding among regions of the same lamella may affect estimates of the total sensory surface area of the olfactory organs because only the region with the most convoluted folds has been assessed [35]. Therefore, to allow for a fair comparison of the functional extent of the olfactory organs of different shark species, both the distribution of sensory epithelium and the varying degree of secondary folding of the lamellae should be considered.

Secondly, while the morphology of the olfactory organs may play an important role in the perception of smells by modifying the hydrodynamics of the water flow carrying odorant molecules to the sensory epithelium [51,52] and partially determining the number of ORNs, other factors may also be relevant in determining the sensitivity and specificity to odorants. Some of these factors include: the diversity of olfactory receptors and their affinity to different odorants [14,53,54], the density of ORNs [55], and the convergence ratio of receptor neurons onto secondary neurons [56,57]. Indeed, electrophysiological studies have shown that the olfactory thresholds of five coastal elasmobranchs to amino acids does not differ significantly among species with olfactory organs that differ in surface area when only the number and size of the lamellae were taken into account [24]. Unfortunately, electrophysiological studies on olfactory ability tend to be restricted to a limited number of substances and to species that can endure these types of tests. Therefore, additional approaches that allow the investigation of a more diverse set of species and compare the whole array of substances that they may be able to detect are necessary to confirm whether differences in olfactory capabilities are related to the morphology and/or habitat of sharks (or otherwise reflect phylogenetic relationships).

One approach that could provide new insights into the olfactory capabilities of this group is to characterise and quantify the olfactory receptors present in the olfactory organ. Olfactory receptors are a type of G-protein coupled receptor expressed in the olfactory organs of vertebrates that bind to specific odorants (ligands), generating an electrical signal in the receptor cell that is transmitted to the brain [58,59]. In other vertebrates, the number of different olfactory receptors varies widely between species according to the need to detect and identify relevant olfactory cues from their surroundings [60–64]. For example, the extensive reduction of the olfactory receptor repertoire of some primates appears to have originated as a consequence of the transition from frugivory to folivory in some species and the acquisition of higher visual acuity in others [64]. Additionally, the expression levels of olfactory receptor

3

genes are a good indicator of the relative number of ORNs present in the olfactory organ in teleost fishes and mammals [65], which is known as an important factor determining the sensitivity to odorants in vertebrates [56]. Furthermore, it has been observed that the number of ORNs correlates with the size of the olfactory receptor repertoire in mammals [66]. Unfortunately, it is not known whether this phenomenon also occurs in other taxa. Therefore, according to these studies, we may expect that if the total sensory surface area is a good proxy of olfactory capabilities for sharks, species with a relatively large sensory surface area will also have a more diverse and/or more highly expressed repertoire of olfactory receptors to differentiate a wider array of substances and/or increase the sensitivity to specific odorants. Alternatively, if the diversity and level of expression of different olfactory receptors are unrelated to the extent of the surface area of the olfactory organs, this traditional anatomical proxy of olfactory capabilities may not fully reflect the importance of this sensory modality in different species of sharks.

The main objective of this thesis was to assess how morphological proxies of olfactory capability relate to the diversity and abundance of olfactory receptors in sharks. To do this, I characterised the anatomical and molecular properties of the olfactory organs of two shark species with contrasting lifestyles: the shortfin mako shark (*Isurus oxyrinchus*), a pelagic and globally distributed species, and the blind shark (*Brachaelurus waddi*), a benthic species endemic to the east coast of Australia. In Chapter 1, I provided a broad introduction to the questions and objectives this thesis aims to address through its following chapters. Therefore, the reader is referred to the introductions of Chapter 2 and 3 for a detailed review of what is currently known about the anatomical and molecular characteristics of the olfactory organs of sharks. In Chapter 2, I used a combination of microscopic techniques to determine the extent of the sensory epithelium and the degree of secondary folding within lamellae to estimate the total sensory surface area of the olfactory organ for each species. In Chapter 3, I then assembled the *de novo* olfactory transcriptomes of each species to characterise the type of olfactory receptors present and their expression levels in the olfactory organs. In Chapter 4, the results obtained from each of these approaches are synthesised to assess the olfactory capabilities of each species in the context of their ecology and lifestyle. The hypothesis was that the greatest total sensory surface area, and therefore, the widest repertoire of olfactory receptors, was going to be found in the mako shark given its pelagic lifestyle and coherent with the results presented in Schluessel et al. [32]. The findings of this study provide new information on the sensory biology of sharks that may generate a new set of tools to better understand the sensory ecology and behaviour of this ancient group of predators and possibly find new strategies to promote their conservation.

Chapter 2 – Anatomical Characteristics of the Olfactory Organ of Sharks

2.1 Introduction

The olfactory organs of all sharks and rays share a common architectural plan [24,32,36,49,50,67–69]. Each of the paired olfactory organs (also called olfactory rosettes) is located symmetrically on either side of the head inside a cartilaginous capsule that forms the olfactory chamber, which is often connected to the exterior by an incurrent and an excurrent nostril (Fig. 2.1A, 2.2). The olfactory organ comprises a series of plate-like structures called lamellae, which are usually (but not always) attached parallel to one another by a central raphe of connective tissue [49] (Fig. 2.1B, 2.2F, 2.3). Each olfactory lamella has several—often elaborate—secondary folds that increase the overall lamellar surface area [35]. The secondary folds of opposing adjacent lamellae form interlamellar channels that guide the water entering the olfactory organ from the incurrent nostril (via the incurrent channel) across the lamellar surface and into the peripheral and excurrent channels before exiting the olfactory cavity by the excurrent nostril [52,70,71]. As the water flows across the sensory epithelium of the lamella, odorant molecules bind to receptors borne on the surface of olfactory receptor neurons (ORNs) [59].

Amongst the elasmobranchs, interspecific variation has been observed in several of the morphological parameters that characterize the peripheral olfactory system; these include the position and shape of the nostrils, the degree of exposure to the environment of the olfactory organs, the presence of nasal valves to redirect the flow of water, the type of lamellar arrangement (circular or ellipsoidal); and the number, size and morphological characteristics of the olfactory lamellae [33,35–37,49,50,67,68,72,73]. Many of these modifications have evolved independently in distantly related shark species, which suggests that these changes reflect functional adaptations to different life styles or sensory requirements [32,35,72,73]. For example, the position of the nares within the snout appears to vary to accommodate the ventilatory needs of the olfactory organs of pelagic and benthic species [72,73]. Most benthic species have their olfactory organs closer to their mouth to allow them to use the flow of water generated through the respiratory oral pump to ventilate the olfactory organ, whereas pelagic species have their nares closer to the tip of the rostrum to optimize water flow through the olfactory organs as the animal moves [73].

The surface area of the olfactory organs of sharks and rays is one morphological trait that appears to vary widely among species; however, the selective pressures driving this diversity and its functional implications for the perception of odours are unclear. Traditionally, a larger surface area has been associated with enhanced olfactory capabilities following the assumption that more extensive olfactory

organs may provide a higher number of ORNs to detect odorants. For example, Schluessel et al. [32] reported that elasmobranchs with bentho-pelagic lifestyles have more numerous lamellae and larger sensory olfactory surface areas than benthic species, suggesting perhaps that bentho-pelagic species may rely more heavily on olfaction to navigate an open water habitat deficient in other sensory cues (e.g. visual) compared to benthic habitats. Moreover, anatomical studies often rely on the surface area of the olfactory organs as an anatomical proxy of olfactory capabilities to infer the sensory ecology of more elusive species that are difficult to keep in captivity or study in the wild [37,39]. However, there is no apparent relationship between the surface area of the olfactory organs and the threshold sensitivity to odorants, either in elasmobranchs or teleost fishes [24,74]. Unfortunately, the surface area of the olfactory organs in these studies is often calculated by simply multiplying the number of lamellae by their size, potentially overlooking the effect of the structural complexity of the lamellae into the available total sensory surface area of the olfactory organ of each species.

Shark olfactory lamellae display two main traits that may affect the amount of sensory epithelium that is exposed to the water carrying odorant molecules through the olfactory rosette: These are: 1) the heterogeneous distribution of the sensory epithelium across the lamellar surface, and 2) the degree of secondary folding of the lamellae. The extent of the sensory epithelium—which is distinguished by the presence of cilia arising from supporting cells—potentially determines the number of individual ORNs available to detect odorants [32,37,68]. Similarly, secondary folds substantially increase the surface area of the lamellae, which in turn may increase the number of ORNs to detect chemical cues [35]. To the best of our knowledge, no study has attempted to determine how these two traits interact with each other and with the overall number and size of the lamellae to determine the total sensory surface area of the olfactory organs in elasmobranchs. Indeed, whereas species-specific variability in the spatial distribution of the sensory epithelium has been reported for the lamellae of some species, these differences have never been quantified [32,37,75]. Similarly, a recent study measured for the first time the degree of secondary folding in several species of elasmobranchs [35]; however, the secondary folds were only characterised in the region of the lamellae with the highest degree of secondary folding, potentially overestimating the contribution of this trait to the total (sensory) surface area of the olfactory organs by discounting the variation in sinuosity observed through different regions of the lamellae [71].

In this study, we used a combination of anatomical techniques to characterize the extent of the sensory epithelium and the degree of secondary folding of the olfactory lamellae and its contribution to the total sensory surface area of the olfactory organ of two shark species: the benthic blind shark (*Brachaelurus waddi*) and the pelagic shortfin mako (*Isurus oxyrinchus*). Scanning electron microscopy (SEM) and

6

light microscopy (LM), respectively, were used to demarcate the sensory epithelium of selected lamellae and to quantify the degree of secondary folding across the entire olfactory organ. Differences in the number and size of the lamellae, the proportion of the epithelium that is sensory (rather than non-sensory) and the degree of secondary folding contributed differently to the total sensory surface area for each species. Additionally, the degree of secondary folding significantly decreased towards the free edges of the lamellae, especially for the blind shark. Estimates of the surface area of the olfactory organs made without consideration of the distribution of sensory epithelium or variability in the degree of secondary folding throughout the lamellae led to significantly different values in almost all comparisons, warning of the potential bias in comparing the surface area of species assessed in different studies that did not consider either of these traits. Although more species are needed to confirm any given trend, and this study does not consider the phylogenetic relationships between the study species, it appears that different species of sharks may be relying on different morphological traits of their olfactory organs—which in turn may be further subjected to additional selective pressures—to reach the total olfactory sensory surface area that characterizes each species. Further comparative analysis should consider each of these morphological traits in relation to the ecology and the phylogeny of different species to help unravel the selective pressures driving the extension of the olfactory organs of this group and its sensory implications.

2.2 Materials and Methods

2.2.1 Specimens

The olfactory organs of blind sharks and shortfin mako sharks were collected from specimens captured in waters off the coast of New South Wales (NSW), Australia. A total of three individuals for each species were examined. Before removing the olfactory organs, the total length, mass, and sex of each specimen were recorded (Table S2.1). Blind sharks were caught by line fishing in coastal waters off Sydney (NSW) from July to August of 2018 under NSW Department of Primary Industries and Fisheries Scientific Collection Permit P17/0055-1.0. These sharks were kept in recirculating seawater aquaria (400L) for up to five months and underwent a series of unrelated electrophysiological experiments on their visual system prior to harvest the tissue under the approval of Macquarie University Animal Ethics Committee (Animal Research Authority 2017/039). Mako sharks were captured as part of game fishing competitions taking place in NSW between February 2019 and March 2020. Animal ethics approvals were not required as the animals were not captured for scientific purposes and the tissue was donated by fishermen.

2.2.2 Tissue collection and storage

From each shark, one of the two olfactory organs were chosen arbitrarily and fixed by immersion in 4% paraformaldehyde in 0.1M phosphate-buffered solution (pH 7.4) and stored at 4°C. The olfactory organs of blind sharks were removed and fixed immediately following euthanasia with an overdose of the fish anaesthetic tricaine methane sulfonate salt (MS222; 500 mg L^{-1} buffered with an equal mass of sodium bicarbonate). The olfactory organs of mako sharks were obtained within 2 to 4 hours of capture. Tissue was stored in fixative for at least two months before it was processed for microscopy.

2.2.3 Olfactory rosette dimensions, olfactory lamellae counts and selection of lamellae

Before dissection, olfactory organs were washed overnight in 0.1M phosphate-buffered solution (pH 7.4) with 0.1% sodium azide (PBS-azide) and the dimensions of the olfactory rosette (length, width, depth, and mass) were measured using a vernier caliper and an electronic balance (Table S2.1). All lamellae in each olfactory rosette were extracted and stored individually in PBS-azide and the number of lamellae per olfactory rosette was counted according to the definition provided by Ferrando et al. [49] (i.e. each fold of tissue extending from the raphe corresponds to a single lamella). From each olfactory organ, five pairs of intact lamellae evenly spaced through the olfactory organ were chosen for SEM and LM, respectively (Fig 2.1A, B). Whenever the quality of one of the lamellae from one of the pairs was unfit to undergo microscopy work, an adjacent lamella was taken instead.

2.2.4 Estimation of gross surface area (GSA)

Extracted lamellae were inspected under a stereomicroscope (Olympus SZX16; Olympus, Japan) and photographed using a digital camera (Olympus DP26; Olympus, Japan). The total surface area (i.e. comprising both sensory and non-sensory regions) of each lamella was calculated from the digital images using Image J, v1.52p [76,77]. To calculate the gross surface area of the olfactory organs of each individual (GSA), measurements of surface area were averaged for all the lamellae within the same olfactory rosette; the result was then multiplied by the number of lamellae and then multiplied by four to account for the two sides of each lamella and the presence of two olfactory organs (Equation S2.1). This measurement would be equivalent to the one used in Kajiura et al. [36] and Meredith and Kajiura [24].

2.2.5 Estimation of sensory surface area (SSA)

SEM was used to determine the boundary of the sensory epithelium of representative lamellae through the olfactory rosette. Lamellae were dehydrated using an ascending ethanol series and dried in a critical point dryer (Leica EM CPD 300 Critical Point Dryer Leica, Germany). Then, each lamella was mounted

on a carbon tab pin stub and sputter-coated with gold (Emitech K550 Gold Sputter Coater; Quorum Technologies, UK). Samples were examined using a JEOL JSM 7100F Field Emission Scanning Electron Microscope (JEOL, Japan) and photographed digitally. The boundary between the sensory and non-sensory epithelium was delineated at > 200x magnification by the presence of cilia over the sensory epithelium and olfactory receptor neurons (Fig 2.1B). Once the distribution of sensory epithelium was established, ImageJ was used to calculate the total surface area and the sensory surface area of the lamellae. Then, the ratio of sensory surface area:total surface area was calculated and multiplied by the gross surface area of the lamella (obtained as above in section 2.2.4) to have a measurement of sensory surface area for each lamella. We did not consider the 'raw' sensory surface area as measured from the SEM micrographs as lamellae experience considerable shrinkage during sample preparation for electron microscopy. The lamellar sensory surface area of all measured lamellae within an olfactory rosette was averaged and multiplied by the number of lamellae and by four to calculate the sensory surface area of the olfactory organs of each individual (SSA) (Equation S2.2). This measurement would be equivalent to the one used in Schluessel et al. [32,33] and Theiss et al. [37].

2.2.6 Estimation of total surface area accounting for secondary folding (TSA-SF)

Selected lamellae were dissected according to a cutting plane that was transverse with respect to most of the secondary folds within a region. This resulted in each olfactory lamella being divided into one to four fragments. Each fragment was dehydrated using an ascending ethanol series and cleared with benzyl benzoate. Then, fragments were embedded in Paraplast (Sigma-Aldrich, USA) and sectioned transversely at 10 μm thickness. These sections were mounted sequentially on microscope slides and stained with hematoxylin and eosin. Histological observations were performed with an Olympus BX53 microscope (Olympus, Japan) and one section every 100–200 μm was photographed with a digital camera (Olympus DP73; Olympus, Japan). When the lamellar section was longer than the camera's field-of-view, a single picture was taken randomly along the length of the lamella. From each image, two different measurements were made on the side of the lamella with the best-preserved secondary folds (if the preservation state of both sides was similar, the side to measure was chosen randomly); firstly, a straight-line (Euclidean distance) measurement from the two furthest points of the lamellae within the photograph, and secondly, a measurement of the convoluted surface of the lamellae (curvilinear length) tracing the perimeter of the secondary folds between the same two start and end points (Fig 2.1C). These measurements were made by independent, trained observers and a sub-set of the measurements cross-validated. The ratio of the increase in the length of a lamellar section considering the secondary folds (i.e. sinuosity) was calculated as the curvilinear length of the secondary folds divided by the straight line

length. The average sinuosity ratio of all the sections within all the fragments of a lamella was used to calculate the surface area of the olfactory organ of each individual accounting for the variation of its secondary folds by multiplying this average against the number of lamellae, the gross lamellar surface area and four (TSA-SF) (Equation S2.3). Also, we calculated a similar measurement but considering only the maximum ratio of increase of the linear length (SAMS) to emulate the method used by Ferrando et al. [35].

2.2.7 Estimation of total sensory surface area accounting for secondary folding (TSSA-SF)

Finally, a novel approach was taken by multiplying simultaneously the average proportion of sensory epithelium and the degree of secondary folding of the olfactory organ against the gross lamellar surface area and four (TSSA-SF) (Equation S2.4).
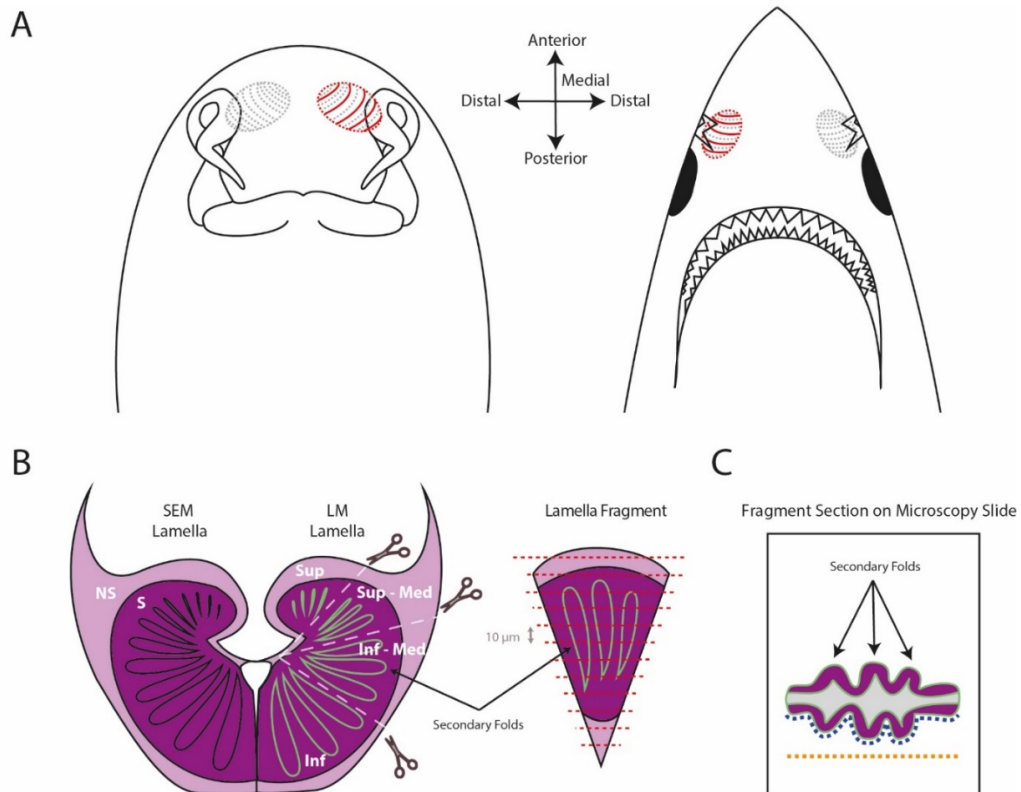
Fig 2.1. Sampling strategy for the olfactory organ and lamellae. (**A**) Illustration showing the relative position of the olfactory organs of *B. waddi* and *I. oxyrinchus* and the relative position of the five lamellae sampled (red lines). (**B**) Schematic representation of the dissection of the lamellae and sectioning method for light microscopy. The lamella for SEM was inspected to determine the distribution of sensory epithelium. Purple areas represent sensory epithelium. Pink areas represent non-sensory epithelium. The lamella for LM was divided into 1–4 fragments containing parallel secondary folds (Inf: inferior; Inf-Med: inferior-medial; Sup-Med: superior-medial; Sup: superior). Fragments were then sectioned at 10 μm thickness for analysis of the secondary folding. Red lines represent sectioning planes. Green lines

highlight the secondary folds (**C**) Scheme on measurements taken from each fragment section. Orange dotted line represents straight-line length. Blue dotted line represents curvilinear length. NS, Non-sensory epithelium; S, Sensory epithelium.

2.2.8 Data Analysis

To determine whether there were differences in the lamellar surface area, the ratio of sensory surface area and the degree of secondary folding of the lamellae of the two species, we constructed generalized linear mixed models (GLMM) in R (version 3.6.1, [78]) using the *lmer* fuction in the *lme4* package [79]. Unfortunately, due to the substantial differences in total body length and mass between the two species, the variables species, total body length and total body mass were confounded. Therefore, we could not incorporate the latter two variables into our models. However, in an attempt to control for total body length, the total sensory surface area was divided by the body length of each individual to determine whether there were still significant differences between species after normalizing for differences in body length. For all the analyses, we included species as a fixed effect and individual as a random effect. Additionally, for the analysis of the secondary folds, we also included the relative position of the fragment where the cuts were obtained as a fixed effect to determine whether there were differences in the degree of secondary folding between the different regions of the lamellae; in this case, the lamella ID where the sections were obtained, and individual were included as nested random effects. To determine whether the different methods of calculating olfactory surface area differed from one another or between species, we also used GLMMs with species and the type of measurement as a fixed effect and the individual ID as a random effect.

Before constructing the models, all numeric variables were log-transformed to ensure normality and homoscedasticity of the residuals of the models [80]. In modelling the gross surface area of the lamellae, the degree of secondary folding and the total sensory surface area normalized by the total length of the individuals, a defensible model where the variance was assumed to grow as a power function of the mean was used to meet the assumption of homoscedasticity of the residuals. Models were fit with Maximum Likelihood and the significance of the variables (p-value < 0.05) was tested using likelihood ratio test (LRT) with the *drop1* function from the *lmertest* package [81]. Post hoc comparisons were performed combining the functions *lsmeans* and *contrast* from the packages *lsmeans* [82] and *pbkrtest* [83], respectively.

2.3 Results

2.3.1 External morphology

The paired olfactory organs of the blind shark are located on the ventral side of the snout close to the mouth (Fig 2.2A). Each olfactory organ receives water from the environment through an incurrent nostril (nare) whose orifice points ventrolaterally (i.e. outwards and downwards towards the substrate). Both incurrent nostrils are characterized by a well-developed circumnarial fold towards the lateral side and a barbel that protrudes towards the substrate on the medial side. The anterior nasal flaps are fused to each other and to their respective upper labial furrow, so no apparent external nasoral grooves are present between the incurrent nostrils and the mouth. No valve flaps penetrate the olfactory cavity. The olfactory cavity is delimitated by a delicate cartilage capsule where the olfactory organ is found. Each olfactory cavity is connected internally to the mouth through an inner cartilage tube (inner nasoral groove) (Fig 2.2B).

The olfactory organs of the shortfin mako are located symmetrically on the lateroventral side of the snout and distant from the mouth (Fig 2.2C). Each olfactory organ is connected to the environment through two narrow and approximately circular nostrils. The incurrent nostril is oriented rostrally towards the oncoming water flow as the shark swims, whereas the excurrent nostril faces caudally (Fig 2.2D,E). The incurrent nostril has a more dorsal and posterior location compared to the excurrent nostril. A posterior nasal flap and an anterior nasal flap arise from the incurrent and the excurrent nostril, respectively, with the latter partially covering the excurrent nostril. Each nasal flap forms a stiff valve flap that fuses together medially before penetrating the olfactory cavity, where it is attached to some of the lamellae of the olfactory organ (Fig 2.2D,F). The olfactory cavity is formed by a thick cartilage capsule that surrounds the olfactory organ.

2.3.2 Morphology of the olfactory organ and number of lamellae

The olfactory organs of both species are elongated and relatively unexposed (i.e. the degree to which the lamellae are visible from the outside, in comparison to other elasmobranch families [50]) but differ in their degree of curvature. The mean dimensions of the olfactory organs of the blind shark of this study were 13.8 ± 5.1 mm in length, 8.8 ± 3.8 mm in width and 10.9 ± 4.6 mm in depth. The dimensions of the olfactory organs of the mako shark in this study were considerably larger, at 38.5 ± 5.3 mm in length, 27.11 ± 2.9 mm in width and 26.14 ± 2.1 mm in depth (Table S2.1). The lamellae (single folds) of both species are arranged in two distinct rows attached by a common raphe, where the lamellae of each row face each other. However, in some instances, the position of the lamellae of the two rows are offset,

presumably because of the curvature of the olfactory organ within the olfactory cavity. The number of pairs of lamellae that were offset is slightly higher in the mako shark than in the blind shark, possibly because of the more pronounced curvature of the organ. The overall number of lamellae was higher in blind sharks with a mean of 84 ± 2 lamellae in comparison to the mako sharks with a mean of 57 ± 3 lamellae per olfactory organ (Table S2.1). The number of lamellae appeared to increase with total body length and body mass, and it was higher in females than males in both species; however, due to the limited sample size, these observations should be interpreted cautiously (Fig S2.1).
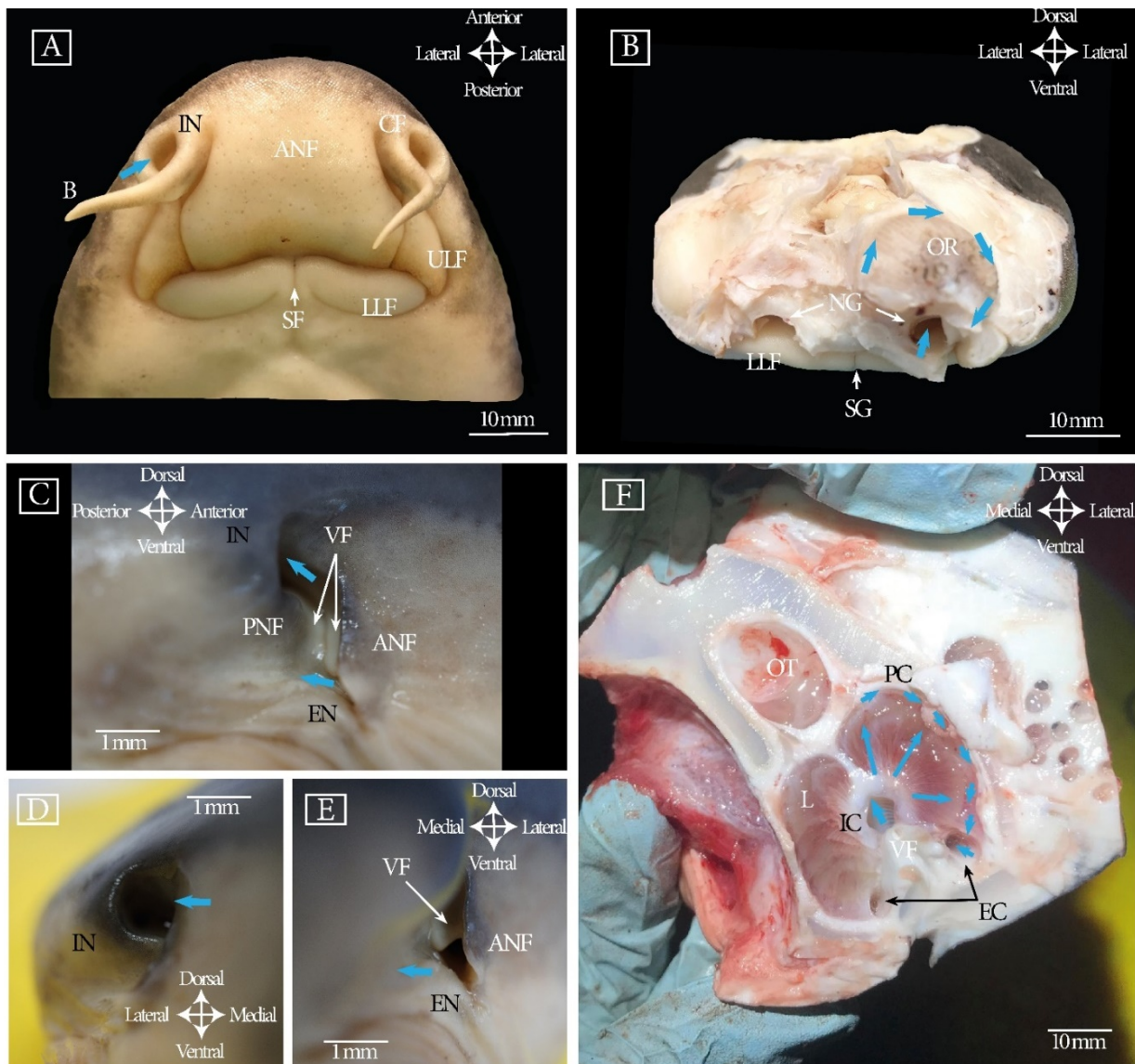
Fig 2.2. External morphology of the olfactory organs. (A) External morphology of *B. waddi;* **(B)** Internal grooves connecting the olfactory organ to the mouth of *B. waddi*; **(C)** External morphology of *I. oxyrinchus*; **(D)** Incurrent nostril of *I.* oxyrinchus; **(E)** Excurrent nostril of *I.* oxyrinchus; **(F)** Transversal section of the olfactory organ of *I. oxyrinchus*. Note the fused valve flaps attached to the

lamellae forming the excurrent channels. Blue arrows represent tentative water flow direction. ANF, anterior nasal flap; B: barbel; CF: circumnarial fold; EC: excurrent channel; EN: excurrent nostril; IC: incurrent channel; IN: incurrent nostril; L: lamellae; LLF: lower labial furrow; NG: inner nasoral groove; OR olfactory rosette; OT: olfactory track; PC: peripheral channel PNF: posterior nasal flap; SG: symphyseal groove; VF: valve flap

2.3.3 Shape and surface area of the olfactory lamellae

In the blind shark, the free edges of opposing lamellae in the middle of the olfactory organ contact each other with finger-like prolongations (a Type I lamellar array according to [50]) (Fig 2.3A). In the mako shark, the free edges of the lamellae in the middle of the organ almost touched each other (a Type II lamellar array) (Fig 2.3B). In both species, the space between the edges of the lamellae increased towards both ends of the olfactory organ. As expected, the mean gross surface area of the lamellae of the blind shark (16.7 ± 8.7 mm^2) was significantly smaller than in the mako shark (193.2 ± 47.6 mm^2) (beta $= 2.66$, t$= 9.93$, p < 0.001) (Table S2.1). The mean surface area of the lamellae appeared to increase with total body length and body mass but there was no sex difference (Fig S2.2).
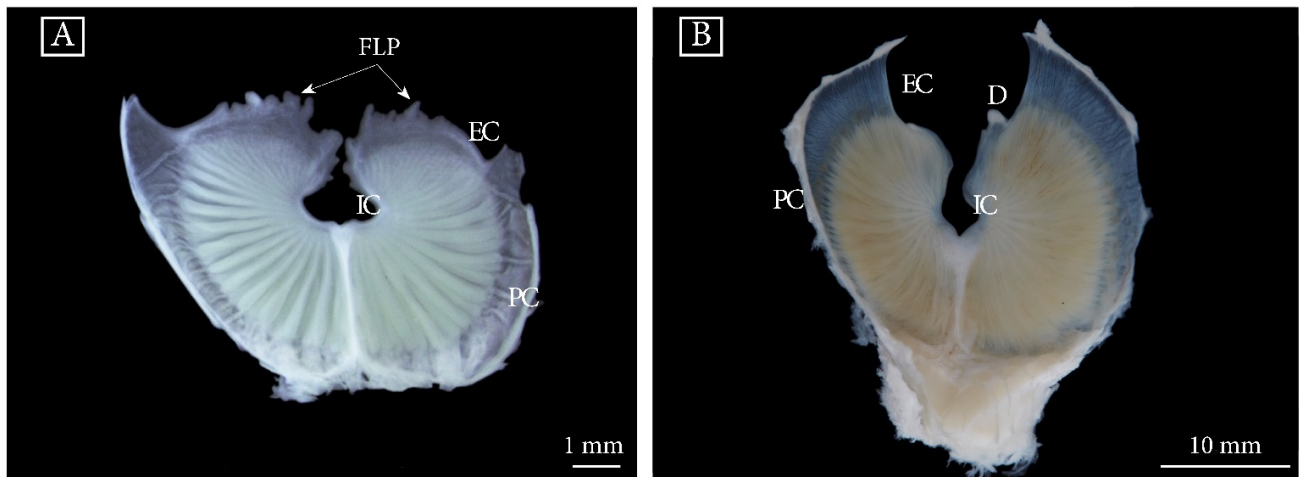
Fig 2.3. Morphology of olfactory lamellae. (**A**) Lamellae of *B. waddi*; (**B**) Lamellae of *I. oxyrinchus*; D: denticles; EC: excurrent channel; FLP: finger-like prolongations; IC: incurrent channel; PC: peripheral channel

2.3.4 Distribution and characteristics of the surface of the sensory and non-sensory epithelium

The distribution of the sensory epithelium across the blind shark lamellae is quite distinct. The epithelium is restricted to a central area of the lamellae, completely covering the secondary folds and its grooves, and it was easily distinguished from the squamous non-sensory epithelium by the presence of numerous cilia arising from supporting cells in the sensory epithelium (Fig 2.4A,C). Olfactory knobs from microvillous olfactory receptor neurons were located mostly near the non-sensory epithelium as swellings covered by microvilli (Fig 2.4E,F). No ciliary olfactory receptor neurons were identified.

Throughout the sensory epithelium, some pore-like structures are observed that appear to be areas where secondary folds are developing (Fig 2.4C). The surface of the non-sensory epithelium displays short microvilli and there is no evidence of cilia arising from supporting cells (Fig 2.4C,I,J). The non-sensory epithelium is restricted to the periphery of the lamellae, including the finger-like prolongations found on the free edges of the lamellae and some isolated non-sensory islets throughout the sensory epithelium (Fig 2.4A, I). In some lamellae, the non-sensory epithelium adjacent to the incurrent channel bears characteristic button-like patterns that may represent points of friction between adjacent lamellae (Fig 2.4J). Goblet cells are sparsely distributed throughout the non-sensory epithelium.

The distinction between sensory and non-sensory epithelium in the mako shark lamellae is not as clearly defined as in the blind shark. The area of the sensory epithelium with the highest density of cilia, as seen in the neuroepithelium of blind shark and all other reported shark species to date, is in the middle of the lamellae and extends slightly further from the secondary folding area into the peripheral channel in some locations (Fig 2.4A,B). However, ciliary supporting cells are also scattered throughout the peripheral channel, decreasing in density away from the secondary folds (Fig 2.4D,H). To the best of our knowledge, this is the first time this phenomenon has been reported; therefore, an attempt was made to determine whether olfactory knobs are present throughout the peripheral channels and whether this epithelium with a lower density of cilia might be sensory in nature. To do this, I first identified the olfactory receptor neurons in the area of the lamellae resembling the neuroepithelium of blind shark (Fig 2.4G). Olfactory knobs are present in clusters towards the bottom of the lamellae as swellings covered by microvilli close to the edge of the lamellae. These olfactory knobs were used as a reference to try to identify any potential olfactory knobs in the peripheral channels, and some dispersed swellings with elongations were identified as potential candidates between the less densely packed cilia (Fig 2.4H,K). These cells are slightly different to the olfactory knobs found elsewhere, and it was difficult to determine whether the cells were covered in microvilli or whether it was instead some type of secretion (Fig 2.4K). Histological examination failed to reveal the presence of any cells with dendrites or axons in the peripheral channels, perhaps due to their sparse distribution. Therefore, we took a conservative approach and considered that the sensory epithelium was restricted to areas with a high abundance of cilia, similar to that observed in the blind shark and other shark species studied previously. However, it is important to note that if further immunohistochemical studies confirm the neuronal nature of these swellings, the sensory surface area of the lamellae of mako may be higher than reported in this study.

The non-sensory epithelium was characterized by the presence of a squamous epithelium bearing microvilli and was restricted to the peripheral channel (ignoring the presence of cilia) and the free edges

of the lamellae (without cilia) (Fig 2.4A,B). Additionally, extensions of non-sensory epithelium were observed on the ridge of most secondary folds next to the incurrent channel. A great number of goblet cells secreting abundant mucus were distributed across the entire surface of the lamellae; however, they appear to be most abundant over the free edges of the lamellae and the non-sensory ridges of the secondary folds. Finally, denticles occur along the borders of the free edges of some lamellae (or only at the inferior tip in some cases) and delimit the excurrent channel of the olfactory organ (Fig 2.4B,L). Denticles were characterized by one triangular cusp and between one and three soft ridges on the crown surface.

Overall, mako shark lamellae had a significantly higher ratio of sensory epithelium area:total lamellae surface area (0.73 ± 0.01) than the blind shark lamellae (0.52 ± 0.02) (beta = 0.34, t= 3.50, p = 0.0248) (Table S2.1). The ratio of sensory surface area within the lamellae appeared to decrease with body length and mass in the blind shark, but not in the mako shark (Fig S2.3). No apparent differences between sex were observed.
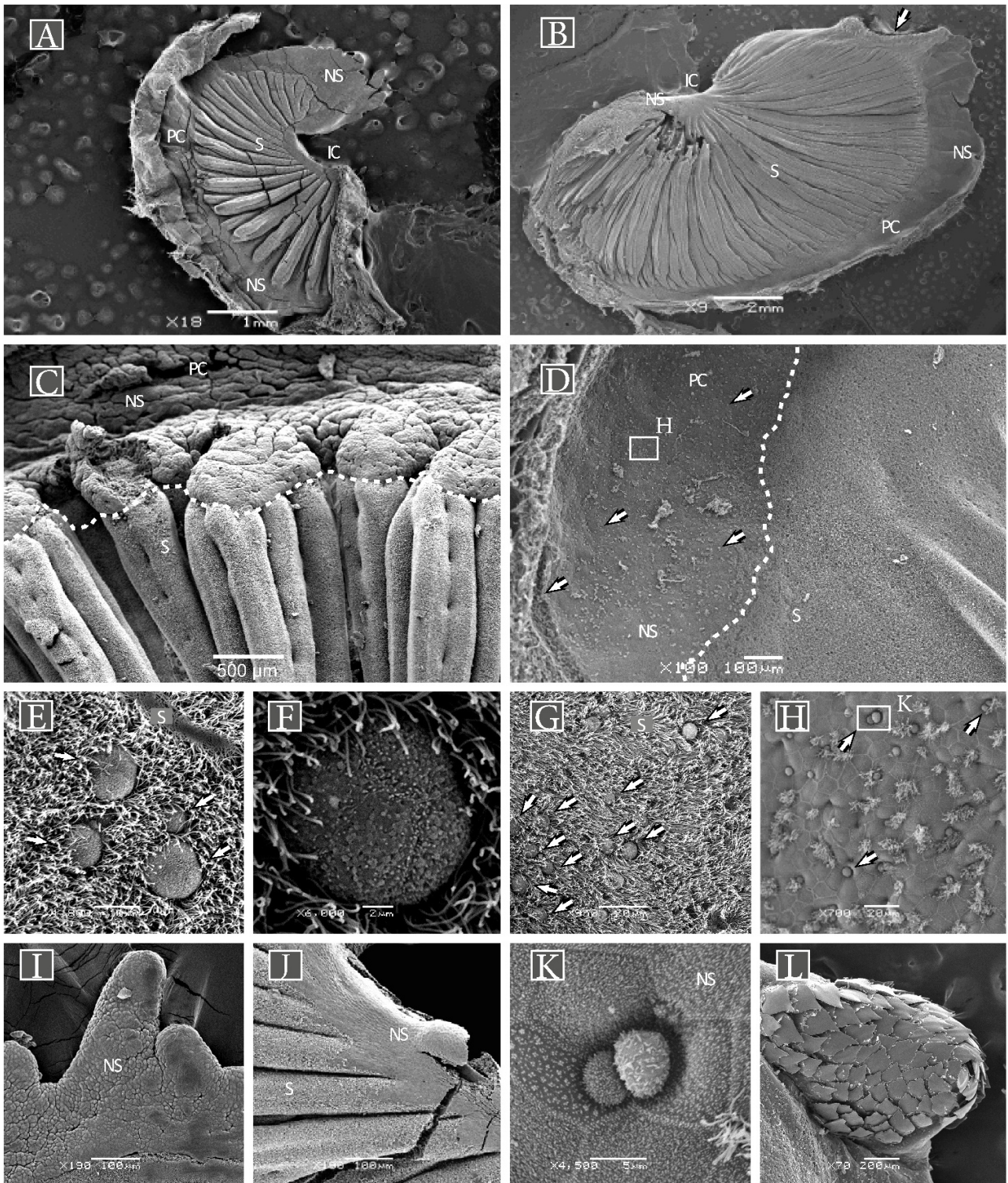
Fig 2.4. Representative scanning electron micrographs of the olfactory lamellae of the blind shark and the mako shark. Blind shark: **(A)** lamellae; **(C)** border between the sensory and non-sensory epithelium (dotted line). Note pore-like structures as secondary folds are developing; **(E-F)** olfactory knobs within the sensory epithelium; **(I)** finger-like prolongations in the free edges of the lamellae; **(J)** non-sensory button like patterns next to the incurrent channel. Mako shark: **(B)** lamellae—note denticles on the free edge of the lamellae (arrow); **(D)** border between the sensory and non-sensory epithelium

17

(dotted line)—note the presence of cilia over the peripheral channel (arrows). Inset: Tentative area picture H was obtained **(G)** olfactory knobs within the sensory epithelium**; (H)** cilia and swellings (arrows) through the non-sensory epithelium. Inset: area picture K was obtained ; **(K)** swellings through the peripheric channel ; **(L)** magnified image of the denticles over the free edge of the lamellae. IC: incurrent channel; PC: peripheral channel S: sensory epithelium; NS: non-sensory epithelium

2.3.5 Degree of secondary folding and histological characteristics of the sensory and non-sensory epithelium

A total of 3390 sections were analysed to determine the degree of secondary folding throughout the lamellae of blind and mako sharks. Unfortunately, some sections were lost during sectioning or staining, and this precluded an analysis of the systematic change in the degree of secondary folding throughout each fragment. However, it may be possible to address this question in the future once the number of missing sections is calculated for each fragment. In any case, the secondary folds are most convoluted towards the middle of each fragment and they decrease in complexity towards the peripheral channels and the raphe. The secondary folds of the blind shark are short, chubby and with few ramifications, whereas the secondary folds of the mako shark are elongated, thin, and possess numerous ramifications (Fig 2.5). In both species, the most elaborate folds are intercalated with short unramified folds. Significant differences in the degree of secondary folding were observed between the different fragment sampling locations across the lamellae in both species. Apical locations (closer to the free edges of the lamellae) have less convoluted secondary folds that become more complex towards the bottom of the lamellae (Fig 2.5). These differences are particularly marked in the blind shark, where the degree of secondary folding increases steadily towards almost the bottom of the lamella (Superior – Superior-Medial: beta = -0.16, t = -6.16, p <0.001; Superior-Medial – Inferior-Medial: beta = -0.13, t = -3.84, p < 0.001; Inferior-Medial – Inferior: beta = -0.04, t = -0.84, p=0.83) (Table S2.2). By contrast, while the degree of secondary folding of the mako increases towards the bottom of the lamellae, the increment in sinuosity was not as marked closer to the middle (Superior – Superior-Medial: beta = -0.26, t = -10.16, p < 0.001; Superior-Medial – Inferior-Medial: beta = -0.08, t = -2.65, p = 0.04; Inferior-Medial – Inferior: beta = -0.01, t = -0.19, p=0.99) (Table S2.2). The increment in the linear length of the lamellae of the secondary folds was significantly higher in the mako shark than in the blind shark (beta = -0.40, t = 6.00, p = 0.039). On average, the increase in surface area was 2.8 times in the mako shark and 1.59 in the blind shark (Table S2.1). However, in the locations where the degree of sinuosity was at its maximum, this increase in surface area was up to 8.41 times more in the mako shark and 3.95 times more in the blind shark. The degree of secondary folding appeared to increase with total body length and mass (Fig S2.4), but, again, no sex differences were apparent.
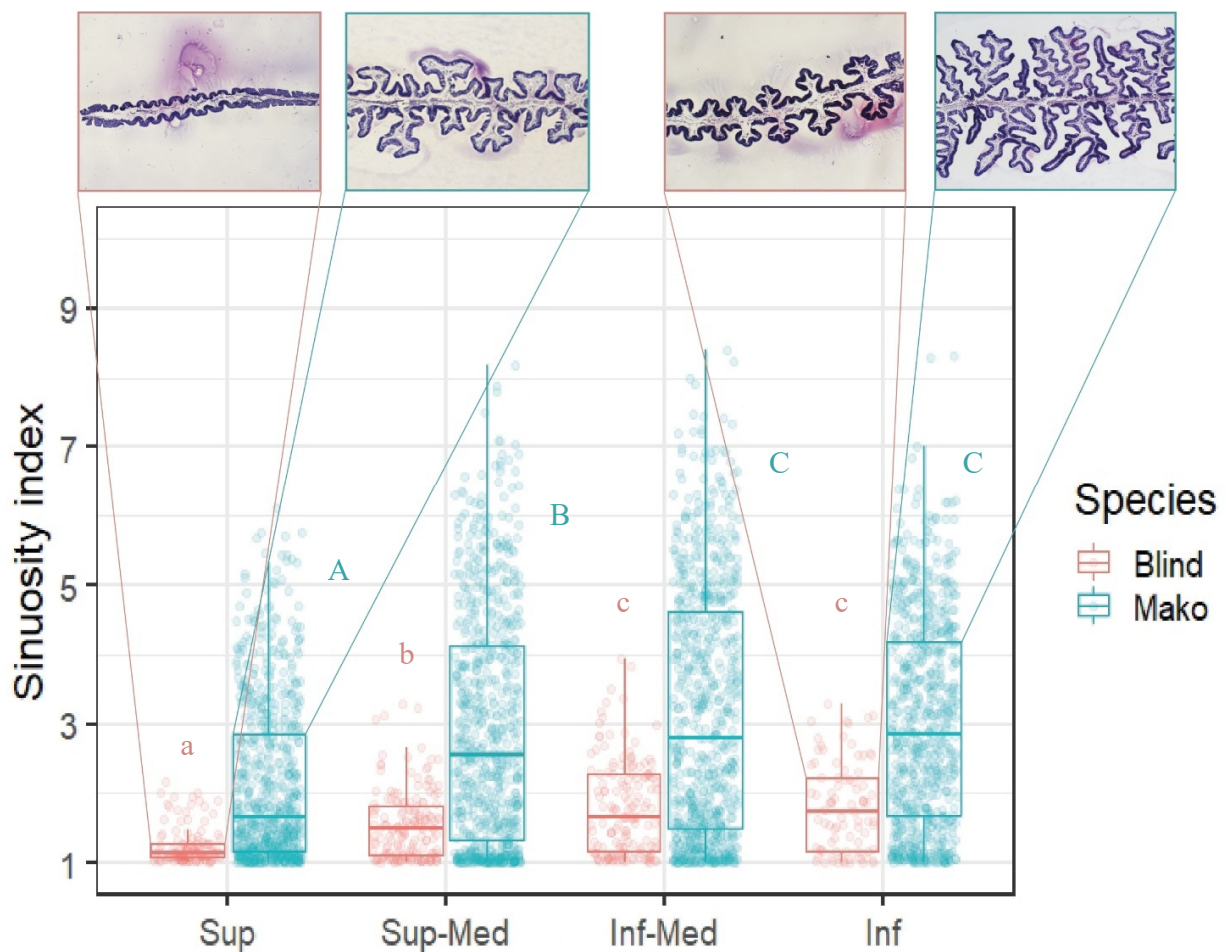
Fig 2.5. Sinuosity index (curvilinear length/straight line length of the lamellae) between species and areas of the lamellae. The degree of secondary folding is higher in the mako shark than the blind shark. Sinuosity index increases towards inferior areas of the lamellae in both species. Letters indicate sinuosity index values that were significantly different from one another. Representative secondary folds from each species for the inferior and superior fragment are provided in the insets as examples. Inf: inferior; Inf-Med: inferior-medial; Sup-Med: superior-medial; Sup: superior. Red: blind shark; blue: mako shark

The transverse sections obtained to characterize the secondary folding also allowed us to inspect the characteristics of the sensory and non-sensory epithelium of both species (Fig 2.6A, B). The sensory epithelium is a ciliated pseudostratified columnar epithelium with olfactory receptor neurons scattered between abundant supporting cells. Supporting cells are the most superficially located within the epithelium and are characterized by the presence of cilia and an oval nucleus. The rounded nuclei of bipolar ORNs are located inferior to the supporting cells, and each receptor cell projects one thin dendrite to the surface of the epithelium and an axon towards the lamina propria. These are the most common ORN cell types observed in both species, and are assumed to be microvillar ORNs, as this is known to be the most common type of ORN in elasmobranchs and resemble those reported in other studies [32,39];

however, we did not manage to visualize the olfactory knobs bearing microvilli that characterize this cell type with this technique.
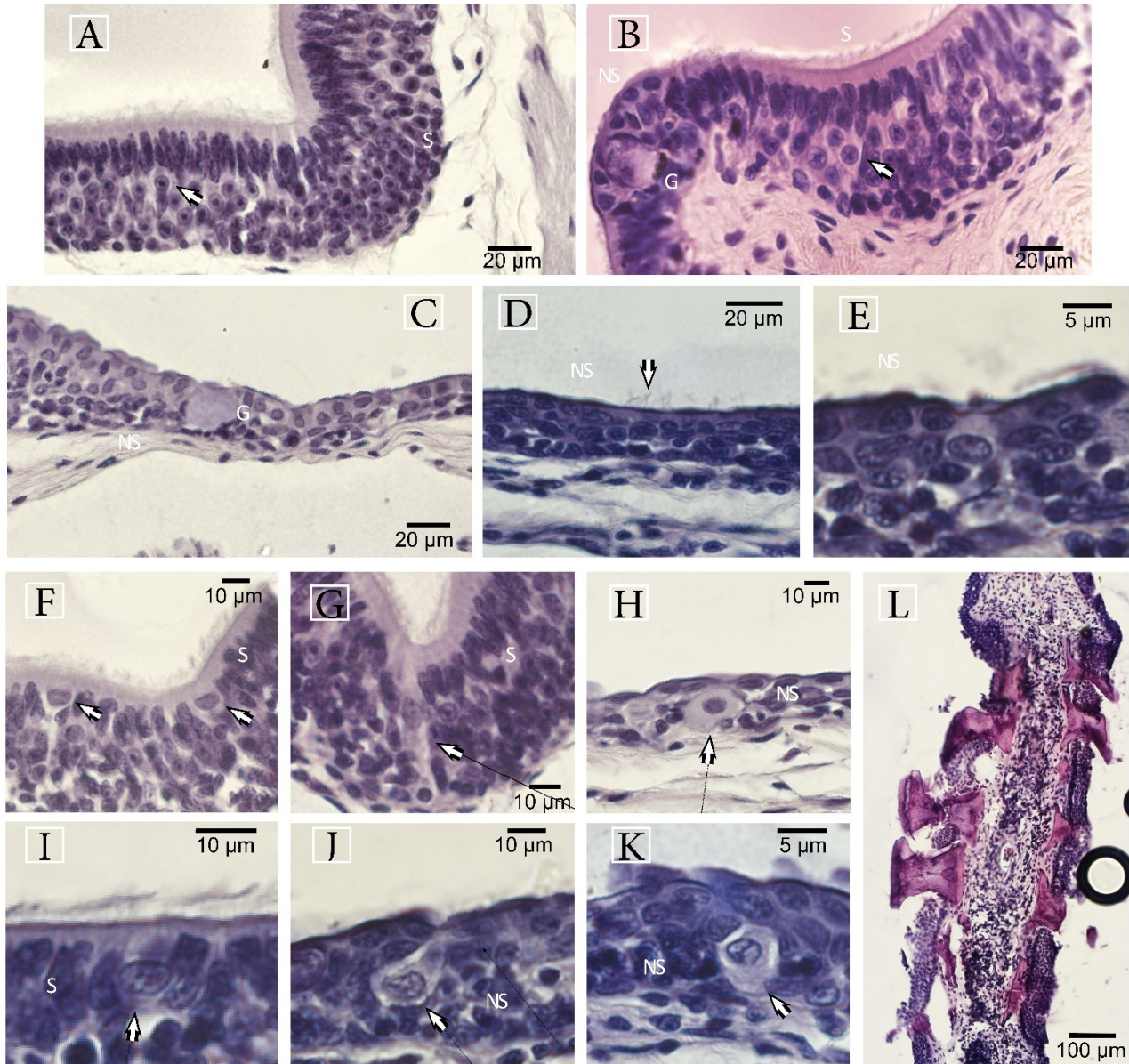
Fig 2.6. Histological sections of blind and mako shark lamellae. (A-B) Sensory epithelium in the blind **(A)** and mako **(B)** shark. Arrows indicate ORN. Note the non-sensory epithelium with a goblet cell on the ridge of the secondary fold of the mako shark; **(C-E)** Non-sensory epithelium in the blind **(C)** and mako shark **(D-E)**. Note the presence of sparse cilia in the mako shark (arrows) and the cell with a clearer colouration in picture E that may be a neuron; **(F, I)** Crypt cells in blind **(F)** and mako shark **(I)**; **(G, J)** Elongated ionocytes in blind **(G)** and mako shark **(J)**; **(H, K)** Rounded ionocytes in blind **(H)** and mako shark **(K)**; **(L)** Transverse section of the denticles on the free edge of a mako shark lamella. G: goblet cell; S: sensory epithelium; NS: non-sensory epithelium.

Crypt olfactory receptor neurons were seen infrequently between the supporting cells in both species (Fig 2.6F, I). These neurons are characterized by a chestnut shape, a wide and clear nucleus restricted to the lower part of the cell, and the presence of a basal projection. In some instances, the crypt of the cells was identified as a dark line on the top of the cell. The non-sensory epithelium is a stratified squamous epithelium of varying thickness with some sparse supporting ciliary cells in the mako shark but none in the blind shark (Fig 2.6C,D,E). Several types of swellings were observed in the non-sensory epithelium of the mako shark; however, there was no indication of an axon, so the neural nature of these cells is unconfirmed (Fig 2.6E). Two other cell types were observed throughout the sensory and non-sensory epithelia: ionocytes and goblet cells. Ionocytes are present as two different morphological types: circular and elongated (Fig 2.6G-K). Goblet cells are particularly abundant in the mako shark, especially on the ridges of the secondary folds and at the free edges of the lamellae (Fig 2.6B), whereas in the blind shark they are restricted mostly to the non-sensory epithelium (Fig 2.6C). Beneath both the sensory and non-sensory epithelia, the lamina propia is characterized by the presence of collagen, fibroblast-like cells, blood capillaries and nerve fibres comprising axons traversing the basal lamina.

2.3.6 Comparison between measurements

For all measurements, the surface area of the olfactory organ was significantly higher in the mako shark than in the blind shark (Table 2.1) (Gross surface area, GSA: beta = -2.16, t = -4.85, p = 0.01; Sensory surface area, SSA: beta = -2.50, t = -5.19, p < 0.01; Surface area with maximum sinuosity, SAMS: beta = -3.16, t = -6.58, p < 0.01; Total surface area with mean sinuosity, TSA-SF: beta = -2.74, t = -5.70, p < 0.01; Total sensory surface area TSSA-SF: beta = -3.09, t = -6.42, p < 0.01). Significant differences were also observed between species when the total sensory surface area was normalized by the total length of the sharks (beta = -1.30, t = 7.99, p = 0.01).

Table 2.1. Comparison of estimates of olfactory organ surface area considering different traits of the lamellae.

Species	Gross surface Area (GSA)	Sensory surface Area (SSA)	Surface area with maximum sinuosity (SAMS)	Total surface area with mean sinuosity (TSA-SF)	Total sensory surface area (TSSA-SF)	Total sensory surface area per cm body length
B. waddi	[a] 56.71 ± 30.05	[b] 27.78 ± 11.62	[c] 153.72 ± 96.65	[d] 92.20 ± 54.93	[a] 44.77 ± 22.76	[e] 0.92 ± 0.10
I. oxyrinchus	[A] 441.06 ± 125.79	[A] 323.82 ± 97.11	[C] 3110.45 ± 1257.76	[D] 1242.86 ± 434.18	[D] 912.78 ± 333.38	[E] 3.45 ± 0.88

Values are mean ± 1 std. dev. and in units of cm². Letters indicate estimates that were significantly different from one another. Darker shades indicate significantly higher values. Orange: blind shark; blue: mako shark.

Statistical analysis revealed that several measurements obtained for each species were significantly different from each other (Table 2.1, Table S2.3). The specific pairs of measurements that were significantly different from each other varied between species. For the blind shark, the gross surface area (GSA) was not statistically different to the total sensory surface area (TSSA-SF). For the mako shark, neither the gross surface area (GSA) was significantly different to the sensory surface area (SSA) nor the surface area with mean sinuosity (TSA-SF) to the total sensory surface area (TSSA-SF). The surface area of the olfactory organs increased with the length and the weight of the shark for all the measurements (Fig 2.7)
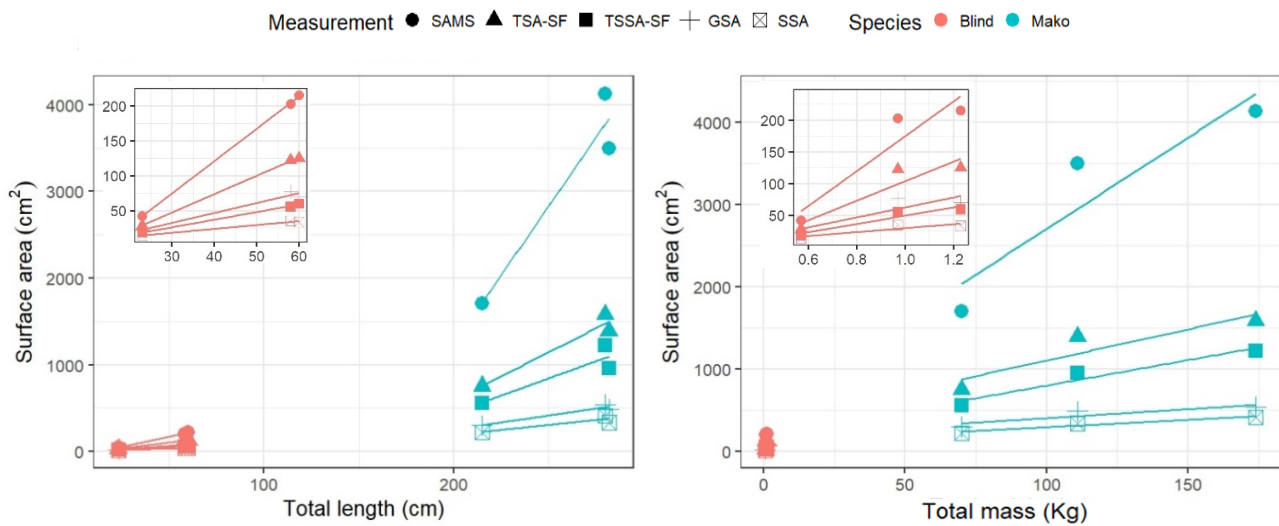
Fig 2.7. Surface area of the olfactory organs of *B. waddi* and *I. oxyrinchus* accounting for different traits of the lamellae. Each data point represents one individual. Insets: enlarged view of blind shark values. **Left panel**: Total sensory surface area in relation to the total length of the shark. Regression coefficients in Table S2.4. **Right panel**: Total sensory surface area in relation to the total mass of the shark. Regression coefficients in Table S2.4. *GSA: Gross surface area; SAMS: surface area with maximum sinuosity; SSA: Sensory surface area.; TSA-SF: total surface area with mean sinuosity; TSSA-SF: total sensory surface area with the mean sinuosity and the proportion of sensory epithelium*

2.4 Discussion

The olfactory organs of sharks display a wide morphological diversity that is thought to be associated with the ecological needs of each species. Previous studies have reported differences in the surface area of the olfactory organ by assessing some of its morphological traits, such as the number of lamellae, their

surface area, the distribution of sensory epithelium, and the degree of secondary folding [24,32,33,35–37]. However, no study to date has attempted to comprehensively characterize how these traits change with respect to one another and, therefore, estimate more accurately the total available sensory surface area of the olfactory rosette of different species of sharks. In this study, we used a multidisciplinary approach to better estimate the total sensory surface area of the olfactory organs of two shark species by characterizing simultaneously the distribution of the sensory epithelium and the degree of secondary folding of their olfactory lamellae. We found that the lamellar surface area, the extent of the sensory epithelium and the degree of secondary folding is higher in the mako shark than in the blind shark, significantly modifying the available total sensory surface area of the olfactory organ despite a lower lamellar count in the mako shark. We also found that the degree of secondary folding significantly decreases towards the free edges of the lamellae in both species, highlighting the need to sample several locations across the lamellae to avoid overestimating the contribution of the secondary folds to the total surface area of the lamellae. We conclude that the consideration of these different sources of variation when comparing the surface area of the olfactory organs of elasmobranchs increases the confidence with which evolutionary or ecological comparisons can be made across species. The very few species examined in this study preclude us from making general assumptions, but we hypothesize that the differences observed in the total sensory surface area are driven by a trade-off between the hydrodynamics of the water flow of the olfactory organ and the olfactory thresholds of each species. Given space limitations of this thesis, this will be discussed in more detail in Chapter 4, where we synthesise these results with those of the molecular studies detailed in Chapter 3, and here we will just focus on how the different traits of the lamellae contribute to the total sensory surface area of the olfactory organ.

The differences observed in the total sensory surface area of the olfactory organs of the mako and blind shark when accounting simultaneously for the distribution of sensory epithelium and the degree of secondary folding are still congruent with the huge variation in surface area observed in other studies. Whereas the absence of individuals of intermediate size precluded us from testing for differences in total sensory surface area accounting for total body length or mass, the higher ratio of sensory epithelium and the increased degree of secondary folding suggests that the mako shark—a pelagic species—has a relatively higher total olfactory sensory surface area compared to the blind shark—a benthic species—regardless of size. Indeed, the mean total sensory surface area divided by the mean total body length of each species (in this study) appears to suggest that the mako shark has approximately 2 cm^2 more surface area per centimetre of body length compared to the blind shark (Table 2.1). This difference in the

extension of the olfactory organs may be further enhanced if the neural nature of the unusual swellings found through the peripheral channels of the mako shark is confirmed, which would effectively increase the proportion of sensory epithelium of this species (Fig. 2.4H). However, note that normalizing the surface area of the olfactory organ by the total length of the sharks has its own caveats as it assumes that the surface area of the olfactory organ grows proportionately with body length rather than with some other type of allometry, as has been seen in other studies [24,33,36,37]. Specifically, we saw some evidence of the proportion of sensory epithelium to decrease with the body length and mass in blind shark and the sinuosity index to increase with body length and mass in both species (Fig. S2.3, 2.4). Therefore, further studies that include more intermediate-sized individuals and different species are required to examine how these morphological traits change with size between species and ontogeny.

The results of this study suggest that different shark species rely on different strategies to reach the total sensory surface area that characterizes their olfactory organs, which in turn may be subjected to independent selective pressures or phylogenetic dependence. For instance, the number of lamellae in the olfactory organ of the mako shark (57), which is quite low compared to other pelagic species [32,49,84] (Fig. S2.5), appears to be compensated for by having larger lamellae, a higher proportion of sensory epithelium, and highly convoluted secondary folds. Perhaps, the number of lamellae of the olfactory organs of the mako shark is restricted by the size and shape of the olfactory cavity. The sharply tapered snout of the mako shark is thought to be an adaptation to streamline its body so as to reduce drag, allowing makos to reach peak speeds of up to 100 km/h [85,86]. Therefore, any benefits of enlarging the olfactory cavity to accommodate more lamellae might be traded-off with losses in hydrodynamic performance associated with a wider snout. Interestingly, the white shark *Carcharodon carcharias* – a close relative of the mako shark - has a higher number of lamellae (81) [84], a wider snout [85], and lower reported burst speeds than the mako shark [87]. In contrast, the number of lamellae in the blind shark is the same as the brownbanded bamboo shark *Chiloscyllium punctatum* (84), which is considerably higher in comparison to other closely related species, such as wobbegong sharks *Orectolobus* spp (40 – 56) or the nurse shark *Nebrius ferrugineus* (72), but lower than in the zebra shark *Stegostoma fasciatum* (105) [32,37,49,84] (Fig. S2.5). In this case, the presence and morphology of nasoral groves that allow some species to ventilate the olfactory organs through the oral pump may have shaped some of the morphological characteristics of their olfactory lamellae. Unfortunately, similarly to the mako and white shark, it is unknown whether the size, the ratio of sensory epithelium or the sinuosity index of the lamellae of orectolobiformes may vary, leading to relatively similar extensions of the olfactory organs despite differences in the lamellar count.

Previous studies have also suggested the elaboration of other traits to overcome reductions in the total surface area of the lamellae due to morphological constraints. For instance, in hammerheads, it has been suggested that the higher lamellar counts of the family Sphyrnidae may have arisen as a compensatory mechanism for the reduced area of the individual lamellae that results from their characteristic dorsoventrally compressed head [36]. Similarly, phylogenetic analysis of the number of the lamellae and the degree of secondary folding in 14 species of elasmobranchs appears to indicate that, at least in some species, a low degree of secondary folding is accompanied by a higher number of lamellae which suggests that these two traits may be used alternatively as two different strategies to increase the surface area of their olfactory organs [35]. While the sensory surface area of the olfactory organs has been measured in other shark species before [32,37], the ratio of sensory epithelium of each species has never been reported, so it is unclear whether the distribution of sensory epithelium may vary with the number and/or size of the lamellae. As the structural complexity of the olfactory organ and the lamellae of more elasmobranch species is characterized, a more solid understanding of the patterns of co-evolution of these traits will be achieved. This may provide new insights to confirm the specific selective pressures driving these adaptations and their effect on the perception of odours in cartilaginous fishes.

Through this study, we also observed that a decrease in secondary folding towards the free edges of the lamellae is a common characteristic of the olfactory lamellae of sharks that has not previously been quantified. Even though the degree of secondary folding differed markedly between the blind and mako shark, both species displayed the most convoluted secondary folds at the inferior parts of the lamellae, which decreased in complexity towards the free edges at different rates in each species (Fig. 2.5, Table S2.2). Examination of micrographs of the complete lamellae of other elasmobranch species shows that this characteristic is also shared by several other shark and ray species [37,67,71,75]. Given that the most sinuous area of the lamella is located where the incurrent water flow is likely to be directed—i.e. at the entry point of the incurrent channel—it is possible that this trait is used as a strategy to canalize and decrease the speed of the water flow. This observation and others reported in this study, such as the presence of denticles tapering the excurrent channels of the mako shark, appears to indicate that control of the water flowing through the olfactory organs may be an important factor driving adaptations of the olfactory lamellae of elasmobranchs. Further studies should aim to characterize the hydrodynamic properties of the water flowing through the olfactory organs in relation to the morphological characteristics considered in this study, as well as other factors such as the diameter/cross-sectional profile and total length of the different channels that made up the circuit that the water flows through.

Finally, interspecific variability in lamellar morphology means that each trait contributes differently to the total sensory surface area of the olfactory organs, highlighting the need to exhaustively consider all these different morphological traits to accurately estimate and compare the 'extension' of the olfactory organs between shark species. For instance, the lower proportion of sensory epithelium in blind shark lamellae significantly decreases the available sensory surface area of the olfactory organ (i.e. there is a significant difference between the gross surface area estimate—GSA—and the estimate that considers the distribution of sensory epithelium—SSA), whereas this is not the case for the mako shark due to their broader distribution of sensory epithelium of their lamellae (Table 2.1, Fig. 2.7, Table S2.1, Table S2.3). Similarly, because the proportion of sensory epithelium in the blind shark is around 50% of the total surface area of the lamellae, it effectively counteracts the increase in surface area of around 1.5 when considering the secondary folds (i.e. there is not a significant difference between the gross surface area estimate—GSA—and the estimate that considers the ratio of sensory surface area and the degree of secondary folding—TSSA-SF). Therefore, studies that may not consider the distribution of sensory epithelium may highly overestimate the available olfactory sensory surface area of some species, which may leave unnoticed trends that could help to explain the different extensions of the olfactory organs of sharks. Moreover, estimating the degree of secondary folding using measurements made only where the sinuosity of the folds is at its maximum (SAMS) significantly overestimates the available surface area differently in each species (Table 2.1, Fig. 2.7, Table S2.3). For instance, the estimate of surface area using only the sections that show the highest degree of secondary folding (SAMS) is 2.5 times higher than the estimate that considers the differences in sinuosity through the lamellae (TSA-SF) in the mako shark, whereas this value is only 1.6 times higher in the blind shark. In consequence, when the olfactory surface area is compared between species, differences are exaggerated when SAMS is used (20 times more extensive surface area in the mako shark in comparison to the blind shark) in comparison to TSA-SF (13 times more extensive surface area in the mako shark in comparison to the blind shark). Given the extensive dataset obtained in this study, it may be possible to generate a model that is able to predict the total sensory surface area accounting for the variation of the secondary folds with a smaller set of measurements, so that a higher number of species and lamellae through the olfactory organ can be assessed. Alternatively, technologies such as micro-CT or nano-CT may provide a faster and more reliable way to obtain such measurements of the organ *in situ*.

Chapter 3 – Molecular Characteristics of the Olfactory Organ of Sharks

3.1 Introduction

Behavioural and anatomical studies have suggested that some shark species rely more heavily than others on olfaction for their survival, but the mechanisms and selective pressures driving these differences are still unclear [20,32,34]. In the past, morphological traits have mostly been used to infer the olfactory capabilities of sharks, especially for species that are difficult to observe in the wild or to test in captivity [32–34,36,37,39,41,42,88]. The two most popular anatomical proxies that have been used are 1) the total sensory surface area of the peripheral olfactory organs (the olfactory rosettes) [32,33,36,37,39], and 2) the relative volume of the primary centres of olfactory processing in the brain (the olfactory bulbs) [34,41,42,88]. The former relies on the assumption that the greater the sensory surface area, the more olfactory receptors will be available to detect odorants in the incurrent water flow; the latter states that a larger olfactory bulb indicates more extensive processing of neural signals and an increased reliance on olfactory information. However, the reliability of these two traits as robust indicators of the olfactory capabilities of sharks remains an open question. For instance, whereas the effect of the relative size of the olfactory bulb on the olfactory capabilities of different shark species has never been assessed, electrophysiological experiments have shown that interspecific differences in the olfactory surface area do not necessarily reflect differences in absolute sensitivity (i.e. detection thresholds) to amino acid-based odorants in several coastal elasmobranchs [24]. Unfortunately, like behavioural studies, electrophysiological tests of olfactory ability are usually restricted to a finite number of odorants that can be tested in a specific set of small and generally benthic or benthopelagic species that are amenable to laboratory studies, which does not permit a broader comparative approach.

Molecular approaches provide an exciting new opportunity to explore the evolution and adaptive radiation of the olfactory system of sharks by identifying the set of olfactory receptors different species use for the perception of relevant odorants in their environments. Olfactory receptors are a type of G-protein-coupled receptor found on the surface of olfactory receptor neurons (ORNs) in the peripheral olfactory organs of vertebrates [58]. These metabotropic receptors are activated when an odorant (ligand) binds to the extracellular domain and, through an intracellular messenger, generates an electrical signal in the receptor cell that is transmitted to the brain [59,89]. Vertebrate olfactory receptors are classified into four canonical gene families: odorant receptors (OR), trace-amine receptors (TAAR), vomeronasal receptors type 1 (V1R or ORA in fish), vomeronasal receptors type 2 (V2R or OlfC in fish) [15,58]. As

each olfactory receptor is activated by a specific set of substances, each olfactory receptor family has undergone considerable lineage-specific expansions and reductions to better adapt organisms to detect useful olfactory cues in their surroundings [63,90–94]. For example, several marine mammals and sea snakes have experienced a substantial depletion of their olfactory receptor repertoire as their olfactory system, originally adapted to detect a broad range of air-borne volatile substances, became less relevant with the transition from land to water [60,95]. Similarly, fish species that release olfactory alarm cues when their skin is damaged to alert conspecifics to the potential of a predator attack have a higher number of V2R receptors than species that do not use this type of anti-predatory mechanism [62]. Consequently, the number and type of olfactory receptors of different species have been extensively used as a proxy of olfactory capabilities in several studies [60,61,63,64,66,96]. Accordingly, we might also expect that species of sharks that rely more heavily on their sense of smell may have an expanded olfactory receptor repertoire to help them identify a wider range of substances compared to species that rely more on other senses such as vision or electroreception.

Currently, there is insufficient information about the olfactory receptor repertoires of chondrichthyans (sharks, rays and chimaeras) to allow a meaningful comparison in relation to the phylogeny and life history of different species. Previous genomic studies have reported the number of olfactory receptor genes in some species; however, the methodology used to search for olfactory receptor genes differs, leading to substantial differences in the number of receptors reported for even the same species. For example, the number of olfactory receptors reported in the elephant shark *Callorhinchus mili,* varies between 43 in Venkatesh et al. 2014 [97], three in Hara et al. 2018 [98], 11 in Marra et al. 2019 [99] to 53 in Sharma et al. 2019 [100]. These differences suggest some of these reported repertoires may be incomplete due to either differences in the gene families being examined or the use of generic databases such as Blast2Go or SwissProt instead of using specific chemoreceptor annotation protocols [101]. The elephant shark (a chimaera) and the catshark *Scyliorhinus canicula* (a selachian) are the only two species whose complete repertoire has potentially been identified (i.e. four canonical olfactory receptor gene families examined using chemoreceptor annotation protocols) [100]. However, whereas differences in the number and composition of their olfactory receptor repertoires were observed, it is unclear whether the olfactory receptor repertoire of cartilaginous fishes may also differ between species at shorter time scales, as these two groups diverged around 420 million years ago [102].

Furthermore, the expression pattern of the complete olfactory receptor repertoire of cartilaginous fishes has never been explored. This is relevant for two main reasons. Firstly, not all olfactory receptors are involved in the perception of odorants as they are not all expressed in olfactory tissue [103,104]. For

example, the TAAR1 receptor gene is not expressed in the olfactory epithelium of vertebrates and is used instead for the detection of brain-derived amine neurotransmitters [103]. Specifically for cartilaginous fishes, it is essential to confirm the expression pattern of OR and TAAR receptors on olfactory tissue as despite being found in the genomes of all chondrichthyan species studied to date [97,99,100], immunohistochemical studies have failed to label any of the G-protein subunits typically coupled to OR and TAAR receptors [105–107]. Secondly, in the sensory olfactory epithelium of mice *Mus musculus* and zebrafish *Danio rerio,* the density of ORNs is highly correlated with the abundance of mRNA transcripts of a given olfactory receptor type [65]. Thus, although the sensitivity to a given odorant may be determined by other factors such as receptor specificity and convergence ratio of receptor neurons to mitral cells [14,53–57], differences in the expression of olfactory receptor gene families by different shark species may provide insights into the relative importance of certain olfactory receptors for the ecology of a given shark species.

In this study, we identified, characterized, and quantified the olfactory receptor genes expressed in the olfactory organs of two shark species with contrasting lifestyles to determine whether their expressed olfactory receptor repertoire may help to identify differences in their olfactory capabilities. To do this, we extracted, isolated and sequenced the mRNA of the olfactory rosette of the blind shark (*Brachaelurus waddi*) and the mako shark (*Isurus oxyrhincus*) and we assembled the first *de novo* transcriptome of the olfactory organs of each species. Next, we identified and quantified the olfactory receptors being expressed by searching against both generic databases (blastnr and blastnt) and phylogenetically validated olfactory receptor queries from the literature. Finally, we estimated the phylogenetic relationships of the olfactory receptors identified in this and other studies constructing maximum likelihood phylogenetic trees to better understand the evolutionary dynamics of these gene families in chondrichthyans. Results of this study indicate that the expressed olfactory receptor repertoire varies between species, with the blind shark having a more extensive receptor repertoire than the mako shark. Due to space limitations of this thesis and to avoid repetition, whether these differences are due to phylogenetic relationships or environmental adaptation and how they may specifically affect the olfactory capabilities of these species will be discussed in more detail in Chapter 4 in relation to the findings already presented in Chapter 2. Moreover, we did not detect any TAAR full transcripts in any of the species, providing new insights into the basic functioning of the olfactory system of cartilaginous fishes. Overall, this study indicates that RNA-seq techniques may be an accessible, efficient and necessary tool that in combination with genomic studies may help us understand the evolution of the

olfactory receptor repertoire of cartilaginous fishes and its potential effect on the olfactory capabilities of different species.

3.2 Materials and Methods

3.2.1 Tissue collection

Blind sharks (n=3) and shortfin mako sharks (n=3) were obtained as indicated in the Materials and Methods section of Chapter 2. One of the two olfactory organs from each shark was selected arbitrarily, dissected out, and stored in RNAlater (Thermo Fisher Scientific, Waltham, USA) (Table S3.1). The period since the death of the animal to the extraction of the olfactory organs ranged from <5 minutes to a maximum of 5 hours. Samples were stored at 4°C overnight to allow penetration of the RNAlater before being transferred to –30°C for long-term storage. Samples were kept between 2 days to up to 16 months before being processed and sequenced in two different batches, as indicated in Table S3.1.

3.2.2 RNA isolation, library preparation and Illumina sequencing

Total RNA was isolated from the whole olfactory organ of blind sharks and from randomly selected pieces across the entire olfactory organ of mako sharks (around one gram of tissue per olfactory organ for both species). We were unable to extract the RNA of the whole olfactory organ in the mako shark due to its large size (~20 grams), whereas the smaller size of the olfactory organ of the blind shark (~1 gram) allowed us to extract the RNA of their whole olfactory organs using the largest reasonable amount of tissue for extracting nucleic acids with TRizol reagent (~1 gram). For RNA isolation, the tissue was homogenized using a stator-rotor type homogenizer (with a disposable tip to prevent cross-contamination) in TRIzol reagent (Invitrogen, Carlsbad, USA) and RNA was purified with Purelink RNA Mini Kit (Ambion, Carlsbad, USA) following the spin column purification method according to the manufacturer´s instructions. The concentration and the purity of the extracted RNA were checked by spectrophotometry using either a NanoDrop One (Thermo Fisher Scientific, Waltham, USA) or an Epock Take3 spectrophotometer (BioTek, Vermont, USA).

RNA samples were submitted to the Ramaciotti Centre for Genomics (UNSW Sydney). The integrity and intactness of the RNA were assessed using an TapeStation System (Agilent, California, USA). Strand-specific libraries were prepared with an average insert size of 350bp using an Illumina Truseq stranded mRNA library prep kit for our first batch and an Illumina stranded mRNA ligation prep for our second batch. Sequencing was performed on an Illumina NextSeq 500 (Illumina, California, USA) with a read length of 2×75bp following standard Illumina protocols for paired-end high output sequencing.

Readers that may not be familiar with the molecular methods and bioinformatic steps indicated in this and the following sections are invited to consult the following references for a thoughtful introductory review of RNA-seq techniques [108,109].

3.2.3 Data pre-processing

Quality of raw and subsequently filtered reads was assessed using MultiQC v1.0 dev0 [110]. First, rRNA was removed from our raw reads using SortMeRNA v4.2.0 [111] by filtering based on the default databases that included 5S for archaea, bacteria and eukarya, 16S and 23S for archaea and bacteria, and 5.8S, 18S and 28S for eukarya. When one of our paired-reads was identified as a potential rRNA, both reads were discarded to keep our sequences paired-ended. Then, adapters were removed from our mRNA reads before they were quality trimmed using Trimmomatic v0.39 [112] with default parameters as implemented in Trinity v2.5.1.

3.2.4 De novo transcriptome assembly, completeness of the assemblies and gene quantification

The *de novo* assembly for each species was performed using Trinity v2.5.1, using processed high-quality reads, with default parameters [113]. The quality and completeness of each assembly was assessed by two methods. First, we determined the proportion of reads for all replicates mapping back to their respective assemblies using the bowtie2 functionality in Trinity. Second, we examined the number of conserved vertebrate single-copy orthologs using BUSCO v4.1.2 [114] using a total of 2254 BUSCO groups on the server usegalaxy.org.au [115]. Gene expression for each sample was then quantified using RNA-Seq by Expectation-Maximization (RSEM) as implemented within Trinity [116]. To test whether any of the gene families are enriched, the total TPM obtained for each receptor family was normalized for its receptor gene number in each species. Statistical tests on transcript abundance were performed using a similar approach as Chapter 2 using generalized linear mixed models after log-transforming the raw and normalized abundance of transcripts to meet normality and homoscedasticity of residuals. For the constructed models, species, receptor type and the interaction between both variables were set as fixed effects and individual as a random effect.

3.2.5 Functional characterization of olfactory receptors within the transcriptome

The assembled contigs were annotated based on similarity searches against the latest release of the NCBI nucleotide (nt) and non-redundant protein (nr) databases using BLASTn v2.7.1+ [117] and Diamond v0.9.13 [118] respectively with an e-value threshold of 1e-05 to identify positive matches. The identified transcripts were filtered to extract all annotated olfactory receptors with the following queries: chemosensory, olfactory, odorant, trace-amine and vomeronasal. We also ran Diamond v0.9.29.130 in

the usegalaxy.org.au server [115] with a custom made database of vertebrate olfactory receptors and the same parameters as indicated before to further detect any potential olfactory receptor that may not have been labelled as such with the previously mentioned databases. Amino acid sequences used as queries were obtained from the following studies: OR [119], TAAR [120], V1R from fish [121] and tetrapods [91] and V2R from fish [122,123] and tetrapods [91]. A total of 2980 OR, 226 TAAR, 239 V1R and 522 V2R were used as queries.

Transcripts with a positive match were translated into amino acid sequences with TransDecoder v.0.39 using homology searches with the latest release of the protein database Uniref90 to predict the most likely coding regions [124]. Any translated protein with less than 170 residues for potential OR, TAAR and V1R transcripts and 200 residues for V2R were removed to ensure the minimum sequence length for each olfactory receptor gene family was warranted. Then, sequences of the same olfactory receptor family were aligned with representative and outgroup sequences to construct phylogenetic trees to confirm the identity of the translated amino acid transcripts as olfactory receptors. Representative vertebrate olfactory receptor sequences categorised in previous studies were selected to recreate the clades presented in their phylogenies [91,119–121,123]. Additional protein sequences from frog, zebrafish, and mouse were retrieved from the databases SwissProt and NCBI nr databases to ensure robust clades of homologous genes were created to classify the newly identified blind and mako shark transcripts. Outgroup sequences for each gene family included: for OR, one adenosine receptor, two adrenergic receptors, one galanin receptor, one histamine receptor, three serotonin receptors and one somatostatin receptor; for TAAR, four adrenergic receptors, five dopamine receptors, five histamine receptors, five hydroxytryptamine receptors and seven rhodopsin receptors; for V1R, 17 taste receptor type 2; for V2R, five metabotropic glutamate receptors, eight taste receptors type 1 and six calcium-sensing receptors. The representative sequences and outgroups for each gene family are provided in FASTA format in Supplementary Electronic Material 1. Sequences were aligned using MAFFT v.7.471 with the L-INS-i strategy and default parameters. Trees were calculated using a Maximum Likelihood Method with IQ-Tree v.2.0.3 using a bootstrap value of 1000 and the ModelFinder functionality as default to ensure the right substitution model was chosen [125,126]. Transcripts were identified as confirmed olfactory receptors when they clustered within one of the olfactory receptor clades with branch support greater than 70%.

3.2.6 Final phylogenetic trees

The amino acid sequences of the olfactory receptors identified with the olfactory receptor database that passed phylogenetic validation were used for the construction of the final phylogenetic trees. We did not

include the olfactory receptors identified using the nt and the nr databases for two reasons: First, some of the transcripts annotated were not accurately identified as olfactory receptors as they showed more similarity with the outgroup clusters during preliminary phylogenetic analyses. Second, all transcripts annotated as olfactory receptors with the nt and nr database were also present when we used our olfactory receptor database if they were longer than 170 residuals for OR, TAAR and V1R and 200 residuals for V2R, and they clustered with one of the olfactory receptor clades in the phylogenetic trees. To contextualize these newly identified olfactory receptors in the light of the evolution of olfactory receptors in chondrichthyans, previously reported olfactory receptor sequences from cartilaginous fishes were extracted from the following studies: the elephant shark *Callorhinchus milii* and the small-spotted catshark *Scyliorhinus canicula* (OR, TAAR, V1R, V2R) [100]; the white shark *Carcharodon carcharias* (OR, TAAR, V1R, V2R) [99]; and the brown-banded bamboo shark *Chiloscyllium punctatum*, the whale shark *Rhincodon typus* and the cloudy catshark *Scyliorhinus torazame* (OR) [98]. For the latter study, nucleotide sequences were translated into amino acid sequences using TransDecoder. Any sequences with fewer residues than the minimum length used in this study were removed to maintain standardization. Sequences were aligned and the phylogenetic trees were drawn following an identical approach to that of the previous section and including the same representatives and outgroups (Supplementary Electronic Material 1). Trees were drawn using iTOL server [127]. Those olfactory receptors newly identified in this study were named according to their closest ortholog/paralog, and their amino acid sequence is provided in Supplementary Electronic Material 2. Alignments are provided in Supplementary Electronic Material 3. Final phylogenetic trees in Newick format are provided as Supplementary Electronic Material 4.

3.3 Results

3.3.1 RNA sequencing and pre-processing of reads

A mean of 37,039,694 and 33,566,748 paired reads per sample were generated from the olfactory organs of blind shark and mako shark, respectively. After rRNA removal and filtering of low-quality reads, the mean number of paired reads that were used for subsequent analysis were 36,483,993 for the blind shark and 33,065,032 for the mako shark with a fragment size between 25 and 76 base pairs (Table 3.1). The GC percentage of these clean reads were around 45% which is common for nucleic genetic material and indicated a correct filtration of any potential rRNA contamination.

Table 3.1. Number of raw, mRNA-only (rRNA removed) and quality filtered reads for each individual of this study. Fragment length, GC content and batch number are provided for each sample.

	Individual	Raw reads	rRNA free reads	Quality filtered Reads	Fragment Length	GC (%)	Batch
Blind	1	38,160,750	37,587,837	37,575,883	25-76	43	1
	2	41,553,722	40,834,205	40,820,472	25-76	43	1
	3	31,404,610	31,061,333	31,055,624	25-75	44	2
	Total	**111,119,082**	**109,483,375**	**109,451,979**	**25-76**	**43**	
Mako	1	35,943,252	35,038,488	35,028,087	25-76	42	1
	2	30,471,679	30,232,941	30,217,845	25-75	45	2
	3	34,285,313	33,961,862	33,949,165	25-75	45	2
	Total	**100,700,244**	**99,233,291**	**99,195,097**	25-76	**44**	

3.3.2 De novo transcriptome assembly and completeness of assemblies

The transcriptome of the olfactory organs of each species was assembled combining the reads of three biological replicates (Table 3.1). For the olfactory transcriptome of the blind shark, a total of 593,974 transcripts were assembled, whereas for the mako shark, 369,296 transcripts were assembled. The average contig length for the blind shark transcriptome was 811 bp and for the mako shark was 853 bp. The N50 was 1834 bp and 1953 bp, respectively.

The quality and completeness of the assemblies were assessed by two methods. First, we determined the proportion of inputted reads mapping back to the generated assemblies, with a 91% overall alignment rate for the blind shark and 93% the mako transcriptome. Second, we examined the number of conserved vertebrate single-copy orthologs using BUSCO. The BUSCO completeness score obtained was 88% and 89% for the blind shark and mako shark transcriptome, respectively (Table 3.2).

Table 3.2. Summary metrics of the assembled olfactory organ transcriptome of the blind shark and mako shark.

	Number of transcripts	Average length	N50	Alignment rate	BUSCO
Blind	593,974	811 bp	1834 bp	91%	88%
Mako	369,296	853 bp	1953 bp	93%	89%

3.3.3 Functional annotation and olfactory receptor mining

The number of transcripts with a hit to a known nucleotide sequence with the NCBI nt database was 136,143 in blind shark and 90,241 in mako shark. From these, seven and 14 sequences were identified as olfactory receptors in blind and mako shark, respectively (Fig 3.1). For the NCBI nr database, 144,155 transcripts for the blind shark and 102,836 for the mako shark were identified to a known protein sequence. In this case, 10 sequences for the blind shark and 13 sequences for the mako shark were reported as olfactory receptors (Fig 3.1). Additionally, up to 1272 transcripts in blind shark and 745 in mako shark had a hit to any of the olfactory receptor amino acid sequences we used as queries in our customised olfactory receptor dataset. After translation, 820 protein sequences in blind shark and 505 in mako shark had sufficient residuals after being translated to be considered potential functional olfactory receptors. Phylogenetic analyses confirmed their identity as olfactory receptors for 58 and 27 of these protein sequences in blind and mako shark, respectively (Fig 3.1).
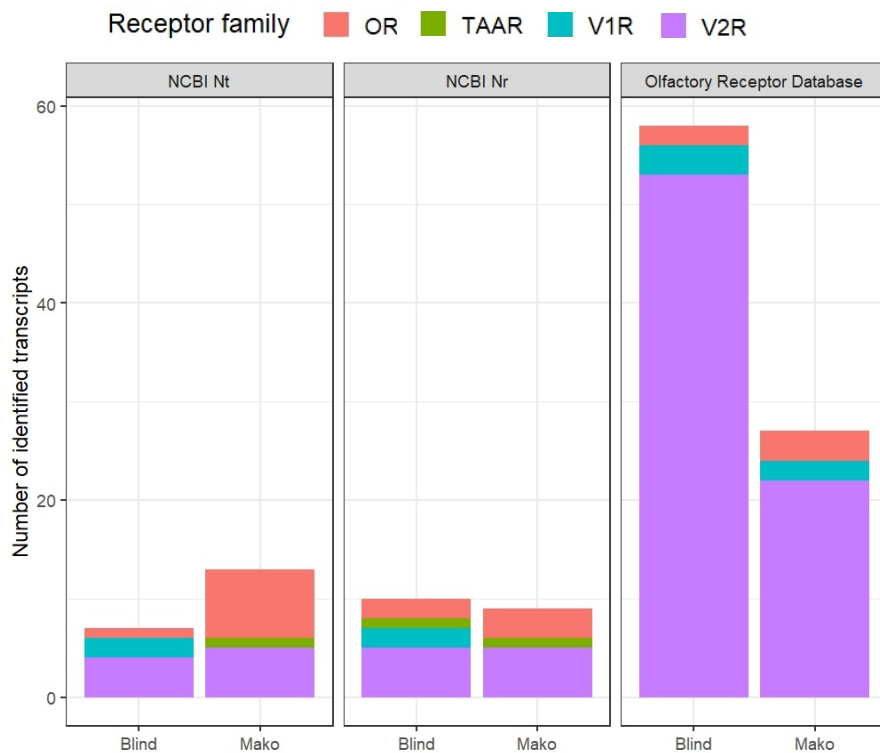
Fig 3.1. Number of olfactory receptor gene transcripts identified with each annotation method for each species. The method involving a custom olfactory receptor database with phylogenetic validation detected a greater number of V2R genes. TAAR receptors were not detected with the latter method because transcripts were either too short or clustered with outgroup sequences during tree construction. Olfactory receptors identified with either the nt or nr database that were long enough and clustered with one of the olfactory receptor clades of the phylogenetic tree were also identified with the olfactory receptor database.

For further downstream analyses and comparisons, only the olfactory receptors identified using the method relying on the olfactory receptor representative database followed by phylogenetic validation were considered for two main reasons. Firstly, this method allowed to identify on average 7 and 2 times more olfactory receptors in blind and mako sharks, respectively, than any of the NCBI databases (Fig 3.3). This was due to a combination of factors such as: incorrect identification of a substantial number of olfactory receptors using the nt and nr databases (e.g. V2Rs were often misidentified as calcium-sensing receptors and V1R's were misidentified as somatostatin or taste receptors), use of non-canonical names to identify olfactory receptor genes (e.g. some OR were identified as GPCR 148 and some V2R were identified as GPCRA Group C) or missing identification (i.e. sequence identified as unknown protein). Secondly, with this method, the quality of the identified olfactory receptors was higher by ensuring that the obtained protein sequences were not instead very similar homologous sequences after phylogenetic validation and confirming that the obtained protein sequences were at least the minimum length expected by olfactory receptors (e.g. some of the sequences identified by the nr and nt database, including the only two potential TAARs identified in this study, were well below our 200 residuals cut-off, compromising the potential functional role and accurate identification of these sequences).

The number of unique olfactory receptor transcripts identified in the transcriptome of blind shark (58) was higher than in the mako shark (27). Whereas the number of OR and V1R were relatively similar and low between both species (2-3 receptor transcripts per family), the number of V2R receptors showed a great expansion in both species, with blind shark displaying 53 different V2R sequences, whereas mako shark had only 22. Surprisingly, no TAAR were detected in either of the transcriptomes. Given we were able to detect transcripts for homologous TAAR sequences such as dopamine and hydroxy-tryptamine receptors [128], it is unlikely this absence was due to a technical error. Additionally, it is important to note that some of the identified olfactory receptor transcripts were different transcriptional isoforms of the same gene. Therefore, only unique genes were considered to compare the number of olfactory receptors identified in the transcriptome of blind and mako shark to the number of receptors identified in the genome of other chondrichthyan species (Fig. 3.2). This was done to avoid overestimating the number of olfactory receptors of blind and mako shark in relation to genomic studies, which cannot report potential isoforms. Overall, the number of identified receptors for all receptor families in the transcriptomes of the blind and the mako shark was lower than in the genomes of either the elephant shark or catshark (Fig 3.2). When only unique genes were considered, the mako shark still had fewer receptor genes than the blind shark (Fig 3.2).
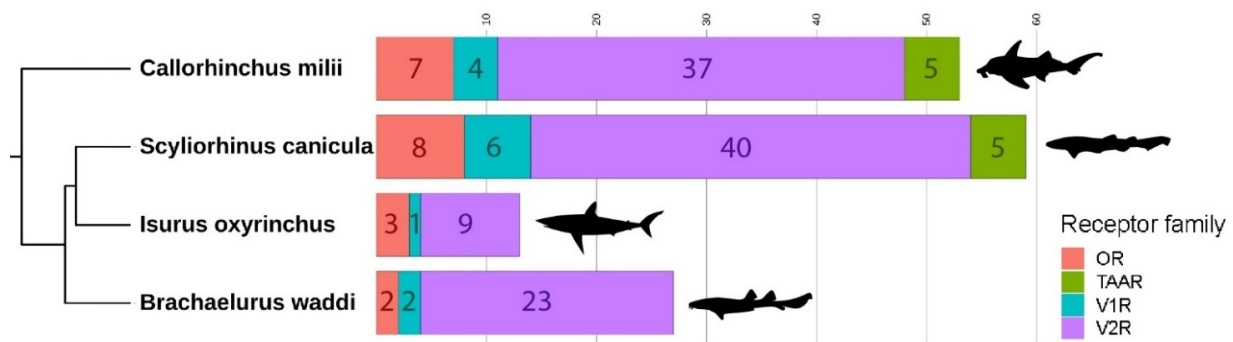
Fig 3.2. Number of unique olfactory receptor genes identified in the complete repertoire of all chondrichthyan species studied to date. Receptors from elephant shark (*C. milli*) and catshark (*S. canicula*) obtained from the genomic study of Sharma et. al [100]. Receptors from blind shark (*B. waddi*) and mako shark (*I. oxyrinchus*) identified in this study from transcriptome analysis. Isoforms of the same gene are not included in the count to ease comparison between genomic and transcriptomic studies.

3.3.4 Phylogenetic analysis of chondrichthyan olfactory receptors

Phylogenetic trees of the olfactory receptor families OR (Fig S3.1), V1R/ORA (Fig. S3.2) and V2R (Fig. S3.3) revealed several genes that were highly conserved in the chondrichthyan lineage, whereas others appeared to be very species-specific. For instance, OR4, ORA3 and V2R1 were identified in all species whose receptor sequences were available. Some genes were shared by several species from different lineages but were completely absent in others, suggesting the potential loss of genes such as V2R2 or ORA2, which were present in all species except carcharhiniform sharks, or OR1, which was only absent in the blind shark. Specifically, the mako shark had a high number of missing receptors that were present in the other species. Alternatively, genes such as V2R20, V2R21 found in the blind shark, V2R9, V2R10 and V2R11 in the catshark, and the V2R21–VR32 chimaera cluster did not have any direct orthologs in any other species and appeared to have undergone gene duplication events. Often, olfactory receptor orthologs were most similar between the most closely related species according to the most accepted chondrichthyan phylogeny [129]; however, it was not always the case (e.g. ORA3). Overall, all trees showed a high level of support in almost all the terminal branches, except for OR1 and V2RL4 in the catshark, suggesting an overall accurate representation of the phylogenetic relationships of the analysed receptors. Those olfactory receptors without a name were reported in other studies, but according to their position within the tree, it is unclear whether they are actual olfactory receptor members.

3.3.5 Expression analysis of olfactory receptors

V2R genes were significantly more highly expressed than any other olfactory receptor family in both species (Table S3.2, Fig. 3.3A). However, there were no significant differences in the abundance of any

of the gene families between species, even though the blind shark had a slightly higher abundance of V2R than the mako (Table S3.3, Fig. 3.3A). There were no significant differences between species nor gene families when the abundance of transcripts was normalized by the number of unique transcript sequences identified for that family in each species (Table S3.3, Fig. 3.3B). However, normalized TPM (transcripts per million) for V1R was slightly higher than OR in mako shark compared to the blind shark, but not significantly. Overall, the expression of unique olfactory receptor sequences was highly variable between different gene families within species, especially for V2R (Fig. 3.3C, D, E). Visual inspection of the expression pattern of the receptors with direct orthologs in both species suggested that gene expression was quite similar for most receptors, except for V2RL1, which was higher in blind shark (Fig. 3.3F).
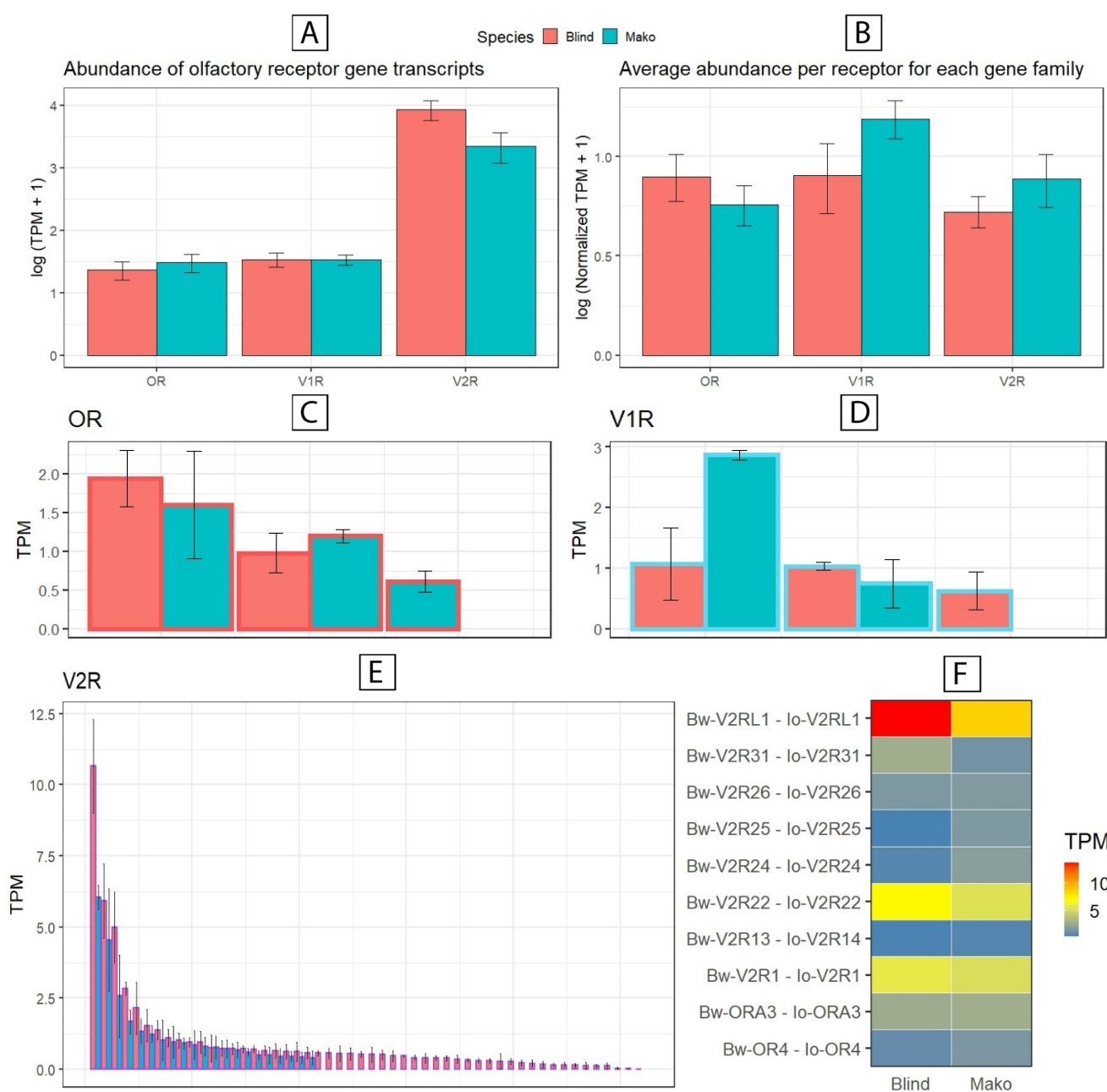
Fig. 3.3. Expression analyses of olfactory receptors in blind and mako shark. (**A**) Total abundance of each olfactory receptor family. V2R is significantly more expressed than other families, but there are no differences between species. TPM represented on log scale (**B**) Normalized abundance by the number of unique sequences for each olfactory receptor family. No significant differences observed between species. TPM represented on log scale. (**C - E**) Distribution of mean TPM expression values for each of the OR (red), V1R (blue), V2R (purple) genes in blind and mako shark, respectively. Abundance for each unique transcript sequence varies widely within each receptor family for each species. Error bars represent the standard error of the mean from three replicates. (**F**) Heatmap of expression pattern of olfactory receptor orthologs between blind and mako shark

3.4 Discussion

Olfactory cues play a critical role in the sensory biology of sharks, allowing them to detect and track prey, avoid potential threats and predators, navigate, and possibly identify conspecifics and potential reproductive mates [2,16,20–22,26,28,29]. However, relatively little is known about the molecular mechanisms that allow different species of sharks to detect relevant olfactory cues from their environments. In this study, I characterized the olfactory receptors expressed in the olfactory organ of two shark species with contrasting lifestyles to determine whether the number of unique olfactory receptor transcripts and their relative expression may indicate differences between the olfactory capabilities of two shark species. I found that the number, type, and relative abundance of specific olfactory receptors varies between the blind shark and the mako shark. However, there were no significant differences between the relative abundance of the different olfactory receptor families per gram of tissue, suggesting that the density of neurons may be similar between species. These findings appear to support the hypothesis that the olfactory receptor repertoire of sharks may have evolved differentially between species and reflect differences in the array of substances each can detect.

The total number of unique olfactory receptor transcripts identified in blind shark was 2.7 times higher than in the mako shark (Fig 3.1). This difference in repertoire size was mostly driven by the lower number of unique V2R receptor transcripts expressed in the mako shark in comparison to the blind shark. The olfactory system of vertebrates is subjected to specific evolutionary processes that determine the diversity and specificity of their olfactory receptor repertoire [15,130]. Receptors fulfilling critical ligand-recognition functions would be subjected to purifying selection and maintained. Alternatively, receptors that are functionally redundant, as a consequence of gene duplications or relaxed selective pressures, would tend to accumulate mutations that might provide them with new useful odorant-binding capabilities or result in functional inactivation. Therefore, the size of the olfactory receptor repertoire has been used as a proxy for the spectrum of odorants an organism can detect in several vertebrate groups [61,63]. This suggests that the wider repertoire of unique receptor transcripts in the blind shark may potentially allow this species to detect and differentiate a wider array of odorants compared to the mako shark. Moreover, these differences were still observed when isoforms were deprecated, and only unique olfactory receptor genes were considered (Fig 3.2); however, the number of unique olfactory receptors identified in this study was lower than those reported in elephant shark and catshark from genomic studies [100]. This may be explained due to a combination of factors, such as the selective expression of certain olfactory receptors (e.g. at different developmental time points) that was not captured in our transcriptomes or an overestimation of the number of olfactory receptors involved in the perception of

odorants in genomics studies because they consider receptors that may not be expressed in olfactory tissue (or not involved in olfaction).

Although we cannot discard the possibility of some olfactory receptors present in the genome were missing from our transcriptome (either for biological or technical reasons), overall, we expect that most of the diversity of the olfactory receptors of each species was captured in this study. Due to the large size of the olfactory organ of the mako shark (~20 grams), it was not feasible to extract the RNA of the whole organ as we did with those of the blind shark (~1 gram); instead, tissue sub-samples were taken from lamella across the whole olfactory organ to obtain the most complete representation of potential olfactory receptor neuron populations obtaining within a gram of tissue. In teleost fishes, the arrangement of olfactory receptor neurons in the epithelium expressing the same receptor is non-random but overlapping [131]. Thus, despite the specific distribution of olfactory receptors types through the olfactory epithelium is unknown in sharks, our random sampling strategy should have captured most of the diversity of olfactory receptors expressed regardless of the type of arrangement they may present, especially as we combined the transcripts obtained from three different individual sharks. Similarly, the expression of olfactory receptors may vary according to life stage, sex and environmental conditions [132–135]. Whereas we managed to obtain blind sharks of different size and sex, and at different times in the year, we were constrained in our ability to obtain high quality olfactory organs from a diverse selection of makos sharks. Additionally, the different capture and euthanasia conditions between species may have generated differences in the expression and degradation of olfactory receptor genes. Further studies need to address how these differences may affect the number of olfactory receptors expressed in a diverse range of individuals of wild caught sharks; however, the high BUSCO scores of the *de novo* assemblies indicate we have successfully assembled most of the transcripts we can expect to be present in the olfactory organs of each species.

On the other hand, the results of this study suggest that some olfactory receptor gene families may not have an olfactory function in chondrichthyans as they are not expressed in olfactory tissue. Despite the presence of OR and TAAR genes in the genomes of all cartilaginous fishes sequenced to date [97,99,100], the receptor neurons and the signalling pathways typically coupled to OR and TAAR have not been determined [106,107], raising the question of whether these receptors are involved in olfaction in this taxon [105]. In this study, V2R were the most numerous and highly expressed receptors, supporting previous results and hypothesis that highlight the important role of vomeronasal receptors for the perception of odours in chondrichthyans [105]. OR receptors were also detected, and they were expressed at the same level as V1R, suggesting that OR receptors are possibly also involved in the

detection of odorants. Intriguingly, four out of the five OR transcripts identified in this study belonged to a clade of OR considered non-olfactory as it is not expressed in the olfactory epithelium of higher vertebrates [119]. Whether these receptors are coupled to an uncharacterized G-protein subunit that would explain why OR receptors have never been visualized in this group before is a topic for further studies. However, no valid TAAR sequences were detected in either of the species. This observation was rather surprising, as TAAR sequences are expressed in the olfactory organs of earlier vertebrate groups [136] and sharks are known to be sensitive to amine compounds [137], which are the principal target for TAAR receptors [128]. Only one partial transcript was identified in very low abundance in each species (Fig. 3.1); however, these sequences were too short (less than 90 amino acids) to be considered functional, making it difficult to accurately identify these sequences as TAAR receptors rather than other homologous sequences. Given we were able to detect full transcripts of other biogenic amine receptors, which are homologous to TAAR genes [128], a procedural or technical error that would have led to TAAR receptors being overlooked seems unlikely. Alternatively, TAAR receptors may have a highly restricted expression pattern either across the sensory epithelium or throughout the lifecycle of sharks that were not captured in this study. In any case, the lack of full TAAR transcripts expressed in the olfactory organ of mako and blind shark appears to suggest TAAR receptors may have a limited role (if any) in the perception of odorants in this group and, therefore, sharks may be relying on an alternative receptor for the detection of amines.

The phylogenetic trees of each of the three olfactory receptor families detected and examined in this study (OR, V1R and V2R) allowed the identification of two distinct evolutionary patterns similar to those observed in other groups of vertebrates [138,139]. Firstly, some olfactory receptor clades were highly conserved as they were present in all species examined (e.g.: OR4, ORA3 and V2R1). Although no shark olfactory receptor has yet been deorphanized, we might expect these genes to fulfil critical and universal olfactory functions, such as detecting common food odorants like amino acids. Secondly, some receptor clades were only present in one or a handful of species, suggesting a potential adaptative role of these olfactory receptors in a species particular ecological niche. Interestingly, orthologues that were either shared by chimaera, catshark and blind shark or solely by catshark and blind shark were not found in the mako shark (e.g.: OR8, ORA2, V2R3L-V2RL5, V2R5-V2R11, V2R16, V2R27, V2R28, V2R32). This suggests that some of the olfactory receptors present in the common ancestor of chondrichthyans and elasmobranchs respectively have become lost/non-functional in the mako shark, perhaps indicating a narrower olfactory sense in the mako shark for the detection of relatively fewer odorants. Future genomic studies would help to confirm the extent of olfactory receptor gene losses in the mako shark through the

identification of pseudogenized olfactory receptor genes in its genome. Although some of the missing orthologs of the mako shark were also absent from the white shark genome annotation [99], it is difficult to determine whether these gene losses are shared with more lamnid sharks as the white shark annotation did not follow olfactory receptor search protocols [101]. Indeed, this study highlights that the number of olfactory receptors is potentially underestimated when using generic nucleotide or protein databases, especially for V2R (Fig. 3.1). Moreover, we saw evidence of two olfactory receptors previously reported (one OR in *S. torazame* and one V1R in *C. carcharias*) that did not cluster with any of the olfactory receptor clades in our phylogenetic trees (Fig S3.1 & Fig S3.2), emphasising the need to validate potential olfactory receptor sequences though phylogenetic analyses.

Finally, although sharks with a larger olfactory receptor repertoire may potentially detect and differentiate between a wider array of substances, sensitivity to odours is another important factor that may determine the reliance of a species on their sense of smell. The number of ORN expressing a given olfactory receptor is one of the key elements that determine sensitivity for given odorants [56]. In vertebrates, each ORN expresses just one type of olfactory receptor, so that the relative number of ORN displaying a given olfactory receptor can be estimated from its gene expression [65]. In this study, the relative abundance of different olfactory receptor transcripts was analysed to determine if the smaller olfactory receptor repertoire of the mako shark is compensated by a higher density of specific ORN. Overall, no significant differences in transcript abundances were observed between species for any of the olfactory receptor gene families, suggesting that overall the relative density of ORN may be quite similar between both species for around a gram of tissue (Fig. 3.3A,B). Additionally, preliminary visual comparison of the expression of one-to-one orthologs indicated very similar values for all shared genes (Fig. 3.3F). Still, there were some differences in the expression level of specific receptors between and within species (Fig. 3.3C-E). For instance, V2RL1, whose orthologs in teleost fish preferentially bind to amino acids [140], was more highly expressed in the blind shark than the mako shark. Similarly, one of the isoforms of Io-ORA3, which may be responsible for the detection of some type of bile salt as observed in several teleost V1R/ORA [141], was highly expressed in the mako shark. Perhaps, the differential expression of specific olfactory receptor sequences may partially explain the observed differences in olfactory threshold to different substances between species of elasmobranchs [24,27]. However, note that other factors such as the olfactory receptor affinity, the functional redundancy of the olfactory receptor repertoire, the total number of ORN, the rate of water flow through the olfactory organ and the degree of summation of ORN may have an important role in the sensitivity to odours of different species [14,53–57].

Chapter 4 – General Discussion

A mechanistic understanding of olfaction in lower vertebrates, such as chondrichthyans, is critical for tracing the evolution of chemoreception in vertebrates. Furthermore, improved knowledge of the sensory biology of this increasingly endangered taxon may provide alternative solutions for their conservation through the development of more effective by-catch reduction and shark deterrent devices [16,45] and identifying potential threats associated with anthropogenic pollution [46–48]. In this study, we explored the relationship between a conventional anatomical measure of olfactory performance in sharks—the total sensory surface area of the olfactory organ, taking into account the ratio of sensory epithelium and variation of secondary folding of the lamellae—and another, potentially more informative, indicator of olfactory capability, i.e., the number of unique odorant receptors expressed on olfactory receptor neurons (ORNs). Based on the assumption that sharks with a more extensive olfactory sensory surface area should rely more heavily on their sense of smell, we hypothesised that they would also possess a more diverse olfactory receptor repertoire to help them discriminate and identify a wider array of substances. The mako shark has a larger total sensory surface area than the blind shark, which is consistent with other studies that have shown that the olfactory organs of more pelagic elasmobranchs are larger than those of benthic species [24,32]. However, the blind shark had the most diverse olfactory receptor repertoire, with 58 expressed receptors transcripts compared to only 27 in the mako shark. These results suggest that while the morphology of the olfactory organ and the extent of its sensory surface area may play a critical role in olfaction, other factors may determine the degree of specialisation of—and even reliance upon—the olfactory sense in different shark species.

4.1 Why is the total sensory surface area of the olfactory organs not correlated with the size of the olfactory receptor repertoire in sharks?

Olfactory stimuli are encoded by the olfactory system through a combinatorial process where each olfactory receptor protein (expressed by a given receptor neuron) is stimulated to a varying degree by one or more odorants [15,138]. Thus, each stimulus generates a specific pattern of activation of several olfactory receptors, allowing the detection and discrimination of a great number of chemical compounds. As the number of olfactory receptor genes with different binding affinities increases, the ability to detect and identify a greater number of olfactory cues should also be enhanced [15]. However, as each olfactory receptor neuron expresses only one type of olfactory receptor gene in vertebrates, it is expected that the total number of olfactory receptor neurons should also be higher to accommodate the wider receptor

repertoire. This relationship is seen in mammals, where the size of the cribriform plate (used as an anatomical proxy for the number of ORN connecting to the olfactory bulb) is a good predictor of the size of the olfactory receptor repertoire and has been used to determine the olfactory receptor repertoire of extinct species [66]. In sharks, we would expect that the higher sensory surface area of the olfactory organs would be correlated with a higher abundance of olfactory receptors if the density of receptors does not differ between species. This assumption was confirmed in our study as the relative abundance of olfactory receptor gene transcripts per gram of tissue was roughly the same in the blind shark and the mako shark. However, in contrast to mammals, the larger total sensory surface area of the mako shark olfactory organ was not accompanied by a more diversified receptor repertoire. Based on this limited study, it is suggested that this relationship may not hold in sharks because the total sensory surface area of the olfactory organs may be partially determined by the rate of water flow through the olfactory organs, whereas other ecological factors such as the background concentration of chemical cues in the environment or diet may have influenced the size of the olfactory receptor repertoire. However, note that this study investigated only two species that differed markedly in body size and from different orders; therefore, data from more species are required to explore further the following hypotheses from a phylogenetic perspective.

4.2 Why is the total sensory surface area of the mako shark higher than in blind shark?

Whereas more extensive olfactory organs have frequently been associated with a higher reliance or sensitivity to odours in elasmobranchs [32,36,37,39], it is possible that the interspecific diversity in total sensory surface area observed is explained by differences in the nature of the water flow through the olfactory organ. The rate of water flow through the rosette is critical for the perception of olfactory stimuli because it determines the availability of odorants in the olfactory organ and the probability they will bind to their target receptors [36]. The speed of the flow entering the olfactory organ is often dependent on the swimming speed of the sharks, which typically rely on passive ventilation to drive water through their olfactory organs [4,50]. A faster flow will reduce the thickness of the slow-moving boundary layer above the sensory epithelium and, therefore, allow more rapid delivery of odorants to the olfactory receptors and faster detection of the stimulus [142]. However, very fast flow rates risk damaging the delicate lamellae of the olfactory organ and increase the likelihood that odorants are flushed away before they bind their target receptors [51,142]. Consequently, sharks have developed several mechanisms to regulate the flow of water entering the olfactory organs. For instance, several aspects of the external morphology of the olfactory organ, including the position, size and shape of the nares, and the presence

of nasal grooves and flaps, are known to either limit or enhance the incurrent flow rate [36,51,52,67,70,143]. Similarly, in the smalleye hammerhead (*Sphyrna tudes*), at high flow speeds, the flow through the incurrent channel is bypassed to the excurrent channel by an apical gap to limit the flow circulating over the surface of the lamellae and potentially avoid tissue damage [51]. Additionally, we might expect that the total sensory surface area is enlarged as a strategy to increase the probability that an odorant will bind to a higher number of ORNs in species that experience faster flow rates. Therefore, it may be possible that the total sensory surface area of the olfactory organs and the morphological traits that determine this (i.e. the number and size of lamellae, the ratio of sensory epithelium and the degree of secondary folding; Chapter 2) are used as alternative mechanisms to regulate the water flow through the olfactory organ while optimizing the number of olfactory receptors necessary to efficiently detect odorants at a given flow regime.

A more extensive olfactory sensory surface area (not accounting for the degree of secondary folding) has been observed in benthopelagic species, and this one also tends to increase with the total length and mass of the organism [24,32,33,36]. Similarly, more pelagic species are thought to reach faster cruising speeds in comparison to benthic sharks thanks to their more hydrodynamic shape, more efficient propulsion, and higher activity levels [144–146], and cruising speed often increases with the total length of sharks [145]. Therefore, the fastest flow reaching the olfactory organs might be expected to occur in larger, more pelagic sharks in comparison to benthic species without considering the effect of the external morphology of the olfactory organs on the water flow entering the olfactory cavities (e.g. size and shape of nares or nasal groves and flaps modifying the speed or volume of the flow). Congruent with these observations, it may be possible that the larger total sensory surface area of the mako shark may help to optimize water flow through the rosette and/or increase the number of ORN exposed to the faster flow this species may experience given their high swimming speeds. Specifically, a larger olfactory organ may be particularly useful for diffusing the energy of the incoming water flow to avoid lamellar damage during burst swimming speeds (that can reach up to 100 km/h) [85], as no muscle tissue was observed around the nares that may allow sealing the olfactory cavity during these events. On the other hand, the reduced total sensory surface area of the blind shark, in comparison to the mako shark, may be partially explained due to their slower swimming speed which is associated with their benthic lifestyle and smaller size [85]. However, the blind shark has a larger sensory surface area in comparison to what has been observed in other benthic species for their size [32] (Fig S2.5). Some benthic species are able to actively ventilate their olfactory organs by coupling respiratory water movements by connecting the olfactory organs to the mouth through nasoral grooves [70,72,73,143]. In this case, the speed of the flow is

expected to be partially determined by the characteristics of the water flow generated through the respiratory pump. However, to the best of our knowledge, the blind shark is the only species reported whose nasoral grooves are completely sealed internally [73]. Therefore, it may be possible that the unusual internal nasoral groove of the blind shark may have increased the speed at which the water flows through the olfactory organ promoting a higher total sensory surface area in this species.

Future studies should explore interspecific differences in the total sensory surface area of the olfactory organ of sharks in relation to the instantaneous volume and speed of the water flowing through their olfactory organ. This may involve an analysis of the effects of various traits such as the external morphology of the olfactory organ, the diameter and sinuosity of the channels made by the secondary folds and the peripheral channels of adjacent lamellae and the heterogeneous distribution of sensory epithelium across the lamellar surface. A combination of techniques such as histology, scanning electron microscopy, and micro or nano-CT may be necessary to accurately characterize these traits to inform comparative multidisciplinary studies that integrate a thoughtful understanding of the hydrodynamics through the olfactory organ and the biology of these organisms.

4.3 Why is the olfactory receptor repertoire larger in blind shark?

The number and type of ORNs found on the olfactory epithelium of vertebrates limits the amount of information an animal can extract from their environment as each olfactory receptor neuron expresses just one type of receptor [15]. In consequence, we may expect that the expression of different types of olfactory receptors on ORNs is optimized to allow animals to maximize the amount of relevant information to inform their behaviour while reducing metabolic costs associated with the development and maintenance of neural tissue [147]. The olfactory requirements for each species may vary according to the number of relevant odorants needed to inform behaviours such as feeding, mating or predator escape, and the concentration at which it is ecologically relevant to detect or distinguish these substances [2]. In turn, these olfactory requirements may be further affected by environmental factors such as the concentration of the odorant and the background level of other chemical cues on the water column [2,74]. Accordingly, we might expect the olfactory organ of sharks to have become optimized for the perception of critical olfactory cues at relevant biological concentrations by either adjusting the number of neurons expressing a given receptor type or diversifying the ligand affinities of its olfactory receptors [147]. Based on the present study, it appears that for the blind shark, it is more ecologically relevant to increase the number of receptors with different binding affinities to potentially detect and discriminate between a wider array of odours, whereas for the mako shark, a higher abundance of a limited number of receptor

types may be more beneficial to increase the sensitivity to given smells or optimize the detection of odorant cues at the potential faster rate of water flow through its olfactory organs.

The relative importance of a wider receptor repertoire to discriminate more odorants may be related to differences in the chemical olfactory 'landscape' of each species. It is well known that the diversity and concentration of chemical cues in the water vary according to both biotic and abiotic factors. For example, the concentration of dissolved organic matter (i.e. pool of organic substances that most olfactory receptors potentially target, such as amino acids, amines, nucleic acids, etc…) is usually higher in coastal waters than in the open ocean [148]. This occurs due to the increased biomass and the higher productivity of coastal ecosystems, whose concentration and diversity of chemical compounds is further enriched through run-offs coming from land [148,149]. Whereas the blind shark is a reef-associated benthic species found close to the coastline [85], the mako shark is an ocean-going pelagic species capable of trans-oceanic migrations [150]. Consequently, the potential number of odorants that the blind shark may encounter and must distinguish as relevant olfactory cues rather than chemical 'noise' may be higher than for the mako shark. By contrast, the relatively limited olfactory receptor repertoire of the mako shark may reflect the lower diversity of behaviourally relevant chemical compounds in the open ocean, which has resulted in the loss of several receptor types present in its common ancestor with the blind shark (Chapter 3). Unfortunately, no other pelagic shark has had its olfactory receptor repertoire properly characterized and future studies should examine a diverse range of species to establish whether a pelagic lifestyle leads to a more specialised olfactory receptor repertoire.

The lower diversity of olfactory receptors of the mako shark may also have arisen as a trade-off to enhance the absolute sensitivity to a limited number of chemical cues by increasing the number of receptors expressing the same receptor type. Sensitivity to a given odorant is determined by the number of receptors expressing a specific olfactory receptor [55], the affinity of the olfactory receptor to that odorant [14,53,54], and the convergence ratio of ORNs to secondary neurons in the glomeruli of the olfactory bulb [56,57]. Given that the total olfactory sensory surface area of the mako shark is substantially larger than that of the blind shark and the relative abundance of ORNs is quite similar in both species (inferred from the similar overall expression levels of olfactory receptor transcripts per gram of tissue in Chapter 3), it appears that the total number of ORNs in the mako shark is higher than in the blind shark. As the number of ORNs expressing the same olfactory receptor is higher in mako sharks because their repertoire is smaller, it is reasonable to speculate that mako sharks may have a much higher sensitivity (lower detection threshold) if the olfactory receptor affinities are similar, although this will depend on the degree of summation/convergence of ORNs onto secondary neurons. Although it has been

shown that the gross surface area of the olfactory organ of elasmobranchs does not reflect the relative sensitivity to amino acids [24], it is unclear how the secondary folds, the distribution of sensory epithelium and the relative abundance of different receptor types may have contributed to differences in the total number of olfactory receptor neurons expressing a given receptor between species. Therefore, it is still important to consider whether the sensitivity to amino acids and other odorants may differ between species when factors other than gross surface area are taken into account.

The potential ability of mako sharks to detect lower concentrations of substances may be related to their ecological needs or the specific flow regime through their olfactory organs. The concentration of organic matter decreases with distance from shore and also with depth [151]. Besides spending a significant amount of time far from the coast, mako sharks are known to perform daily vertical migrations to depths of up to 800 meters to forage [85]. By contrast, blind sharks typically feed close to shore in depths less than 140 metres [85]. Therefore, it may be more relevant for the mako shark to be able to detect olfactory cues that are present at very low concentrations rather than being able to distinguish between a wider array of odorants. Alternatively, if the speed of the water flow differs between species, a higher number of ORNs expressing the same olfactory receptor type may be an adaptation of the olfactory organ of the mako shark to detect substances that spend significantly less time in the olfactory cavity as the water flowing through the olfactory organ is faster. In that case, we may expect that the relative sensitivity to odours of the mako shark may not differ from other species under flow rate conditions that resemble those typically experienced by the olfactory organ of this species as they move.

These potential inferred differences in diversity and sensitivity to odours between species may be alternatively related to ecological factors such as diet, navigational demands and reproductive behaviour. For instance, blind sharks have a more diverse diet, including crustaceans, small teleosts, squid and sea anemones [85], whereas mako sharks in the west Pacific primarily feed on tuna and eventually squid [152]. The more generalist diet of the blind shark may explain the larger olfactory receptor repertoire to detect a wider range of olfactory cues released from different prey items, whereas the mako shark may have lost some of the ancestral olfactory receptors because they were no longer useful for the detection of their specific prey. Alternatively, mako sharks may just rely on a limited number of odorants that they are very sensitive to for oceanic navigation. For instance, marine organisms able to perform long-range movements—such as sea turtles and seals—are outstandingly sensitive to dimethyl sulphite which is released in areas of high productivity where prey is more likely to be found [153–155]. Similarly, mako sharks may rely on specific chemical mixtures to navigate between specific grounds [29,156]. Moreover, the degree of reliance on pheromones for sexual reproduction between species may also have an effect

shaping the olfactory receptor repertoire of different species, as it potentially occurs in some teleost fishes [94].

Finally, the reduced olfactory receptor repertoire of the mako shark in comparison with the blind shark may indicate that this species relies less on olfactory cues in comparison to the blind shark. Interestingly, a comparative analysis of the olfactory bulb of 58 species of cartilaginous fishes indicated that the mako shark has a relatively smaller olfactory bulb [34], which in combination with their enlarged optic tectum may suggest that this species relies more heavily on vision rather than olfaction compared to other species [157]. Although the blind shark was not assessed in that study, relatively smaller olfactory bulbs are found in benthic/reef-associated species that are similar to the blind shark [34]. However, another comparative study found that the blind shark has a relatively reduced mesencephalon and enlarged medulla, suggesting that this species may rely more on other sensory modalities other than vision [158,159]. Therefore, without further information about the olfactory bulbs of the blind shark, it is difficult to determine whether the size of the olfactory bulb may correlate with the size of the olfactory receptor repertoire in sharks. Further research should examine whether the olfactory receptor repertoire is increased in species with the largest olfactory bulbs, including species inhabiting coastal-oceanic habitats such as the white shark, the blue shark *Prionace glauca* and the tiger shark *Galeocerdo cuvier*. Alternatively, whereas it has traditionally been assumed that the size of the olfactory bulb in vertebrates is related to their reliance on olfaction, this anatomical proxy may also be affected by other factors [34]. For instance, the size of the olfactory bulb is dependent on the size and number of its mitral cells [55], and therefore, a small olfactory bulb may still provide high sensitivity to odorants if the convergence ratio of olfactory receptor neurons to mitral cells is high. Additionally, it has been suggested that the size of the olfactory bulb may just reflect individual properties that determine the olfactory performance of an animal rather than overall reliance, such as coupling to the central nervous system or ability to track odours for spatial navigation [160,161]. Therefore, a comprehensive characterization of the anatomical and physiological traits of the peripheral and central olfactory system and its behavioural effects may be required to fully understand the olfactory capabilities of different species of sharks.

Final Conclusions and Further directions

The olfactory system of cartilaginous fishes is a highly diversified sensory modality that has adapted to suit the different ecological requirements of each species. On one hand, the total sensory surface area of the olfactory organs may vary to optimize the hydrodynamics of the water flow going through the olfactory organs or to maximize the number of olfactory receptor neurons available for the detection of odorants. On the other hand, the diversity of olfactory receptors used for the perception of relevant olfactory cues may also vary—regardless of the size of the olfactory organs—to optimize the detection and discrimination of olfactory cues in different environments or under the different flow regimes experienced by the olfactory organ of different species of chondrichthyans. Identifying the olfactory capabilities of different shark species is critical to better understand the evolution of this sensory modality in vertebrates and the ecology of species that are difficult to observe in the wild or test under lab conditions. The results of this study suggest that a comprehensive and multidisciplinary approach of the different elements that conform the olfactory system of this successful group of predators needs to be undertaken to fully appreciate the olfactory capabilities of this group. Future studies should explore the hydrodynamics of the water flow through the olfactory cavity considering the fine-scale traits of the olfactory organs and the lamellae, the composition of the olfactory receptor repertoire and the relative size of the olfactory bulbs of more species to characterize which selective pressures are driving the diversity of these traits and how they may affect the perception of odours. Subsequently, a mechanistic approach in which the specific binding properties and the structural evolution of the olfactory receptors of chondrichthyans are explored may provide opportunities to identify the range of substances these species can detect. This knowledge may help to identify negative impacts on sensory function and sensory-driven behaviours of changes in water quality arising from pollution and climate change or develop improved shark deterrents that may save lives of sharks through sensory-based bycatch reduction techniques in commercial fisheries and those of humans though improved shark deterrents.

Supplementary Electronic Material

Electronic supplementary material regarding olfactory receptor sequences, alignments and phylogenetic trees can be accessed at: https://cloudstor.aarnet.edu.au/plus/s/oKzztajuzNR6Cbb

References

1. Galizia CG, Lledo P. Olfaction. In: Galizia CG, Lledo P, editors. Neurosciences - From molecule to behavior: a university textbook. Berlin, Heidelberg: Springer Spektrum; 2013. pp. 253–284. doi:10.1007/978-3-642-10769-6_13

2. Müller-Schwarze D. Chemical ecology of vertebrates. 1st ed. Cambridge: Cambridge University Press; 2006. doi:10.1017/CBO9780511607233

3. Zielinski BS, Hara TJ. Olfaction. In: Hara TJ, Zielinski BS, editors. Fish physiology. San Diego: Elsevier; 2006. pp. 1–43. doi:10.1016/S1546-5098(06)25001-5

4. Cox JPL. Hydrodynamic aspects of fish olfaction. Journal of the Royal Society Interface. 2008. pp. 575–593. doi:10.1098/rsif.2007.1281

5. Hara TJ. Olfaction in fish. Prog Neurobiol. 1975;5: 271–335.

6. Saraiva LR, Kondoh K, Ye X, Yoon KH, Hernandez M, Buck LB. Combinatorial effects of odorants on mouse behavior. Proc Natl Acad Sci U S A. 2016;113: E3300–E3306. doi:10.1073/pnas.1605973113

7. Martinez Q, Lebrun R, Achmadi AS, Esselstyn JA, Evans AR, Heaney LR, et al. Convergent evolution of an extreme dietary specialisation, the olfactory system of worm-eating rodents. Sci Rep. 2018;8. doi:10.1038/s41598-018-35827-0

8. Brokaw AF, Smotherman M. Role of ecology in shaping external nasal morphology in bats and implications for olfactory tracking. PLoS One. 2020;15: e0226689. doi:10.1371/journal.pone.0226689

9. Bibliowicz J, Alié A, Espinasa L, Yoshizawa M, Blin M, Hinaux H, et al. Differences in chemosensory response between eyed and eyeless Astyanax mexicanus of the Rio Subterráneo cave. Evodevo. 2013;4: 25. doi:10.1186/2041-9139-4-25

10. Niimura Y. Evolutionary dynamics of olfactory receptor genes in chordates: interaction between environments and genomic contents. Hum Genomics. 2009;4: 107–118. doi:10.1186/1479-7364-4-2-107

11. Hashiguchi Y, Nishida M. Evolution of Trace Amine–Associated Receptor (TAAR) Gene Family in Vertebrates: Lineage-Specific Expansions and Degradations of a Second Class of Vertebrate Chemosensory Receptors Expressed in the Olfactory Epithelium. Mol Biol Evol.

2007;24: 2099–2107. doi:10.1093/molbev/msm140

12. Li Q, Tachie-Baffour Y, Liu Z, Baldwin MW, Kruse AC, Liberles SD. Non-classical amine recognition evolved in a large clade of olfactory receptors. Elife. 2015;4: e10441. doi:10.7554/eLife.10441

13. Hansen A, Zielinski BS. Diversity in the olfactory epithelium of bony fishes: Development, lamellar arrangement, sensory neuron cell types and transduction components. J Neurocytol. 2005;34: 183–208. doi:10.1007/s11068-005-8353-1

14. Hussain A, Saraiva LR, Ferrero DM, Ahuja G, Krishna VS, Liberles SD, et al. High-affinity olfactory receptor for the death-associated odor cadaverine. Proc Natl Acad Sci U S A. 2013;110: 19579–19584. doi:10.1073/pnas.1318596110

15. Bear DM, Lassance JM, Hoekstra HE, Datta SR. The Evolving Neural and Genetic Architecture of Vertebrate Olfaction. Curr Biol. 2016;26: R1039–R1049. doi:10.1016/J.CUB.2016.09.011

16. Hart NS, Collin SP. Sharks senses and shark repellents. Integr Zool. 2015;10: 38–64. doi:10.1111/1749-4877.12095

17. Collin SP, Kempster RM, Yopak KE. How Elasmobranchs Sense Their Environment. 1st ed. In: Shadwick RE, Farrell AP, Brauner CJ, editors. Physiology of Elasmobranch Fishes: Structure and Interaction with Environment. 1st ed. New York: Elsevier; 2015. pp. 19–99. doi:10.1016/B978-0-12-801289-5.00002-X

18. Heithaus MR. Predator-Prey Interactions. In: Carrier JC, Musick JA, Heithaus MR, editors. Biology of sharks and their relatives. 1st ed. Boca Raton: CRC Press; 2004. pp. 487–521.

19. Heithaus MR, Frid A, Wirsing AJ, Worm B. Predicting ecological consequences of marine top predator declines. Trends Ecol Evol. 2008;23: 202–210. doi:10.1016/J.TREE.2008.01.003

20. Gardiner JM, Atema J, Hueter RE, Motta PJ. Multisensory integration and behavioral plasticity in sharks from different ecological niches. PLoS One. 2014;9: e93036. doi:10.1371/journal.pone.0093036

21. Hobson ES. Feeding behavior in three species of sharks. Pacific Sci. 1963;17: 171–194.

22. Huber D, Wilga C, Dean M, Ferry L, Gardiner J, Habegger L, et al. Feeding in Cartilaginous Fishes: An Interdisciplinary Synthesis. In: Bels V, Whishaw I, editors. Feeding in vertebrates. Berlin: Springer; 2019. pp. 231–295. doi:10.1007/978-3-030-13739-7_8

23.   Tricas TC, Kajiura SM, Summers AP. Response of the hammerhead shark olfactory epithelium to amino acid stimuli. J Comp Physiol A Neuroethol Sensory, Neural, Behav Physiol. 2009;195: 947–954. doi:10.1007/s00359-009-0470-3

24.   Meredith TL, Kajiura SM. Olfactory morphology and physiology of elasmobranchs. J Exp Biol. 2010;213: 3449–3456. doi:10.1242/jeb.045849

25.   Hodgson ES, Mathewson RF, Gilbert PW. Electroencephalographic studies of chemoreception in sharks. In: Gilbert PW, Mathewson RF, Rall DP, editors. Sharks, Skates and Rays. Baltimore: Johns Hopkins Press; 1967. pp. 491–501.

26.   Gardiner JM, Maruska KP, Sisneros J, Casper B. Sensory physiology and behavior of elasmobranchs. In: Carrier JC, Musick JA, Heithaus MR, editors. Biology of Sharks and Their Relatives. 2nd ed. Boca Raton: CRC Press; 2012. pp. 349–402. doi:10.1201/b11867-15

27.   Meredith TL, Caprio J, Kajiura SM. Sensitivity and specificity of the olfactory epithelia of two elasmobranch species to bile salts. J Exp Biol. 2012;215: 2660–2667. doi:10.1242/jeb.066241

28.   Nosal AP, Chao Y, Farrara JD, Chai F, Hastings PA. Olfaction Contributes to Pelagic Navigation in a Coastal Shark. PLoS One. 2016;11: e0143758. doi:10.1371/journal.pone.0143758

29.   Gardiner JM, Whitney NM, Hueter RE. Smells like home: The role of olfactory cues in the homing behavior of blacktip sharks, *Carcharhinus limbatus*. Integr Comp Biol. 2015;55: 495–506. doi:10.1093/icb/icv087

30.   Papastamatiou YP, Bodey TW, Caselle JE, Bradley D, Freeman R, Friedlander AM, et al. Multiyear social stability and social information use in reef sharks with diel fission–fusion dynamics. Proc R Soc B Biol Sci. 2020;287: 20201063. doi:10.1098/rspb.2020.1063

31.   Schluessel V. Who would have thought that 'Jaws' also has brains? Cognitive functions in elasmobranchs. Anim Cogn. 2015;18: 19–37. doi:10.1007/s10071-014-0762-z

32.   Schluessel V, Bennett MB, Bleckmann H, Blomberg S, Collin SP. Morphometric and ultrastructural comparison of the olfactory system in elasmobranchs: The significance of structure-function relationships based on phylogeny and ecology. J Morphol. 2008;269: 1365–1386. doi:10.1002/jmor.10661

33.   Schluessel V, Bennett MB, Bleckmann H, Collin SP. The role of olfaction throughout juvenile development: Functional adaptations in Elasmobranchs. J Morphol. 2010;271: 451–461.

doi:10.1002/jmor.10809

34. Yopak KE, Lisney TJ, Collin SP. Not all sharks are "swimming noses": variation in olfactory bulb size in cartilaginous fishes. Brain Struct Funct. 2015;220: 1127–1143. doi:10.1007/s00429-014-0705-0

35. Ferrando S, Amaroli A, Gallus L, Aicardi S, Di Blasi D, Christiansen JS, et al. Secondary folds contribute significantly to the total surface area in the olfactory organ of chondrichthyes. Front Physiol. 2019;10: 245. doi:10.3389/fphys.2019.00245

36. Kajiura SM, Forni JB, Summers AP. Olfactory morphology of carcharhinid and sphyrnid sharks: Does the cephalofoil confer a sensory advantage? J Morphol. 2005;264: 253–263. doi:10.1002/jmor.10208

37. Theiss SM, Hart NS, Collin SP. Morphological indicators of olfactory capability in wobbegong sharks (Orectolobidae, Elasmobranchii). Brain Behav Evol. 2009;73: 91–101. doi:10.1159/000209865

38. Sheldon RE. The sense of smell in selachians. J Exp Zool. 1911;10: 51–62. doi:10.1002/jez.1400100105

39. Ferrando S, Gallus L, Ghigliotti L, Vacchi M, Nielsen J, Christiansen JS, et al. Gross morphology and histology of the olfactory organ of the Greenland shark *Somniosus microcephalus*. Polar Biol. 2016;39: 1399–1409. doi:10.1007/s00300-015-1862-1

40. Ferrando S, Gallus L, Amaroli A, Gambardella C, Waryani B, Di Blasi D, et al. Gross anatomy and histology of the olfactory rosette of the shark *Heptranchias perlo*. Zoology. 2017;122: 27–37. doi:10.1016/j.zool.2017.02.003

41. Lisney TJ, Collin SP. Brain morphology in large pelagic fishes: A comparison between sharks and teleosts. J Fish Biol. 2006;68: 532–554. doi:10.1111/j.0022-1112.2006.00940.x

42. Lisney TJ, Bennett MB, Collin SP. Volumetric analysis of sensory brain areas indicates ontogenetic shifts in the relative importance of sensory systems in elasmobranchs. Raffles Bull Zool. 2007;55: 7–15.

43. Camilieri-Asch V, Shaw JA, Yopak KE, Chapuis L, Partridge JC, Collin SP. Volumetric analysis and morphological assessment of the ascending olfactory pathway in an elasmobranch and a teleost using diceCT. Brain Struct Funct. 2020;225: 2347–2375. doi:10.1007/s00429-020-02127-1

44. Collin SP. The neuroecology of cartilaginous fishes: Sensory strategies for survival. Brain Behav Evol. 2012;80: 80–96. doi:10.1159/000339870

45. Jordan LK, Mandelman JW, McComb DM, Fordham S V, Carlson JK, Werner TB. Linking sensory biology and fisheries bycatch reduction in elasmobranch fishes: A review with new directions for research. Conserv Physiol. 2013;1: 1–20. doi:10.1093/conphys/cot002

46. Cave EJ, Kajiura SM. Effect of Deepwater Horizon Crude Oil Water Accommodated Fraction on Olfactory Function in the Atlantic Stingray, *Hypanus sabinus*. Sci Rep. 2018;8: 15786. doi:10.1038/s41598-018-34140-0

47. Pistevos JCA, Nagelkerken I, Rossi T, Olmos M, Connell SD. Ocean acidification and global warming impair shark hunting behaviour and growth. Sci Rep. 2015;5: 16293. doi:10.1038/srep16293

48. Dixson DL, Jennings AR, Atema J, Munday PL. Odor tracking in sharks is reduced under future ocean acidification conditions. Glob Chang Biol. 2015;21: 1454–1462. doi:10.1111/gcb.12678

49. Ferrando S, Gallus L, Ghigliotti L, Amaroli A, Abbas G, Vacchi M. Clarification of the Terminology of the Olfactory Lamellae in Chondrichthyes. Anat Rec. 2017;300: 2039–2045. doi:10.1002/ar.23632

50. Cox JPL. Ciliary function in the olfactory organs of sharks and rays. Fish Fish. 2012;14: 364–390. doi:10.1111/j.1467-2979.2012.00476.x

51. Rygg AD, Cox JPL, Abel R, Webb AG, Smith NB, Craven BA. A Computational Study of the Hydrodynamics in the Nasal Region of a Hammerhead Shark (Sphyrna tudes): Implications for Olfaction. PLoS One. 2013;8: e59783. doi:10.1371/journal.pone.0059783

52. Abel RL, Maclaine JS, Cotton R, Xuan VB, Nickels TB, Clark TH, et al. Functional morphology of the nasal region of a hammerhead shark. Comp Biochem Physiol - A Mol Integr Physiol. 2010;155: 464–475. doi:10.1016/j.cbpa.2009.10.029

53. Hamdani EH, Døving KB. The functional organization of the fish olfactory system. Progress in Neurobiology. Pergamon; 2007. pp. 80–86. doi:10.1016/j.pneurobio.2007.02.007

54. Trimmer C, Keller A, Murphy NR, Snyder LL, Willer JR, Nagai MH, et al. Genetic variation across the human olfactory receptor repertoire alters odor perception. Proc Natl Acad Sci U S A. 2019;116: 9475–9480. doi:10.1073/pnas.1804106115

55. Smith TD, Bhatnagar KP. Microsmatic primates: Reconsidering how and when size matters. Anat Rec. 2004;279B: 24–31. doi:10.1002/ar.b.20026

56. Meisami E. A proposed relationship between increases in the number of olfactory receptor neurons, convergence ratio and sensitivity in the developing rat. Dev Brain Res. 1989;46: 9–19. doi:10.1016/0165-3806(89)90139-9

57. Apfelbach R, Russ D, Slotnick BM. Ontogenetic changes in odor sensitivity, olfactory receptor area and olfactory receptor density in the rat. Chem Senses. 1991;16: 209–218. doi:10.1093/chemse/16.3.209

58. Korsching S. Aquatic Olfaction. In: Zufall F, Munger SD, editors. Chemosensory Transduction: The Detection of Odors, Tastes, and Other Chemostimuli. 1st ed. Boston: Academic Press; 2016. pp. 81–100. doi:10.1016/B978-0-12-801694-7.00005-6

59. Bargmann CI. Comparative chemosensation from receptors to ecology. Nature. 2006;444: 295–301. doi:10.1038/nature05402

60. Kishida T, Go Y, Tatsumoto S, Tatsumi K, Kuraku S, Toda M. Loss of olfaction in sea snakes provides new perspectives on the aquatic adaptation of amniotes. Proc R Soc B Biol Sci. 2019;286: 20191828. doi:10.1098/rspb.2019.1828

61. Hayden S, Bekaert M, Crider TA, Mariani S, Murphy WJ, Teeling EC. Ecological adaptation determines functional mammalian olfactory subgenomes. Genome Res. 2010;20: 1–9. doi:10.1101/gr.099416.109

62. Yang L, Jiang H, Wang Y, Lei Y, Chen J, Sun N, et al. Expansion of vomeronasal receptor genes (OlfC) in the evolution of fright reaction in Ostariophysan fishes. Commun Biol. 2019;2: 235. doi:10.1038/s42003-019-0479-2

63. Wang G, Shi P, Zhu Z, Zhang YP. More functional V1R genes occur in nest-living and nocturnal terricolous mammals. Genome Biol Evol. 2010;2: 277–283. doi:10.1093/gbe/evq020

64. Niimura Y, Matsui A, Touhara K. Acceleration of olfactory receptor gene loss in primate evolution: Possible link to anatomical change in sensory systems and dietary transition. Mol Biol Evol. 2018;35: 1437–1450. doi:10.1093/molbev/msy042

65. Saraiva LR, Ahuja G, Ivandic I, Syed AS, Marioni JC, Korsching SI, et al. Molecular and neuronal homology between the olfactory systems of zebrafish and mouse. Sci Rep. 2015;5: 11487. doi:10.1038/srep11487

66.   Bird DJ, Murphy WJ, Fox-Rosales L, Hamid I, Eagle RA, Van Valkenburgh B. Olfaction written in bone: cribriform plate size parallels olfactory receptor gene repertoires in Mammalia. Proc R Soc B Biol Sci. 2018;285: 20180100. doi:10.1098/rspb.2018.0100

67.   Theisen B, Zeiske E, Breucker H. Functional Morphology of the Olfactory Organs in the Spiny Dogfish (*Squalus acanthias* L.) and the Small-spotted Catshark (*Scyliorhinus canicula* (L.)). Acta Zool. 1986;67: 73–86.

68.   Zeiske E, Theisen B, Gruber SH. Functional morphology of the olfactory organ of two carcharhinid shark species. Can J Zool. 1987;65: 2406–2412. doi:10.1139/z87-362

69.   Zeiske E, Theisen B, Breucker H. Structure, development, and evolutionary aspects of the peripheral olfactory system. In: Hara TJ, editor. Fish Chemorreception. Dordrecht: Springer; 1992. pp. 13–39.

70.   Agbesi MPK, Naylor S, Perkins E, Borsuk HS, Sykes D, Maclaine JS, et al. Complex flow in the nasal region of guitarfishes. Comp Biochem Physiol -Part A Mol Integr Physiol. 2016;193: 52–63. doi:10.1016/j.cbpa.2015.12.007

71.   Fishelson L, Baranes A. Ontogenesis and cytomorphology of the nasal olfactory organs in the Oman shark, *Iago omanensis* (Triakidae), in the Gulf of Aqaba, Red Sea. Anat Rec. 1997;249: 409–421. doi:10.1002/(SICI)1097-0185(199711)249:3<409::AID-AR13>3.0.CO;2-S

72.   Bell MA. Convergent Evolution of Nasal Structure in Sedentary Elasmobranchs. Copeia. 1993; 144. doi:10.2307/1446305

73.   Timm LL, Fish FE. A comparative morphological study of head shape and olfactory cavities of sharks inhabiting benthic and coastal/pelagic environments. J Exp Mar Bio Ecol. 2012;414–415: 75–84. doi:10.1016/j.jembe.2012.01.016

74.   Caprio J. High sensitivity and specificity of olfactory and gustatory receptors of catfish to amino acids. In: Hara TJ, editor. Chemoreception in Fishes. Amsterdam: Elsevier; 1982. pp. 109–134.

75.   Takami S, Luer CA, Graziadei PPC. Microscopic structure of the olfactory organ of the clearnose skate, *Raja eglanteria*. Anat Embryol (Berl). 1994;190: 211–230. doi:10.1007/BF00234300

76.   Schneider CA, Rasband WS, Eliceiri KW. NIH Image to ImageJ: 25 years of image analysis. Nat Methods. 2012;9: 671–675. doi:10.1038/nmeth.2089

77. Schindelin J, Arganda-Carreras I, Frise E, Kaynig V, Longair M, Pietzsch T, et al. Fiji: An open-source platform for biological-image analysis. Nat Methods. 2012;9: 676–682. doi:10.1038/nmeth.2019

78. R Core Team. R: A Language and Environment for Statistical Computing. Vienna, Austria: R Foundation for Statistical Computing; 2019.

79. Bates D, Mächler M, Bolker BM, Walker SC. Fitting linear mixed-effects models using lme4. J Stat Softw. 2015;67: 1–48. doi:10.18637/jss.v067.i01

80. Zar JH. Biostatistical Analysis. Englewood Cliffs: Prentice-Hall; 1994.

81. Kuznetsova A, Brockhoff PB, Christensen RHB. lmerTest Package: Tests in Linear Mixed Effects Models. J Stat Softw. 2017;82. doi:10.18637/jss.v082.i13

82. Lenth R V. Least-Squares Means: The R Package Ismeans. J Stat Softw. 2016;69. doi:10.18637/jss.v069.i01.

83. Halekoh U, Højsgaard S. A kenward-roger approximation and parametric bootstrap methods for tests in linear mixed models–the R package pbkrtest. J Stat Softw. 2014;58: 1–30.

84. Meng Q, Yin M. A study of the olfactory organ of the sharks. Trans Chinese Ichthyol Soc. 1981; 1–24.

85. Elbert DA, Fowler S, Compagno L. Sharks of the World. A fully illustrated guide. Plymouth: Wild Nature Press; 2013.

86. Bernal D, Dickson KA, Shadwick RE, Graham JB. Review: Analysis of the evolutionary convergence for high performance swimming in lamnid sharks and tunas. Comp Biochem Physiol - A Mol Integr Physiol. 2001;129: 695–726. doi:10.1016/S1095-6433(01)00333-6

87. Semmens JM, Payne NL, Huveneers C, Sims DW, Bruce BD. Feeding requirements of white sharks may be higher than originally thought. Sci Rep. 2013;3: 1471. doi:10.1038/srep01471

88. Camilieri-Asch V, Yopak KE, Rea A, Mitchell JD, Partridge JC, Collin SP. Convergence of Olfactory Inputs within the Central Nervous System of a Cartilaginous and a Bony Fish: An Anatomical Indicator of Olfactory Sensitivity. Brain Behav Evol. 2020;95: 139–161. doi:10.1159/000510688

89. Corey EA, Ache BW. Comparative Olfactory Transduction. In: Zufall F, Munger SD, editors. Chemosensory Transduction: The Detection of Odors, Tastes, and Other Chemostimuli. 1st ed.

Boston: Academic Press; 2016. pp. 207–223. doi:10.1016/B978-0-12-801694-7.00012-3

90. Yoshihito Niimura. Olfactory Receptor Multigene Family in Vertebrates: From the Viewpoint of Evolutionary Genomics. Curr Genomics. 2012;13: 103–114. doi:10.2174/138920212799860706

91. Shi P, Zhang J. Comparative genomic analysis identifies an evolutionary shift of vomeronasal receptor gene repertoires in the vertebrate transition from water to land. Genome Res. 2007;17: 166–174. doi:10.1101/gr.6040007

92. Nikaido M, Suzuki H, Toyoda A, Fujiyama A, Hagino-Yamagishi K, Kocher TD, et al. Lineage-Specific Expansion of Vomeronasal Type 2 Receptor-Like (OlfC) Genes in Cichlids May Contribute to Diversification of Amino Acid Detection Systems. Genome Biol Evol. 2013;5: 711–722. doi:10.1093/gbe/evt041

93. Eyun S Il, Moriyama H, Hoffmann FG, Moriyama EN. Molecular evolution and functional divergence of trace amine-associated receptors. PLoS One. 2016;11: e0151023. doi:10.1371/journal.pone.0151023

94. Nikaido M, Ota T, Hirata T, Suzuki H, Satta Y, Aibara M, et al. Multiple Episodic Evolution Events in V1R Receptor Genes of East-African Cichlids. Genome Biol Evol. 2014;6: 1135–1144. doi:10.1093/gbe/evu086

95. Liu A, He F, Shen L, Liu R, Wang Z, Zhou J. Convergent degeneration of olfactory receptor gene repertoires in marine mammals. BMC Genomics. 2019;20: 997. doi:10.1186/s12864-019-6290-0

96. Tsagkogeorga G, Müller S, Dessimoz C, Rossiter SJ. Comparative genomics reveals contraction in olfactory receptor genes in bats. Sci Rep. 2017;7: 259. doi:10.1038/s41598-017-00132-9

97. Venkatesh B, Lee AP, Ravi V, Maurya AK, Lian MM, Swann JB, et al. Elephant shark genome provides unique insights into gnathostome evolution. Nature. 2014;505: 174–179. doi:10.1038/nature12826

98. Hara Y, Yamaguchi K, Onimaru K, Kadota M, Koyanagi M, Keeley SD, et al. Shark genomes provide insights into elasmobranch evolution and the origin of vertebrates. Nat Ecol Evol. 2018;2: 1761–1771. doi:10.1038/s41559-018-0673-5

99. Marra NJ, Stanhope MJ, Jue NK, Wang M, Sun Q, Pavinski Bitar P, et al. White shark genome reveals ancient elasmobranch adaptations associated with wound healing and the maintenance of genome stability. Proc Natl Acad Sci U S A. 2019;116: 4446–4455.

doi:10.1073/pnas.1819778116

100. Sharma K, Syed AS, Ferrando S, Mazan S, Korsching SI. The chemosensory receptor repertoire of a true shark is dominated by a single olfactory receptor family. Genome Biol Evol. 2019;11: 398–405. doi:10.1093/gbe/evz002

101. Niimura Y. Identification of chemosensory receptor genes from vertebrate genomes. In: Touhara K, editor. Pheromone signaling Methods in molecular biology (methods and protocols). Totowa: Humana Press; 2013. pp. 95–105. doi:10.1007/978-1-62703-619-1_7

102. Inoue JG, Miya M, Lam K, Tay B-H, Danks JA, Bell J, et al. Evolutionary Origin and Phylogeny of the Modern Holocephalans (Chondrichthyes: Chimaeriformes): A Mitogenomic Perspective. Mol Biol Evol. 2010;27: 2576–2586. doi:10.1093/molbev/msq147

103. Li Q, Liberles SD. Odor Sensing by Trace Amine-Associated Receptors. In: Zufall F, Munger SD, editors. Chemosensory Transduction: The Detection of Odors, Tastes, and Other Chemostimuli. 1st ed. Boston: Academic Press; 2016. pp. 67–80. doi:10.1016/B978-0-12-801694-7.00004-4

104. Vanderhaeghen P, Schurmans S, Vassart G, Parmentier M. Olfactory receptors are displayed on dog mature sperm cells. J Cell Biol. 1993;123: 1441–1452. doi:10.1083/jcb.123.6.1441

105. Ferrando S, Gallus L. Is the olfactory system of cartilaginous fishes a vomeronasal system? Front Neuroanat. 2013;7. doi:10.3389/fnana.2013.00037

106. Ferrando S, Gambardella C, Ravera S, Bottero S, Ferrando T, Gallus L, et al. Immunolocalization of G-Protein Alpha Subunits in the Olfactory System of the Cartilaginous Fish *Scyliorhinus Canicula*. Anat Rec Adv Integr Anat Evol Biol. 2009;292: 1771–1779. doi:10.1002/ar.21003

107. Ferrando S, Gallus L, Gambardella C, Vacchi M, Tagliafierro G. G protein alpha subunits in the olfactory epithelium of the holocephalan fish *Chimaera monstrosa*. Neurosci Lett. 2010;472: 65–67. doi:10.1016/J.NEULET.2010.01.059

108. Conesa A, Madrigal P, Tarazona S, Gomez-Cabrero D, Cervera A, McPherson A, et al. A survey of best practices for RNA-seq data analysis. Genome Biol. 2016;17: 13. doi:10.1186/s13059-016-0881-8

109. Delhomme N, Mähler N, Schiffthaler B, Sundell D, Mannapperuma C, Hvidsten TR, et al. Guidelines for RNA-Seq data analysis. Epigenesys. 2014.

110. Ewels P, Magnusson M, Lundin S, Käller M. MultiQC: Summarize analysis results for multiple tools and samples in a single report. Bioinformatics. 2016;32: 3047–3048. doi:10.1093/bioinformatics/btw354

111. Kopylova E, Noé L, Touzet H. SortMeRNA: Fast and accurate filtering of ribosomal RNAs in metatranscriptomic data. Bioinformatics. 2012;28: 3211–3217. doi:10.1093/bioinformatics/bts611

112. Bolger AM, Lohse M, Usadel B. Trimmomatic: A flexible trimmer for Illumina sequence data. Bioinformatics. 2014;30: 2114–2120. doi:10.1093/bioinformatics/btu170

113. Haas BJ, Papanicolaou A, Yassour M, Grabherr M, Blood PD, Bowden J, et al. De novo transcript sequence reconstruction from RNA-seq using the Trinity platform for reference generation and analysis. Nat Protoc. 2013;8: 1494–1512. doi:10.1038/nprot.2013.084

114. Simão FA, Waterhouse RM, Ioannidis P, Kriventseva E V, Zdobnov EM. BUSCO: Assessing genome assembly and annotation completeness with single-copy orthologs. Bioinformatics. 2015;31: 3210–3212. doi:10.1093/bioinformatics/btv351

115. Afgan E, Baker D, Batut B, Van Den Beek M, Bouvier D, Ech M, et al. The Galaxy platform for accessible, reproducible and collaborative biomedical analyses: 2018 update. Nucleic Acids Res. 2018;46: W537–W544. doi:10.1093/nar/gky379

116. Li B, Dewey CN. RSEM: Accurate transcript quantification from RNA-Seq data with or without a reference genome. BMC Bioinformatics. 2011;12: 323. doi:10.1186/1471-2105-12-323

117. Camacho C, Coulouris G, Avagyan V, Ma N, Papadopoulos J, Bealer K, et al. BLAST+: Architecture and applications. BMC Bioinformatics. 2009;10: 421. doi:10.1186/1471-2105-10-421

118. Buchfink B, Xie C, Huson DH. Fast and sensitive protein alignment using DIAMOND. Nat Methods. 2014;12: 59–60. doi:10.1038/nmeth.3176

119. Niimura Y. On the Origin and Evolution of Vertebrate Olfactory Receptor Genes: Comparative Genome Analysis Among 23 Chordate Species. Genome Biol Evol. 2009;1: 34–44. doi:10.1093/gbe/evp003

120. Eyun S, Moriyama H, Hoffmann FG, Moriyama EN. Molecular Evolution and Functional Divergence of Trace Amine–Associated Receptors. PLoS One. 2016;11: e0151023. doi:10.1371/journal.pone.0151023

121. Zapilko V, Korsching SI. Tetrapod V1R-like ora genes in an early-diverging ray-finned fish species: The canonical six ora gene repertoire of teleost fish resulted from gene loss in a larger ancestral repertoire. BMC Genomics. 2016;17: 83. doi:10.1186/s12864-016-2399-6

122. Hashiguchi Y, Nishida M. Evolution and origin of vomeronasal-type odorant receptor gene repertoire in fishes. BMC Evol Biol. 2006;6: 76. doi:10.1186/1471-2148-6-76

123. Alioto TS, Ngai J. The repertoire of olfactory C family G protein-coupled receptors in zebrafish: candidate chemosensory receptors for amino acids. BMC Genomics. 2006;7: 309. doi:10.1186/1471-2164-7-309

124. Haas B. TransDecoder (Find Coding Regions Within Transcripts). 2016.

125. Nguyen L-T, Schmidt HA, von Haeseler A, Minh BQ. IQ-TREE: A Fast and Effective Stochastic Algorithm for Estimating Maximum-Likelihood Phylogenies. Mol Biol Evol. 2014;32: 268–274. doi:10.1093/molbev/msu300

126. Kalyaanamoorthy S, Minh BQ, Wong TKF, Von Haeseler A, Jermiin LS. ModelFinder: Fast model selection for accurate phylogenetic estimates. Nat Methods. 2017;14: 587–589. doi:10.1038/nmeth.4285

127. Letunic I, Bork P. Interactive Tree of Life (iTOL) v4: Recent updates and new developments. Nucleic Acids Res. 2019;47: W256–W259. doi:10.1093/nar/gkz239

128. Liberles SD. Trace amine-associated receptors: Ligands, neural circuits, and behaviors. Curr Opin Neurobiol. 2015;34: 1–7. doi:10.1016/j.conb.2015.01.001

129. Naylor GJP, Caira JN, Jensen K, Rosana KAM, Straube N, Lakner C. Elasmobranch Phylogeny: A Mitochondrial Estimate Based on 595 Species. In: Carrier JC, Musick JA, Heithaus MR, editors. Biology of Sharks and Their Relatives. 2nd ed. Boca Raton: CRC Press; 2012. pp. 31–56. doi:10.1201/b11867-9

130. Nei M, Niimura Y, Nozawa M. The evolution of animal chemosensory receptor gene repertoires: Roles of chance and necessity. Nat Rev Genet. 2008;9: 951–963. doi:10.1038/nrg2480

131. Ahuja G, Reichel V, Kowatschew D, Syed AS, Kotagiri AK, Oka Y, et al. Overlapping but distinct topology for zebrafish V2R-like olfactory receptors reminiscent of odorant receptor spatial expression zones. BMC Genomics. 2018;19: 383. doi:10.1186/s12864-018-4740-8

132. Johnstone KA, Lubieniecki KP, Koop BF, Davidson WS. Expression of olfactory receptors in

different life stages and life histories of wild Atlantic salmon (*Salmo salar*). Mol Ecol. 2011;20: 4059–4069. doi:10.1111/j.1365-294X.2011.05251.x

133. Zhu G, Wang L, Tang W, Liu D, Yang J. De Novo Transcriptomes of Olfactory Epithelium Reveal the Genes and Pathways for Spawning Migration in Japanese Grenadier Anchovy (*Coilia nasus*). PLoS One. 2014;9: e103832. doi:10.1371/journal.pone.0103832

134. Zhang S, Zhang Z, Wang H, Kong X. Antennal transcriptome analysis and comparison of olfactory genes in two sympatric defoliators, *Dendrolimus houi* and *Dendrolimus kikuchii* (Lepidoptera: Lasiocampidae). Insect Biochem Mol Biol. 2014;52: 69–81. doi:10.1016/J.IBMB.2014.06.006

135. van der Linden C, Jakob S, Gupta P, Dulac C, Santoro SW. Sex separation induces differences in the olfactory sensory receptor repertoires of male and female mice. Nat Commun. 2018;9: 5081. doi:10.1038/s41467-018-07120-1

136. Libants S, Carr K, Wu H, Teeter JH, Chung-Davidson YW, Zhang Z, et al. The sea lamprey Petromyzon marinus genome reveals the early origin of several chemosensory receptor families in the vertebrate lineage. BMC Evol Biol. 2009;9: 180. doi:10.1186/1471-2148-9-180

137. Mathewson RF, Hodgson ES. Klinotaxis and rheotaxis in orientation of sharks toward chemical stimuli. Comp Biochem Physiol -- Part A Physiol. 1972;42: 79–84. doi:10.1016/0300-9629(72)90369-6

138. Ache BW, Young JM. Olfaction: Diverse species, conserved principles. Neuron. 2005;48: 417–430. doi:10.1016/j.neuron.2005.10.022

139. Taylor JS, Raes J. Duplication and Divergence: The Evolution of New Genes and Old Ideas. Annu Rev Genet. 2004;38: 615–643. doi:10.1146/annurev.genet.38.072902.092831

140. Luu P, Acher F, Bertrand HO, Fan J, Ngai J. Molecular determinants of ligand selectivity in a vertebrate odorant receptor. J Neurosci. 2004;24: 10128–10137. doi:10.1523/JNEUROSCI.3117-04.2004

141. Cong X, Zheng Q, Ren W, Chéron JB, Fiorucci S, Wen T, et al. Zebrafish olfactory receptors ORAs differentially detect bile acids and bile salts. J Biol Chem. 2019;294: 6762–6771. doi:10.1074/jbc.RA118.006483

142. Weissburg MJ, Browman HI, Fields DM, Hemmi JM, Zeil J, Higgs DM, et al. Sensory biology: Linking the internal and external ecologies of marine organisms. Mar Ecol Prog Ser. 2005;287:

263–307. doi:10.3354/meps287263

143. Timm-Davis LL, Fish FE. Flow through the nasal cavity of the spiny dogfish, *Squalus acanthias*. Eur Phys J Spec Top. 2015;224: 3407–3417. doi:10.1140/epjst/e2015-50037-1

144. Bigman JS, Pardo SA, Prinzing TS, Dando M, Wegner NC, Dulvy NK. Ecological lifestyles and the scaling of shark gill surface area. J Morphol. 2018;279: 1716–1724. doi:10.1002/jmor.20879

145. Ryan LA, Meeuwig JJ, Hemmi JM, Collin SP, Hart NS. It is not just size that matters: shark cruising speeds are species-specific. Mar Biol. 2015;162: 1307–1318. doi:10.1007/s00227-015-2670-4

146. Wilga CAD, Lauder G V. Biomechanics of locomotion in sharks, rays, and chimeras. In: Carrier JC, Musick JA, Heithaus MR, editors. Biology of Sharks and Their Relatives. 1st ed. Boca Raton: CRC Press; 2004. pp. 148–157. doi:10.1201/b11867-13

147. Teşileanu T, Cocco S, Monasson R, Balasubramanian V. Adaptation of olfactory receptor abundances for efficient coding. Elife. 2019;8: e39279. doi:10.7554/eLife.39279

148. Barrón C, Duarte CM. Dissolved organic carbon pools and export from the coastal ocean. Global Biogeochem Cycles. 2015;29: 1725–1738. doi:10.1002/2014GB005056

149. Hyndes GA, Nagelkerken I, Mcleod RJ, Connolly RM, Lavery PS, Vanderklift MA. Mechanisms and ecological role of carbon transfer within coastal seascapes. Biol Rev. 2014;89: 232–254. doi:10.1111/brv.12055

150. Corrigan S, Lowther AD, Beheregaray LB, Bruce BD, Cliff G, Duffy CA, et al. Population Connectivity of the Highly Migratory Shortfin Mako (*Isurus oxyrinchus* Rafinesque 1810) and Implications for Management in the Southern Hemisphere. Front Ecol Evol. 2018;6: 187. doi:10.3389/fevo.2018.00187

151. Hansell DA, Carlson CA, Repeta DJ, Schlitzer R. Dissolved organic matter in the ocean: A controversy stimulates new insights. Oceanography. 2009;22: 202–211. doi:10.5670/oceanog.2009.109

152. Rogers PJ, Huveneers C, Page B, Hamer DJ, Goldsworthy SD, Mitchell JG, et al. A quantitative comparison of the diets of sympatric pelagic sharks in gulf and shelf ecosystems off southern Australia. ICES J Mar Sci. 2012;69: 1382–1393. doi:10.1093/icesjms/fss100

153. Nevitt GA. The Neuroecology of Dimethyl Sulfide: A Global-Climate Regulator Turned Marine

Infochemical. Integr Comp Biol. 2011;51: 819–825. doi:10.1093/icb/icr093

154. Kowalewsky S, Dambach M, Mauck B, Dehnhardt G. High olfactory sensitivity for dimethyl sulphide in harbour seals. Biol Lett. 2006;2: 106–109. doi:10.1098/rsbl.2005.0380

155. Endres CS, Lohmann KJ. Perception of dimethyl sulfide (DMS) by loggerhead sea turtles: A possible mechanism for locating high-productivity oceanic regions for foraging. J Exp Biol. 2012;215: 3535–3538. doi:10.1242/jeb.073221

156. Yamamoto Y, Shibata H, Ueda H. Olfactory Homing of Chum Salmon to Stable Compositions of Amino Acids in Natal Stream Water. Zoolog Sci. 2013;30: 607. doi:10.2108/zsj.30.607

157. Yopak KE, Lisney TJ. Allometric Scaling of the Optic Tectum in Cartilaginous Fishes. Brain Behav Evol. 2012;80: 108–126. doi:10.1159/000339875

158. Yopak KE. Neuroecology of cartilaginous fishes: The functional implications of brain scaling. J Fish Biol. 2012;80: 1968–2023. doi:10.1111/j.1095-8649.2012.03254.x

159. Yopak KE, Lisney TJ, Collin SP, Montgomery JC. Variation in Brain Organization and Cerebellar Foliation in Chondrichthyans: Sharks and holocephalans. Brain Behav Evol. 2007;69: 280–300. doi:10.1159/000100037

160. Jacobs LF. From chemotaxis to the cognitive map: The function of olfaction. Proc Natl Acad Sci U S A. 2012;109: 10693–10700. doi:10.1073/pnas.1201880109

161. Finlay BL, Hinz F, Darlington RB. Mapping behavioural evolution onto brain evolution: The strategic roles of conserved organization in individuals and species. Proc R Soc B Biol Sci. 2011;366: 2111–2123. doi:10.1098/rstb.2010.0344

Supplementary Material

Chapter 2

Table S2.1 Dimensions of the whole animal and the olfactory epithelium of the specimens of blind shark and mako shark of this study

| Species | ID | Sex | Individual | | Olfactory Epithelium | | | | | | | |
			Length (cm)	Mass (kg)	Length (mm)	Width (mm)	Depth (mm)	Mass (g)	Number of lamellae	Area of lamellae (mm^2)	Ratio sensory	Sinuosity ratio
B. waddi	1	Male	60	1.23	17.15	11.88	12.51	1.72	84	20.93 ± 18.23	0.47 ± 0.07	1.78 ± 0.67
	2	Female	58	0.97	16.42	10.23	14.57	1.67	86	22.54 ± 12.28	0.45 ± 0.05	1.57 ± 0.54
	3	-	23	0.57	7.87	4.54	5.73	0.23	83	6.70 ± 2.32	0.64 ± 0.03	1.29 ± 0.26
I. oxyrinchus	1	Female	215	70	32.41	24.56	23.64	10.13	54	138.40 ± 54.16	0.74 ± 0.03	2.52 ± 1.26
	2	Female	280	174	41.41	26.41	27.55	20.04	60	224.23 ± 90.03	0.77 ± 0.07	2.94 ± 1.71
	3	Male	282	111	41.86	30.38	27.23	22.75	56	217.00 ±89.54	0.86 ± 0.06	2.86 ± 1.64

Values are mean ± 1 std. dev.

Table S2.2 Coefficients from linear mixed-effects model investigating the change in secondary folding between different areas of the lamellae in the blind and mako shark.

Species	Fragment comparison	Estimate	SE	df	*t-value*	*P*
B. waddi	Superior – Superior-Medial	-0.162	0.026	3354	-6.161	**<0.0001**
	Superior – Inferior-Medial	-0.300	0.033	3354	-9.207	**<0.0001**
	Superior – Inferior	-0.342	0.043	3354	-7.991	**<0.0001**
	Superior-Medial – Inferior-Medial	-0.139	0.036	3354	-3.84	**0.0007**
	Superior-Medial – Inferior	-0.180	0.046	3354	-3.921	**0.0005**
	Inferior-Medial – Inferior	-0.041	0.049	3354	-0.846	0.8326
I. oxyrinchus	Superior – Superior-Medial	-0.261	0.026	3354	-10.161	**<0.0001**
	Superior – Inferior-Medial	-0.342	0.027	3354	-12.554	**<0.0001**
	Superior – Inferior	-0.348	0.028	3354	-12.636	**<0.0001**
	Superior-Medial – Inferior-Medial	-0.081	0.030	3354	-2.651	**0.0402**
	Superior-Medial – Inferior	-0.087	0.031	3354	-2.818	**0.0251**
	Inferior-Medial – Inferior	-0.006	0.032	3354	-0.199	0.9972

SE: Standard error; df: degrees of freedom, P: p-value.

Table S2.3 Coefficients from linear mixed-effects model investigating the surface area of the olfactory organs obtained between measurements considering different morphological traits for the blind and mako shark.

Species	Method comparison	Estimate	SE	df	*t-value*	*P*
B. waddi	GSA - SSA	0.654	0.106	16.000	6.179	**0.0001**
	GSA - SAMS	-0.909	0.106	16	-8.591	**<.0001**
	GSA - TSA-SF	-0.431	0.106	16	-4.07	**0.0068**
	GSA - TSSA-SF	0.223	0.106	16	2.109	0.2636
	SSA- SAMS	-1.562	0.106	16	-14.77	**<0.0001**
	SSA- TSA-SF	-1.084	0.106	16	-10.249	**<.0001**
	SSA- TSSA-SF	-0.431	0.106	16	-4.07	**0.0068**
	SAMS- TSA-SF	0.478	0.106	16	4.521	**0.0028**
	SAMS- TSSA-SF	1.132	0.106	16	10.7	**<.0001**
	TSA-SF - TSSA-SF	0.654	0.106	16	6.179	**0.0001**
I. oxyrinchus	GSA - SSA	0.31	0.106	16	2.935	0.0637
	GSA - SAMS	-1.917	0.106	16	-18.125	**<0.0001**
	GSA - TSA-SF	-1.019	0.106	16	-9.63	**<.0001**
	GSA - TSSA-SF	-0.708	0.106	16	-6.694	**<.0001**
	SSA- SAMS	-2.228	0.106	16	-21.061	**<.0001**
	SSA- TSA-SF	-1.329	0.106	16	-12.565	**<0.0001**
	SSA- TSSA-SF	-1.019	0.106	16	-9.63	**<.0001**
	SAMS- TSA-SF	0.899	0.106	16	8.496	**<.0001**
	SAMS- TSSA-SF	1.209	0.106	16	11.431	**<.0001**
	TSA-SF - TSSA-SF	0.31	0.106	16	2.935	0.0637

SE: Standard error; df: degrees of freedom, P: p-value. GSA: Gross surface area; SSA: Sensory surface area.; SAMS: surface area with maximum sinuosity; TSA-SF: total surface area with mean sinuosity; TSSA-SF: total sensory surface area with the mean sinuosity and the proportion of sensory epithelium

Table S2.4 Regression lines (allometric equations) for the surface area of the olfactory organ of the blind and mako shark described in Fig. 2.7.

Species	Total Length (cm)					Total Mass (Kg)				
	GSA	SSA	SAMS	TSA-SF	TSSA-SF	GSA	SSA	SAMS	TSA-SF	TSSA-SF
Blind shark	$y = 2.35x^{0.033}$	$y = 2.11x^{0.024}$	$y = 2.73x^{0.044}$	$y = 2.43x^{0.040}$	$y = 2.20x^{0.031}$	$y = 2.19x^{1.86}$	$y = 1.99x^{1.37}$	$y = 2.42x^{2.59}$	$y = 2.17x^{2.35}$	$y = 1.97x^{1.86}$
	$R^2 = 0.986$	$R^2 = 0.991$	$R^2 = 0.999$	$R^2 = 0.999$	$R^2 = 0.999$	$R^2 = 0.793;$	$R^2 = 0.810$	$R^2 = 0.869$	$R^2 = 0.857$	$R^2 = 0.885$
Mako shark	$y = 3.96x^{0.008}$	$y = 3.74x^{0.007}$	$y = 4.85x^{0.012}$	$y = 4.43x^{0.010}$	$y = 4.21x^{0.009}$	$y = 5.43x^{0.005}$	$y = 5.06x^{0.005}$	$y = 7.03x^{0.008}$	$y = 6.28x^{0.006}$	$y = 5.91x^{0.007}$
	$R^2 = 0.965$	$R^2 = 0.865$	$R^2 = 0.959$	$R^2 = 0.964$	$R^2 = 0.889$	$R^2 = 0.785$	$R^2 = 0.915$	$R^2 = 0.796$	$R^2 = 0786$	$R^2 = 0.899$

GSA: Gross surface area; SSA: Sensory surface area.; SAMS: surface area with maximum sinuosity; TSA-SF: total surface area with mean sinuosity; TSSA-SF: total sensory surface area with the mean sinuosity and the proportion of sensory epithelium

Supplementary Equation 2.1. Gross surface area (GSA).

$$GSA = \bar{X}\{Gross\ Lamellar\ Surface\ Area\} \times No.lamellae \times 4$$

Supplementary Equation 2.2. Sensory surface area (SSA).

$$SSA = \bar{X}\left\{\frac{Lamellar\ Sensory\ Surface\ Area\ (SEM)}{Lamellar\ Surface\ Area\ (SEM)}\right\} \times \bar{X}\{Gross\ Lamellar\ Surface\ Area\}$$
$$\times No.\ lamellae \times 4$$

Supplementary Equation 2.3. Total surface area accounting for secondary folding (TSA-SF).

$$TSA\text{-}SF = \bar{X}\left\{\frac{Curvilinear\ Length\ (LM)}{Straight\ length\ (LM)}\right\} \times \bar{X}\{Gross\ Lamellar\ Surface\ Area\} \times No.lamellae \times 4$$

Supplementary Equation 2.4 Total sensory surface area accounting for mean secondary folding and the proportion of sensory epithelium (TSSA-SF).

$$TSSA\text{-}SF = \bar{X}\left\{\frac{Curvilinear\ Length\ (LM)}{Straight\ length\ (LM)}\right\} \times \bar{X}\left\{\frac{Lamellar\ sensory\ surface\ area\ (SEM)}{Lamellar\ surface\ area\ (SEM)}\right\}$$
$$\times\ \bar{X}\left\{Gross\ Lamellar\ Surface\ Area\right\} \times No.lamellae \times 4$$
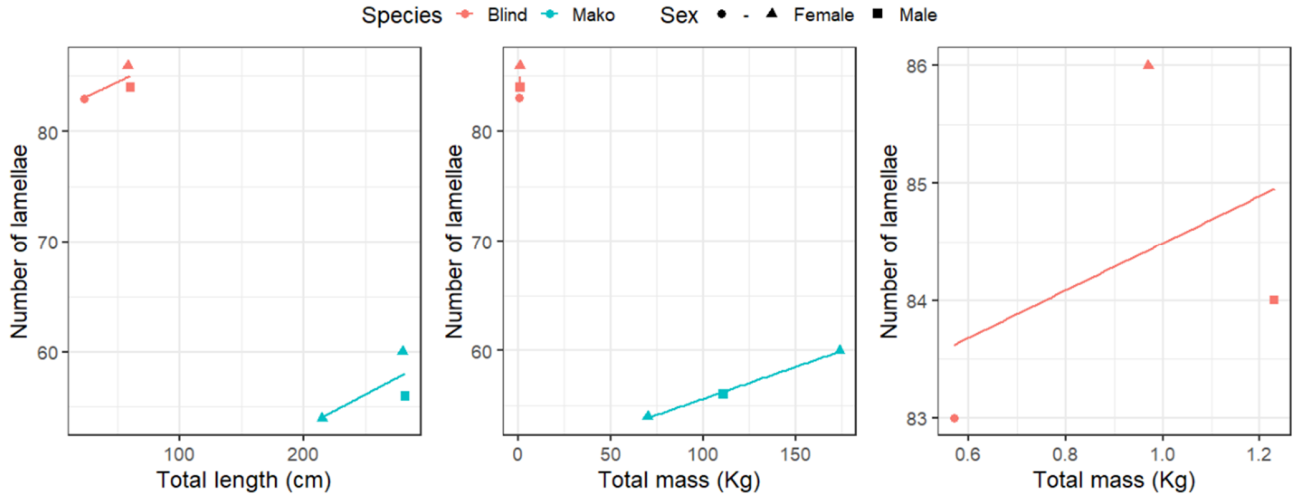
Fig S2.1

Fig S2.1. Number of lamellae of the olfactory organ of *B. waddi* and *I. oxyrinchus* in relation to total size. **Left panel**, Number of lamellae in relation to the total length of the shark. Regression coefficients: *B. waddi*: $y = 4.41x^{0.0006}$, $R^2 = 0.528$; *I oxyrinchus*: $y = 3.76x^{0.0010}$, $R^2 = 0.559$. **Middle panel**: Number of lamellae in relation to the total body mass of the shark. **Right panel**: Close up of the number of lamellae of *B. waddi* in relation to the total mass. Regression coefficients *B. waddi*: $y = 4.41x^{0.0241}$, $R^2 = 0.197$; *I. oxyrinchus*: $y = 3.92x^{0.0010}$, $R^2 = 0.997$.
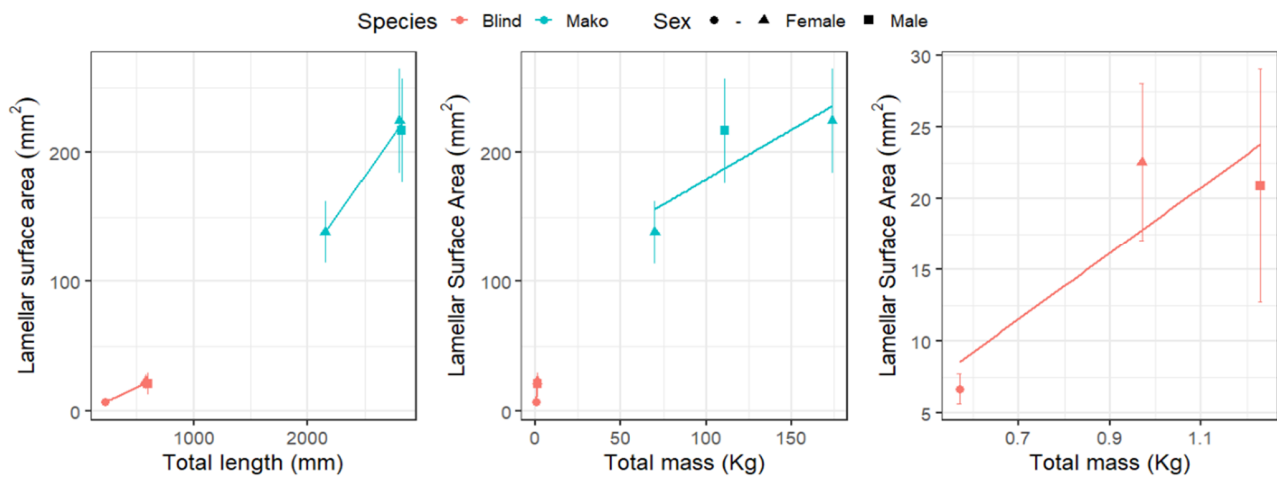
Fig S2.2

Fig S2.2. Gross surface area of the olfactory lamellae of *B. waddi* and *I. oxyrinchus* in relation to total size. Each data point represents the average surface area of five lamellae from one individual. Error bars represent standard deviation. **Left panel**: Lamellar surface area in relation to the total length of the shark. Regression coefficients: *B. waddi*: $y = 1.16x^{0.0032}$, $R^2 = 0.989$; *I. oxyrinchus*: $y = 3.42x^{0.0007}$, $R^2 = 0.992$. **Middle panel**: Lamellar surface area in relation to the total mass of the shark. **Right panel**: Close up of the lamellar surface area of *B. waddi* in relation to the total mass. Regression coefficients: *B. waddi*: $y = 0.99x^{1.83}$, $R^2 = 0.806$; *I. oxyrinchus*: $y = 4.73x^{0.0042}$, $R^2 = 0.696$.
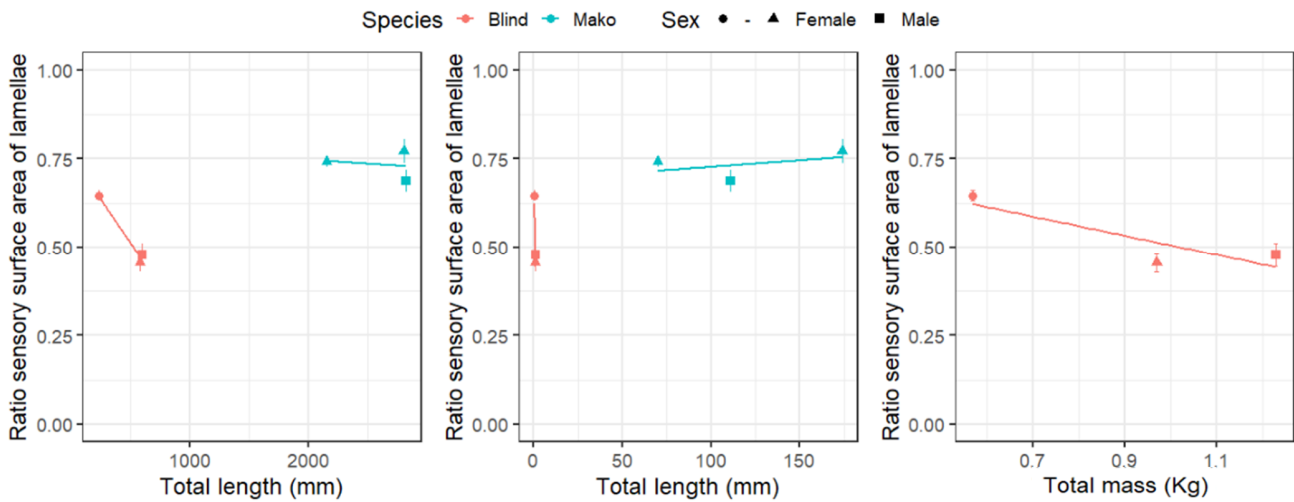
Fig S2.3

Fig S2.3. Ratio of sensory surface area:total surface area of the lamellae of *B. waddi* and *I. oxyrinchus* in relation to total size. Each data point represents the average ratio of five lamellae from one individual. Error bars represent standard deviation. **Left panel**: Ratio of lamellar sensory surface area in relation to the total length of the shark. Regression coefficients: *B. waddi*: $y = -0.23x^{-0.0008}$, $R^2 = 0.969$; *I. oxyrinchus*: $y = -0.22x^{-0.0001}$, $R^2 = 0.04$. **Middle panel:** Ratio of lamellar sensory surface area in relation to the total mass of the shark. **Right panel**: Ratio of lamellar sensory surface area of *B. waddi* in relation to the total mass. Regression coefficients: *B. waddi*: $y = -0.20x^{-0.492}$, $R^2 = 0.744$; *I. oxyrinchus*: $y = -0.36x^{0.0004}$, $R^2 = 0.194$.
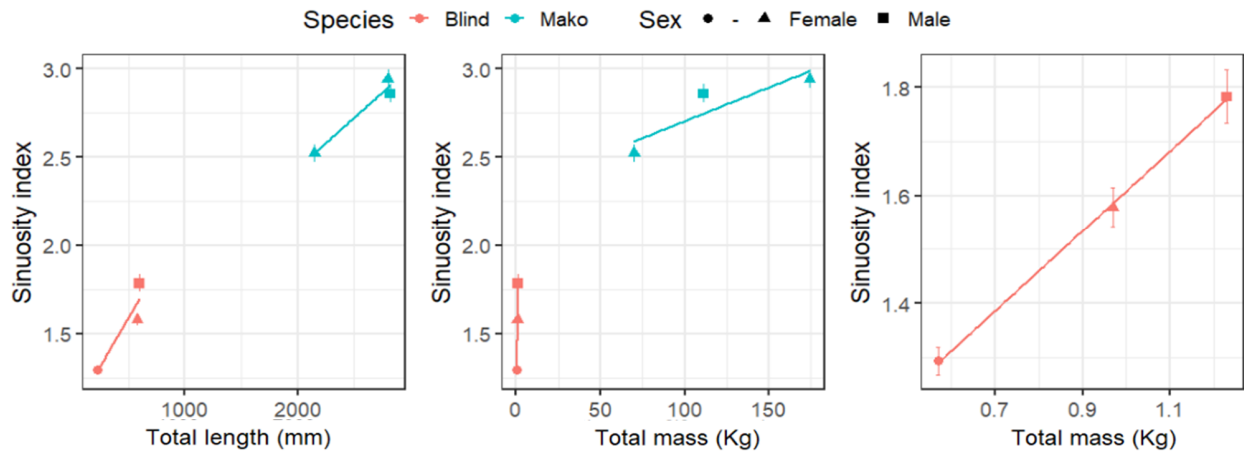
Fig S2.4

Fig S2.4. Sinuosity index of the lamellae of *B. waddi* and *I. oxyrinchus* in relation to total size.
Each data point represents the average ratio of all the sections of five lamellae from one individual.
Error bars represent standard deviation. **Left panel**: Ratio of lamellar sensory surface area in relation
to the total length of the shark. Regression coefficients: *B. waddi*: $y = 0.08x^{0.0007}$, $R^2 = 0.891$;
I. oxyrinchus: $y = 0.47x^{0.0002}$, $R^2 = 0.96$. **Middle panel**: Ratio of lamellar sensory surface area in
relation to the total mass of the shark. **Right panel**: Ratio of lamellar sensory surface area of *B. waddi*
in relation to the total mass. Regression coefficients: *B. waddi*: $y = -0.01x^{0.488}$, $R^2 = 0.999$;
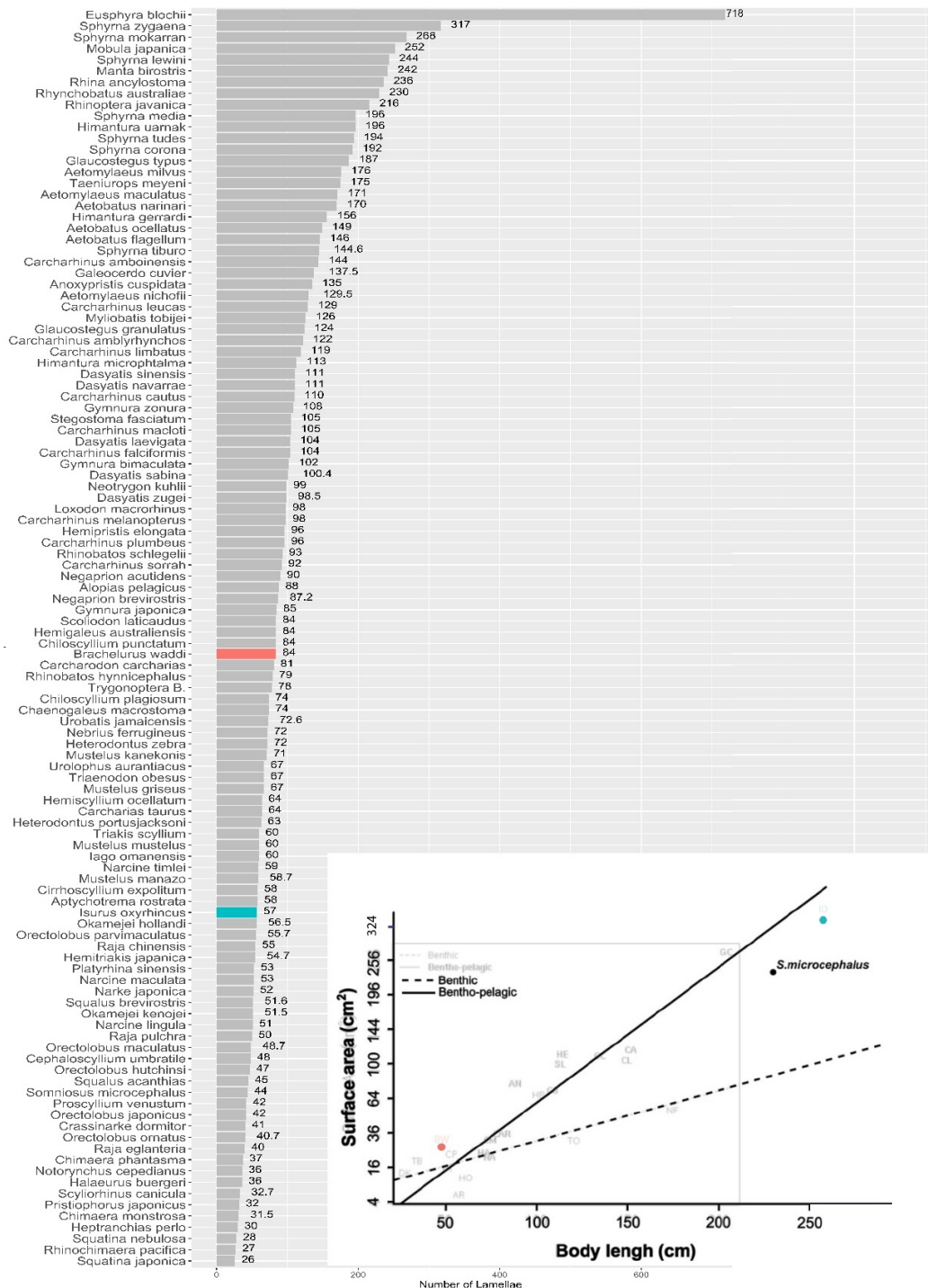*I. oxyrinchus*: $y = 0.85x^{0.0014}$, $R^2 = 0.793$.

Fig S2.5

Fig S2.5. Number of lamellae and sensory surface area of *B. waddi (red)* and *I. oxyrinchus (blue)* in relation to other studies. Number of lamellae recompiled from Ferrando et al. [49]. Inset: Sensory surface area in relation to the total length of benthic and bentho-pelagic species modified from Schluessel et al. [32] and Ferrando et al. [39].

Chapter 3

Table S3.1. Morphometric information on the specimens of blind shark and mako shark used in this study, RNA integrity number (RIN), and sequencing batch.

	ID	Sex	Length (cm)	Weight (Kg)	Delay of extraction after death	RIN	Batch Number
Brachaelurus waddi	1	Female	55.5	0.942	<5 min	9.2	1
	2	Male	13	0.183	<5 min	9.5	1
	3	Male	66	1.82	<5 min	9	2
Isurus oxyrinchus	1	Female	247	100.5	~ 5 hours	6.2	1
	2	Female	275	155.8	~ 2 hours	8.8	2
	3	Female	260	111.4	~ 4 hours	8.8	2

Table S3.2. Coefficients from linear mixed-effects model investigating expression differences of the three canonical olfactory receptor gene families in blind and mako shark.

Species	Receptor family comparison	Estimate	SE	df	*t-value*	*P*
B. waddi	OR – V1R	-0.2399	0.204	8	-1.173	0.500
	OR – V2R	-2.8496	0.204	8	-13.936	**<.0001**
	V1R – V2R	-2.6096	0.204	8	-7.991	**<.0001**
I. oxyrinchus	OR – V1R	-0.0893	0.204	8	-0.437	0.9014
	OR – V2R	-2.0564	0.204	8	-10.057	**<.0001**
	V1R – V2R	-1.9671	0.204	8	-9.620	**<.0001**

SE: Standard error; df: degrees of freedom, P: p-value.

Table S3.3. Coefficients from linear mixed-effects model investigating differences between species in raw and normalized abundance (number of transcripts/number of genes) of the three canonical olfactory receptor gene families in blind and mako shark.

Abundance	Receptor family comparison	Estimate	SE	df	t-value	P
TPM	OR	-0.15086	0.275	4	-0.549	0.6121
	V1R	-0.00026	0.275	4	-0.001	0.9993
	V2R	0.642272	0.275	4	2.338	0.0795
Normalized TPM	OR	0.255	0.294	4	0.867	0.4351
	V1R	-0.502	0.294	4	- 1.707	0.1629
	V2R	-0.267	0.204	4	-0.907	0.4156

SE: Standard error; df: degrees of freedom, P: p-value.

Table S3.4. Coefficients from linear mixed-effects model investigating differences in the normalized abundance of the three canonical olfactory receptor gene families found in blind and mako shark.

Species	Normalized family comparison	Estimate	SE	df	t-value	P
B. waddi	OR – V1R	0.0304	0.292	8	0.104	0.9940
	OR – V2R	0.3068	0.292	8	1.052	0.5676
	V1R – V2R	0.2765	0.292	8	0.948	0.6276
I. oxyrinchus	OR – V1R	-0.7258	0.292	8	-2.488	0.0861
	OR – V2R	-0.2143	0.292	8	-0.735	0.7508
	V1R – V2R	0.5115	0.292	8	1.753	0.2449

SE: Standard error; df: degrees of freedom, P: p-value.

Fig S3.1

Fig S3.1 Maximum likelihood phylogenetic tree of OR. Phylogenetic tree with 33 OR sequences from chondrichthyans obtained in this study and from Hara et al. [98], Marra et al. [99] and Sharma et al. [100]. Number of unique OR transcripts for blind shark was two, whereas for mako it was three. Newly identified genes in mako and blind shark were named according to closest ortholog/paralog. Outgroup genes belonged to nine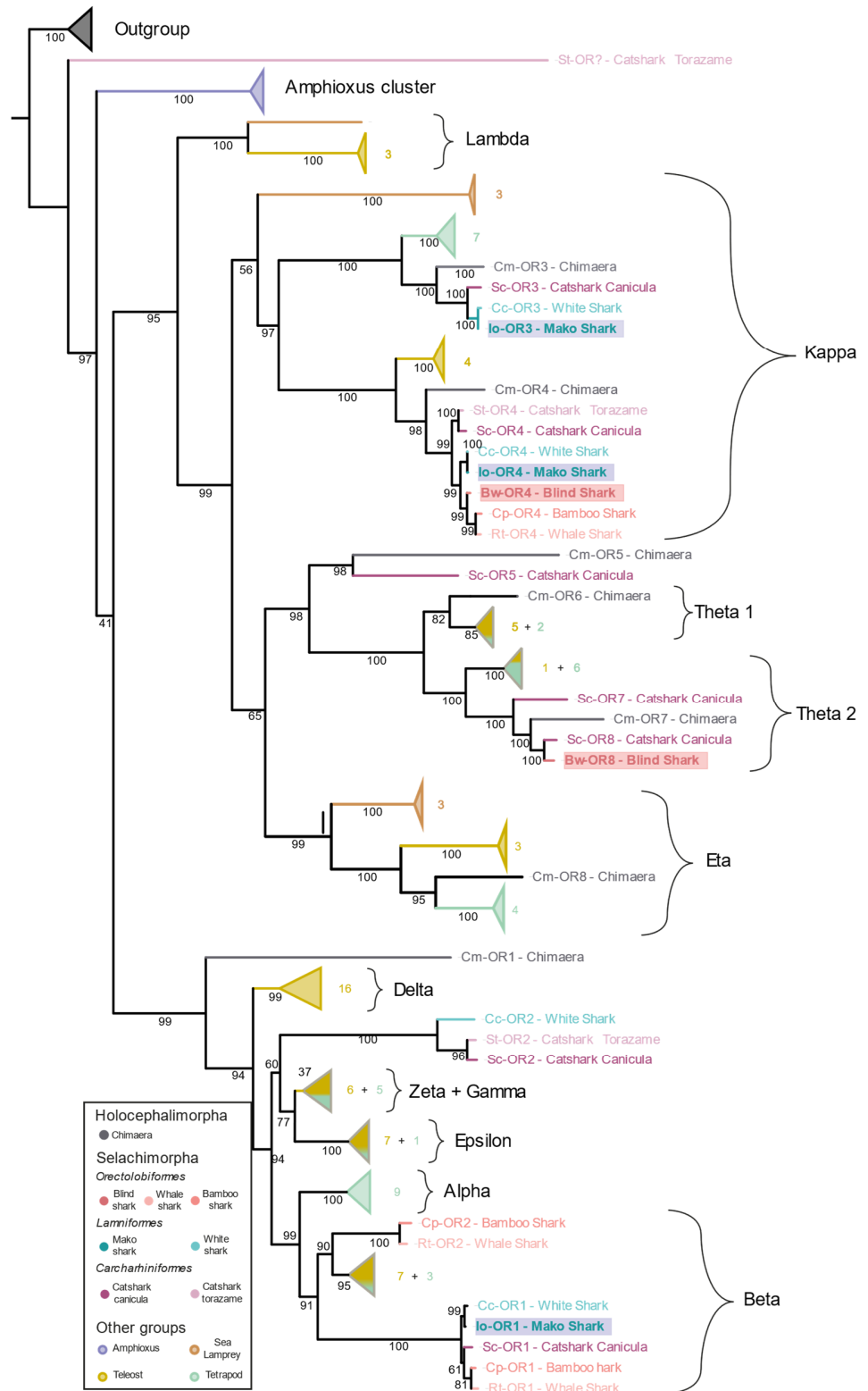 non-OR rhodopsin-like GPCR genes. Bootstrap values shown as a percentage are displayed at nodes. Coloured numbers next to collapsed clades indicate the number of sequences of each vertebrate group

in that branch. Note that one of the reported receptors for *S. torazame* does not cluster with any other of the OR clades, and therefore, its identification should be revisited.
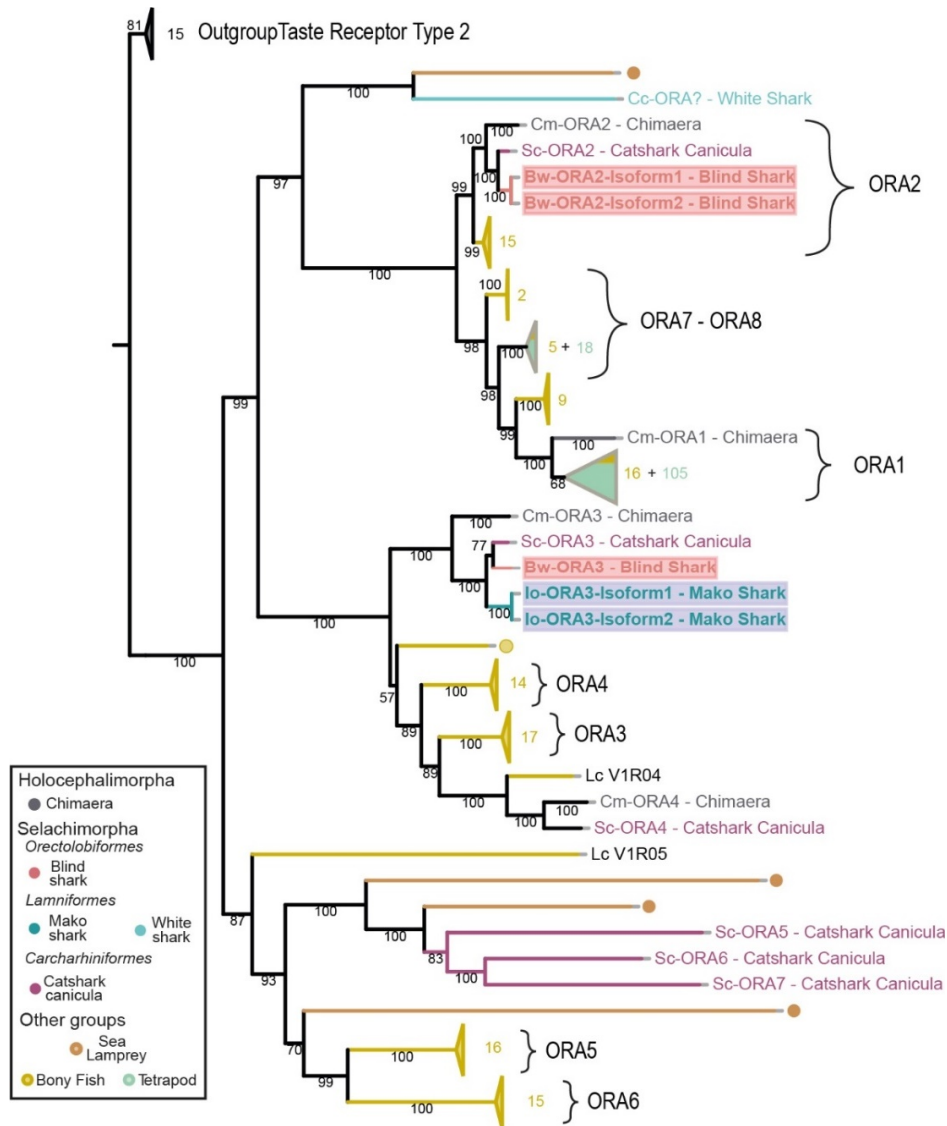
Fig S3.2

Fig S3.2 Maximum likelihood phylogenetic tree of V1R/ORA. Phylogenetic tree with 16 V1R sequences from chondrichthyans obtained in this study and from Marra et al. [99] and Sharma et al. [100]. Number of unique V1R transcripts for blind shark was three, whereas for mako it was two. Newly identified genes in mako and blind shark were named according to closest ortholog/paralog. Outgroup genes included 15 taste receptor type 2 genes (T2R). Bootstrap values shown as a percentage are displayed at nodes. Coloured numbers next to collapsed clades indicate the number of sequences of each vertebrate group in that branch. Note the only white shark gene obtained from Marra et al. [99] had an unusual position in the tree that does not cluster with other chondrichthyan clades, and therefore, its identification as an olfactory receptor should be revisited.

Fig S3.3

Fig S3.3. Maximum likelihood phylogenetic tree of V2R.

Phylogenetic tree with 164 V2R sequences from chondrichthyans obtained in this study and from Marra et al. [99] and Sharma et al. [100]. Number of unique V2R transcripts for blind shark was 53, whereas for mako it was 22. Newly identified genes in mako and blind shark were named according to closest ortholog/paralog. As V2R is a paraphyletic gene family, three different outgroup genes were used: 18 Taste receptor type 1 (TS1R) sequences for the GPRC6A/V2RL clade; five calcium-sensing receptor sequences for family A, B, and C of V2R; five metabotropic glutamate receptors for both groups (V2R). Bootstrap values shown as a percentage are displayed at nodes. Coloured numbers next to collapsed clades indicate the number of sequences of each vertebrate group in that branch.
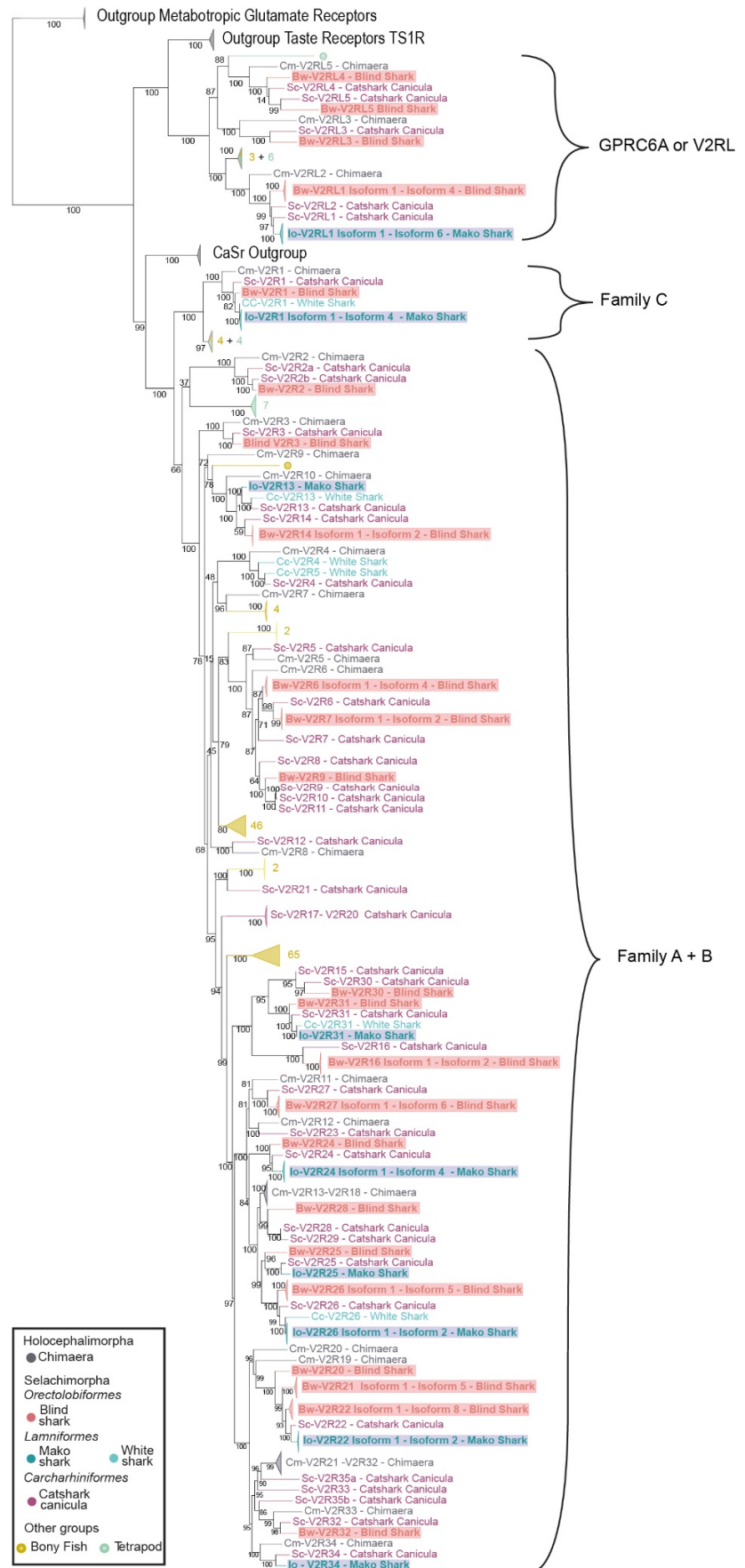
Pages 79-80 of this thesis has been removed as it may contain sensitive/confidential content